CHARACTERIZING THE REGULATORY MECHANISMS IN *FUSARIUM VERTICILLIOIDES* SECONDARY METABOLISM USING FUNCTIONAL GENOMICS APPROACHES

A Dissertation

by

YOON E. CHOI

Submitted to the Office of Graduate Studies of
Texas A&M University
in partial fulfillment of the requirements for the degree of

DOCTOR OF PHILOSOPHY

May 2008

Major Subject: Plant Pathology

CHARACTERIZING THE REGULATORY MECHANISMS IN *FUSARIUM VERTICILLIOIDES* SECONDARY METABOLISM USING FUNCTIONAL GENOMICS APPROACHES

A Dissertation

by

YOON E. CHOI

Submitted to the Office of Graduate Studies of
Texas A&M University
in partial fulfillment of the requirements for the degree of

DOCTOR OF PHILOSOPHY

Approved by:

Chair of Committee,	Won-Bo Shim
Committee Members,	Brian D. Shaw
	Herman B. Scholthof
	Wayne Versaw
Head of Department,	Dennis C. Gross

May 2008

Major Subject: Plant Pathology

ABSTRACT

Characterizing the Regulatory Mechanisms in *Fusarium verticillioides* Secondary Metabolism Using Functional Genomics Approaches. (May 2008)

Yoon E. Choi,

B.S., Korea University;

M.S., Pohang University of Science and Technology, Korea

Chair of Advisory Committee: Dr. Won-Bo Shim

Fusarium verticillioides is one of the most important fungal pathogens of maize and has also received increasing attention due to its ability to produce various secondary metabolites, including fumonisin B_1 (FB_1) and bikaverin. However, little is known about the regulatory mechanisms associated with *F. verticillioides* secondary metabolism. In this study, I utilized functional genomics, forward and reverse genetics, proteomics, and high efficiency homologous recombination, to better understand the complex secondary metabolism regulations in *F. verticillioides*. First, using the reverse genetics approach, I characterized a putative protein phosphatase gene, *CPP1* as a negative regulator of FB_1 biosynthesis. *CPP1* gene deletion also affected multiple phenotypes such as radial growth, conidia germination rates, macroconidia formation, and hyphal swelling. Through gene complementation, I also demonstrated that the *F. verticillioides CPP1* and *Neurospora crassa* wild-type *ppe-1* gene are functionally conserved. Second, I used proteomics and quantitative real-time (qRT)-PCR, to advance our understanding of

genes associated with fumonisin production. I analyzed the proteomic changes associated with the mutation in *FCC1*, a key positive regulator of fumonisins biosynthesis. I isolated proteins that were significantly up-regulated in either the wild-type or the *fcc1* mutant, and transcriptional profiles of the genes corresponding to the selected proteins were analyzed via qRT-PCR. These genes showing expression patterns concomitant with fumonisin biosynthesis can be identified as primary targets for functional analysis. Next, I utilized REMI (Restriction Enzyme Mediated Integration) to isolate *GAC1* gene, which encodes a GTPase activating protein, that serve as a negative regulator of bikaverin biosynthesis in *F. verticillioides*. *AREA* and *PKS4* are downstream genes that are regulated positively and negatively by *GAC1*, respectively. Lastly, I generated a highly efficient homologous recombination strain of *F. verticillioides*. In eukaryotes, *KU70* and *KU80* play important roles in nonhomologous end-joining process, which leads to a high percentage of ectopic integration events during fungal transformation. By generating a *KU70* gene deletion mutant (SF41), I have established a resource that will contribute to functional genomic research in *F. verticillioides*.

DEDICATION

To my wife, Eun-Jung Kim and my parents, Mr. Jong-Eul Choi and Ms. Keum-Soon Kim.

ACKNOWLEDGEMENTS

I am thankful for everyone who helped me make it to this point in my life. I am especially thankful for the passionate guidance and unlimited support during my Ph.D. studies from Dr. Won-Bo Shim. I also would like to thank my committee members, Dr. Brian D. Shaw, Dr. Herman B. Scholthof, and Dr. Wayne Versaw for their helpful discussion and advice throughout the course of this research.

I would like to acknowledge the support and friendship of all the faculty, staff, and graduate students of the Department of Plant Pathology and Microbiology.

Finally, I greatly appreciate the love and encouragement of my wife Eun-Jung, my mother, Keum-Soon Kim, my father, Jong-Eul Choi, my mother-in law, Young-Ran Joo, and my father-in law, Yong-Dae Kim.

TABLE OF CONTENTS

CHAPTER Page

LIST OF FIGURES

LIST OF TABLES

CHAPTER I

INTRODUCTION

FUNGAL SECONDARY METABOLISM

Metabolic processes in biological systems can largely be classified into primary and secondary metabolisms (Bennett & Ciegler, 1983). Primary metabolic processes are considered vital to all living organisms, e.g. glycolosis, fatty acid metabolism, amino acid biosynthesis, and photosynthesis. These are essential metabolic processes for exploiting or utilizing nutrient sources to obtain energy or assemble macromolecules of cellular structure/functions for own survival. In contrast, secondary metabolisms are those excluded from the primary metabolisms and are considered dispensable for the survival of organisms. Unlike primary metabolites, secondary metabolites are not directly associated with normal growth and are produced under select conditions (Bennett & Ciegler, 1983). Notably, via secondary metabolism, a wide variety of metabolites with low-molecular weight can be synthesized, some with potent physiological activities (Bennett & Bentley, 1989).

Fungi are of particular interest due to their capacity to produce an extensive array of secondary metabolites. While many secondary metabolites have no known functions to the producing fungal organisms (Bu'Lcok, 1961), these metabolites have tremendous importance to humans with beneficial (e.g., antibiotics) or detrimental (e.g., mycotoxins)

This dissertation follows the style of *Microbiology*.

properties (Demain & Fang, 2000).

For example, one of the most notable fungal secondary metabolites, penicillin, was identified from the culture of *Penicillium notatum* and has a broad-spectrum of antibiotic activities. It had enormous impact on the development of medicine and saved innumerable lives all across the world. Significantly, recent investigations demonstrated that more than 700 fungal secondary metabolites have antibacterial, antifungal, or antitumor activities (Demain & Fang, 2000; Pelaez, 2005). On the opposite spectrum in terms of human interest are mycotoxins, which are responsible for a number of disease incidences due to their toxicity (Bennet & Klich, 2003). For example, in the early 1960s, aflatoxins were first discovered by scientist searching for the cause of 'turkey X disease', which was responsible for thousands of turkey deaths in Argentina. It turned out that these turkeys were fed with peanut meals contaminated with *Aspergillus flavus* (Blount, 1961). Further research showed that aflatoxins, a group of mycotoxins produced by *A. flavus*, was directly responsible for these deaths (Blount, 1961). To date, aflatoxins remain as one of the most toxic mycotoxins known to man with high carcinogenic activity (Eaton & Groopman, 1998). In addition to *A. flavus*, other fungal organisms are capable of producing various mycotoxins, which are common and widespread in nature posing a great threat to humans and animals.

Due to the significant impact of fungal secondary metabolites, it is critical that we gain a better understanding of the molecular mechanisms associated with secondary metabolites in fungi. While there has been good progress made toward the functional characterization of fungal secondary metabolism genes in the past decade, we still do not

understand the details of how these metabolic pathways are intricately regulated in fungal cells.

FUSARIUM SPECIES AND SECONDARY METABOLISM

Fusarium species are filamentous ascomycete fungi widely distributed in soil and plants. The genus *Fusarium* contains over 20 species and includes several economically important plant pathogens, most notably *F. verticillioides*, *F. graminearum*, and *F. oxysporum*. Studies on *Fusarium* species have been very active lately, mostly due to the concerns regarding various mycotoxins in crops infected with toxigenic *Fusarium* (Desjardins, 2006). The three forementioned *Fusarium* species are responsible for the significant economic loss by *Fusarium*-caused plant diseases worldwide (Di Pietro *et al*., 2003; McMullen *et al*., 1997; Munkvold & Desjardins, 1997).

F. graminearum is the casual agent of head blight (scab) of wheat and barley. The economic loss due to this disease was estimated as more than $3 billion during the wheat scab outbreaks in the 1990s (McMullen *et al*., 1997). The fungus produces several important mycotoxins, such as trichothecene and deoxynivalenol (DON, vomitoxin), posing additional economic threats. Trichothecenes are powerful modulators of mammalian immune functions, and deoxynivalenol are potent inhibitors of protein biosynthesis in eukaryoyes (Rubella *et al*., 2004). Genes involved in production of trichothecenes are clustered and are referred to as the 'Tri cluster'. So far, two positive regulators within the cluster were identified: *Tri 6* and *Tri 10*. Tri6 is Cys_2-His_2 zinc

finger protein associated with activation of Tri cluster genes, and Tri10 is required for expression of Tri cluster acting upstream of Tri6 (Tag *et al*., 2001).

Fusarium oxysporum is the most abundant *Fusarium* in nature and they are responsible for vascular wilts in over 100 cultivated plant species, including tomato, potato, sugarcane, bean, cowpea (Di Pietro *et al*., 2003). Tomato wilt, caused by *F. oxysporum* f. sp. *lycopersici*, has been reported in at least 32 countries worldwide (Jones *et al*., 1991). Panama disease of banana (*F. oxysporum*) is a devastating disease that is widespread in Asia, Africa, Australia, the Pacific Islands, the Caribbean, and Central and South America. This disease nearly eliminated the banana export trade in Central America during a 1950s outbreak (Ploetz 1994) and remains one of the most important diseases of banana worldwide (Kung'u & Jeffries 2001, Viljoen 2002).

Fusarium verticillioides (Sacc.) Nirenburg (teleomorph *Gibberella moniliformis* Wineland) causes severe stalk rot and ear rot of maize and is found in plant residues in almost every maize field at harvest (White, 1999). Fungal stalk rots, including fusarium stalk rot, are the most devastating diseases of maize in terms of average yield loss. Recently, attention to maize diseases caused by *F. verticillioides* have increased due to the fact that the fungus can produce a wide variety of secondary metabolites, which include fumonisins, bikaverin, fusaric acid, fusarin C, and moniliformin (Bacon *et al*. 2004; Nelson *et al*. 1993). Of these secondary metabolites, fumonisins have been reported to possess a high cancer promoting activity (Gelderblom *et al*., 1988). The ingestion of fumonisin-contaminated corn by humans and animals has been linked to a variety of illnesses, including leukoencephalomalasia and neural tube defects

(Gelderblom *et al*., 1988; Marasas, 2001; Minorsky, 2002; Missmer *et al*., 2006). More than 28 fumonisin analogs have been identified to date, and among them, fumonisin B_1 (FB_1) is the major fumonisin found in contaminated commodities (Rheeder *et al*., 2002). To date, efficient management strategies against *F. verticillioides* have not been developed (Munkvold & Desjardins, 1997). Moreover, the chemical structure of FB_1 is so stable that it cannot be completely eliminated by post-harvest treatment (Munkvold & Desjardins, 1997).

SECONDARY METABOLITE BIOSYNTHESIS IN *F. VERTICILLIOIDES*

Over the past decade, significant progress has been made in elucidating the molecular genetic mechanisms associated with fumonisin biosynthesis in *F. verticillioides*. FB_1 is synthesized via a polyketide biosynthetic pathway (Seo *et al*., 2001). The genes involved in FB_1 biosynthesis are clustered in a fashion similar to other well-defined fungal secondary metabolite gene clusters. The fumonisin (*FUM*) gene cluster is known to contain 22 genes with a length of 42 kb (Brown *et al*., 1996; Proctor *et al*., 2003; Sagaram *et al*., 2006b; Seo *et al*., 2001). Of the 22 genes, 15 genes are co-regulated including the key gene in the *FUM* gene cluster, *FUM1*, which encodes a polyketide synthase (Proctor *et al*., 1999). The FB_1 structure suggests at least 8 enzymatic steps are required for its synthesis (Seo *et al*., 2001). *In silico* analysis of the *FUM* cluster suggest that the Fum1 protein is involved in the formation of a linear polyketide. An aminotransferase, the Fum8 protein, attaches an alanine to the polyketide

backbone and P450 monoxygenase, the Fum6 protein, catalyzes further modification of side chains. Gene disruption of *FUM1*, *FUM6*, and *FUM8* demonstrated that these genes are indispensable for FB_1 biosynthesis (Seo *et al*., 2001; Proctor *et al*., 2003). Biochemical functions of the Fum3 protein, a 2-ketoglutarate dependent dioxygenase, and the Fum13 protein, a dehydrogenase/reductase, were characterized recently (Butchko *et al*., 2003; Ding *et al*., 2004). Genes for self-protection, such as longevity assurance factor (*FUM17* and *FUM18*) and an ABC transporter (*FUM19*), are also present in the *FUM* cluster (Proctor *et al*., 2003).

While our knowledge of the *FUM* gene cluster is nearly complete, we still lack a clear understanding of the regulatory mechanisms involved in fumonisin biosynthesis. Therefore, recent research has been mostly directed at the regulatory mechanisms of FB_1 biosynthesis. Interestingly, specific regulatory gene(s) that are often present in fungal secondary metabolite gene clusters have not been reported in the *FUM* gene cluster. Environmental factors, mainly acidic pH and nitrogen stress, have been shown to enhance FB_1 production (Shim & Woloshuk, 1999). In addition, maize kernel composition was identified as a factor in FB_1 biosynthesis (Bluhm & Woloshuk, 2005; Shim *et al*., 2003). Among the regulatory genes associated with FB_1 biosynthesis, *FCC1* was the first regulatory gene characterized in *F. verticillioides* (Shim & Woloshuk, 2001). *FCC1* encodes a C-type cyclin, and the *FCC1* knock-out mutant (FT536) failed to produce FB_1 on corn kernels. In addition, FT536 showed significant reduction in conidia production in synthetic media (Shim & Woloshuk, 2001). Based on this phenotypic analysis, it was suggested that *FCC1* plays an important role in fumonisin biosynthesis

and conidiation in *F. verticillioides*. Since *FCC1* is associated with multiple signaling pathways, it has been emphasized that identification of additional downstream signaling genes is necessary to better understand the *FCC1*-mediated signaling pathway that directly impacts FB_1 biosynthesis. However, we still have limited knowledge of downstream genes of *FCC1*. To date, studies have only revealed a limited number of regulatory genes associated with fumonisin biosynthesis, e.g., *PAC1, FCC1, ZFR1*, *GBP1*, and *FUM21* (Brown *et al*., 2007; Flaherty *et al*., 2003; Flaherty & Woloshuk, 2004; Sagaram *et al*., 2006a; Shim & Woloshuk, 2001). *GBP1* and *PAC1* are negative regulatory genes, while *FCC1* and *ZFR1* positively regulate FB_1 biosynthesis. Two genes, *ZFR1* and *GBP1*, were determined as *FCC1*-downstream genes acting on FB1 biosynthesis (Flaherty & Woloshuk, 2004; Sagaram *et al*., 2006a). Significantly, other than *FUM21*, none of these genes are physically linked to the *FUM* gene cluster, and we have limited understanding of fumonisin regulatory signaling network in *F. verticillioides*.

F. verticillioides secondary metabolites are not limited to fumonisins. There are a variety of the other mycotoxins (e.g, fusaric acid) and pigments (Bacon *et al*., 2004; Nelson *et al*., 1993) synthesized by the fungus. While studies have begun revealing the regulatory mechanism associated with FB_1 biosynthesis, little is known about the biosynthesis of other *F. verticillioides* secondary metabolites, such as bikaverin, fusarin C, and moniliformin. The genes and signaling pathways associated with biosynthesis of these metabolites are not fully understood. Moreover, it is important to recognize that

secondary metabolism in *F. verticillioides* is complex and that these biosynthetic processes are interlinked and intricately regulated.

RESOURCES FOR STUDYING *F. VERTICILLIOIDES*

There are several advantages to studying *F. verticillioides* as the organism of choice for fungal secondary metabolism research. The full genome sequence of *F. verticillioides* was recently released and publicly available. Also, the *F. verticillioides* research community assembled a wealth of molecular, genetic, and genomic resources. A genetic map consisting of 150 biochemical, molecular and morphological markers and 486 AFLP markers is available (Jurgenson *et al*., 2002; Xu & Leslie, 1996). Brown *et al* (2007) reported generating over 87,000 ESTs from *F. verticillioides* and analysis of this extensive collection of ESTs, which is estimated to represent over 80% of the expressed genes in the fungus. Fungal protoplast generation and a gene knock-out strategy is now routine and well-established - albeit low efficiency- in *F. verticillioides* (Proctor *et al*., 1999; Shim & Woloshuk, 2001). Using the double-joint PCR strategy, gene disruption vector construction is no longer the bottleneck step in *F. verticillioides* gene knock-out procedure (Yu *et al*., 2004). Furthermore, *F. verticillioides* is also capable of sexual cross, which provides traditional genetic experiments.

RESEARCH OBJECTIVES

Due to the significance of *F. verticillioides* in maize diseases as well as the threat of fumonisins to humans and animals, it is critical that we gain a better understanding of *F. verticillioides* biology. My research goal is focused on characterizing the regulatory mechanisms associated with *F. verticillioides* secondary metabolisms. Here, I have outlined four research objectives that are aimed to achieve this goal:

1. **Identify and characterize genes that are downstream of *FCC1* via a reverse genetics approach.** *F. verticillioides FCC1* encodes a protein highly similar to yeast C-type cyclin Ume3, which is associated with the RNA polymerase II holoenzyme. Unlike other cyclins that are involved in cell cycle regulation, C-type cyclins, including Ume3, are known to regulate transcriptional machinery in *S. cerevisiae* (Cooper *et al*., 1997). A study by Shim and Woloshuk (2001) demonstrated that functional *FCC1* is necessary for proper FB_1 biosynthesis and fungal development. Also, previous cDNA microarray and suppressive subtraction hybridization (SSH) analyses identified genes that are expressed differentially downstream of *FCC1* leading to the hypothesis that select group of genes are directly associated with FB_1 biosynthesis (Pirttilä *et al*., 2004; Shim and Woloshuk, 2001). Here, I selected a gene designated *CPP1*, which encodes a putative cell shape control protein phosphatase, for functional characterization. Phosphorylation/dephosphrylation of proteins is central to regulating a wide variety of cellular functions including signal transduction

and gene expression (Dickman & Yarden, 1999). Protein phosphatases play a fundamental role in a variety of cellular processes, where they catalyze the dephosphorylation of proteins. Despite of their importance, little is known about protein phosphatases in *F. verticillioides*. Expression of *CPP1* was highly up-regulated in a fumonisin suppressing condition. Therefore I hypothesize that *CPP1* is involved in fumonisin production in a negative manner. If this hypothesis is true, *CPP1* gene deletion will result in elevated FB_1 production.

2. **Identify novel FB_1 regulatory genes by studying the differential protein expression in wild-type and FT536.** The correlation between transcription and translation is known to be less than 50% (King & Sinha, 2001). Thus, there are limitations to identifying *FCC1*-mediated FB_1 biosynthesis signaling genes by only focusing on the changes that occur at the transcriptional level. It is possible that genes downstream of *FCC1* involved in FB_1 biosynthesis are regulated at the post-transcriptional level. I hypothesize that proteins that are differentially regulated in wild-type and fcc1-deletion mutant will lead to identification of novel genes that are associated with fumonsin regulation in *F. verticillioides*.
3. **Identify novel regulatory gene(s) associated with *F. verticillioides* secondary metabolism.** In contrast to the fumonisin biosynthesis mechanism, little is known about the biosynthetic mechanisms of other secondary metabolites in *F. verticillioides*. Here, I will utilize REMI (Restriction Enzyme Mediated Integration) mutagenesis to screen for novel genes in *F. verticillioides* that impact secondary metabolism. In order to generate mutants, vector pBP15, which harbors hygromycin

B phosphotransferase gene as the selectable marker, will be linearized using restriction enzyme and subsequently will be transformed into *F. verticillioides* protoplasts. Random integration of the vector may result in inactivation of functional genes. *F. verticillioides* spends most of its life cycle as a haploid, which makes the REMI approach more feasible for identifying gene mutations and aberrant phenotypes (Kahmann *et al*., 1999; Maier *et al*., 1999). The aim of this objective is to discover new genes that are involved in *F. verticillioides* secondary metabolism.

4. **Develop an efficient gene characterization system suitable for high-throughput functional genomic research in *F. verticillioides*.** In order to understand and characterize the functional roles of genes involved in *F. verticillioides* secondary metabolism, we depend heavily on gene disruption as the key experimental procedure. However, the major problem encountered in the mutagenesis process is the low efficiency of homologous recombination in *F. verticillioides*. While the efficiency varies depending on the locus, in general it is less than 2% in *Fusarium verticillioides* (Choi *et al*., unpublished data). This low efficiency is due to a high number of ectopic integration events that occur during transformation. Homologous recombination events, which have been utilized for generating gene deletion mutants in filamentous fungi, are based on spontaneous repairing mechanisms for double strand breaks (DSB) in eukaryotes. When exogenous disruption vectors are introduced to protoplasts, they are recognized as DSB, therefore are subject to DSB repairs in fungal cell. Two independent pathways are involved in repairing DSB. One is homologous recombination (HR) depending on sequence similarity and the

other is nonhomologous end-joining (NHEJ), which directly integrates exogenous DNA fragments (e.g. disruption vector) into the genome without sequence homology (Ninomiya *et al*., 2004). NHEJ is the mechanisms responsible for ectopic integration competing with HR. NHEJ is a major mechanism for repairing DSB in filamentous fungi, whereas HR is dominant over NHEJ in *Saccharomyces cerevisiae* (Meyer *et al*., 2007). To overcome the problems of low efficiency of HR in filamentous fungi, one solution is to inhibit NHEJ, which in turn, will increase HR efficiency (Goins *et al*., 2006). Here, my aim is to enhance the homologous recombination efficiency in *F. verticillioides*, and this will be accomplished by disrupting the NHEJ mechanism. This high HR efficient strain will contribute to functional genomics research in *F. verticillioides*.

CHAPTER II

FUNCTIONAL CHARACTERIZATION OF *FUSARIUM VERTICILLIOIDES CPP1*, A GENE ENCODING A PUTATIVE PROTEIN PHOSPHATASE 2A CATALYTIC SUBUNIT*

INTRODUCTION

The fungal pathogen *Fusarium verticillioides* (Sacc.) Nirenburg (teleomorph *Gibberella moniliformis* Wineland) has been the topic of extensive research based on its production of the mycotoxin fumonisin B_1 (FB_1) on maize. FB_1 is a potent carcinogen, and ingestion of fumonisin-contaminated corn by humans and animals has been linked to a variety of illnesses, including leukoencephalomalasia and neural tube defects (Gelderblom *et al*., 1988; Marasas, 2001; Minorsky, 2002; Missmer *et al*., 2006). Due to these serious concerns, the US Food and Drug Administration has established guidelines for the fumonisin level in feed and foodstuff (Park & Troxell, 2002).

Significant progress has been made in elucidating the fumonisin biosynthetic pathway and regulatory mechanisms associated with the toxin production. The biosynthetic gene cluster, including the polyketide synthase (PKS) gene, *FUM1*, (Proctor

* Reprinted with permission from "Functional characterization of *Fusarium verticillioides CPP1*, a gene encoding putative protein phosphatase 2A catalytic subunit" by Choi, Y. E. & Shim, W. B, 2008a. *Microbiol* 154, 326-336, Copyright [2008] by Microbiology.

et al., 1999; Proctor *et al*., 2003; Seo *et al*., 2001), and a number of regulatory genes involved in fumonisin biosynthesis, namely *PAC1, FCC1,* and *ZFR1*, have been identified and characterized (Flaherty *et al*., 2003; Flaherty & Woloshuk, 2004; Shim & Woloshuk, 2001). These genes however do not show clear epistatic relationships, and therefore it is conceivable that multiple signaling pathways are associated with fumonisin regulation. Moreover, a putative regulatory gene within the *FUM* cluster, *FUM21*, has recently been identified and characterized, but it was shown that the deletion of the *FUM21* gene did not completely block fumonisin biosynthesis (Brown *et al*., 2007). This report suggests that transcriptional regulation of *FUM* genes can also be affected by putative regulatory gene(s) outside the *FUM* cluster. Additionally, the complexity of fumonisin regulation is further enhanced by a variety of physiological and nutritional conditions, notably acidic pH and nitrogen stress, which are known to favor or perhaps trigger fumonisin biosynthesis (Flaherty *et al*., 2003; Shim & Woloshuk, 1999).

In an effort to identify additional genes associated with fumonisin regulation, Shim & Woloshuk (2001) constructed a subtractive suppression hybridization (SSH) cDNA library to screen genes differentially expressed during fumonisin biosynthesis in *F. verticillioides* wild-type and FT536 strains. FT536 harbors a mutation in the *FCC1* gene, resulting in reduced conidiation and drastic reduction in fumonisin production when grown on maize kernels (Shim & Woloshuk, 2001). Microarray analysis using *F. verticillioides* oligoarrays has further verified genes that are expressed concomitantly with fumonisin production (Pirttilä *et al*., 2004). A number of these genes have been

selected for characterization of their role in fumonisin biosynthesis. For instance, cDNA encoding a putative zinc binuclear cluster-type transcriptional factor, later designated *ZFR1*, was shown to be positively associated with fumonisin biosynthesis (Flaherty & Woloshuk, 2004). Deletion of *ZFR1* in *F. verticillioides* resulted in greater than 90% reduction in fumonisin production when compared to that of wild-type. Also, Sagaram *et al.* (2006a) recently demonstrated that *GBP1*, a gene originally identified in the FT536 SSH cDNA library, encodes a monomeric G-protein that is negatively associated with fumonisin biosynthesis.

In the FT536 SSH cDNA library, we isolated a 300-bp cDNA fragment (ft536_ 0_M14) that showed a high level of similarity to a *Neurospora crassa* gene that encodes a probable cell shape control protein phosphatase 2A catalytic subunit, PPE-1 (E=5e-45). Protein phosphatases catalyze the dephosphorylation of specific substrates that are important for processing various biological and cellular functions (Ceulemans & Bollen, 2004; Dickman & Yarden, 1999; Hunter, 1995), and this catalytic action is known to de-activate signaling pathways induced by a variety of protein kinases (Hunter, 1995). In *Arabidopsis*, for instance, protein phosphatase type 2C is involved in the negative regulation of abscisic acid signaling pathway (Saez *et al*., 2004). Overall, we have limited understanding of the role of protein phosphatases in filamentous fungi, particularly in association with secondary metabolism. Moreover, protein phosphatases in *F. verticillioides* have not been functionally characterized to date.

The cDNA fragment ft536_ 0_M14 was identified in FT536 SSH cDNA library, which represents the collection of genes up-regulated during fumonisin suppression, and

therefore we hypothesize that this gene, designated *CPP1*, is negatively associated with fumonisin biosynthesis in *F. verticillioides*. To test this hypothesis, we generated a *CPP1* gene deletion mutant and investigated the role of *CPP1* in *F. verticillioides*. In this study, we report that deletion of *CPP1* results in elevated fumonisin production via de-repression (or up-regulation) of *FUM1* expression. We also show that a mutation in *CPP1* results in pleiotropic phenotypes suggesting that *CPP1* is associated with multiple signaling pathways that control fungal development and differentiation. Lastly, we demonstrate that *Neurospora crassa* wild-type *ppe-1* gene can complement *F. verticillioides CPP1* gene deletion.

METHODS

Fungal strain and culture media. *Fusarium verticillioides* strain 7600 (Fungal Genetics Stock Center, University of Missouri, Kansas City, MO, USA) was stored in 20% glycerin at –80°C. Conidia were produced for inoculum by growing the fungus on V8 juice agar (200 ml of V8 juice L^{-1}, 3 g of $CaCO_3$ L^{-1}, and 20 g of agar L^{-1}) at 25°C. For genomic DNA extraction, the fungus was grown in YPD medium (Difco, Detroit, MI, USA) on a rotary shaker (150 rpm). For RNA isolation, hyphal growth assay, and conidia germination assay, the fungus was grown in defined liquid (DL) medium, pH 6.0 (Shim & Woloshuk, 1999). The medium (100 ml) was inoculated with 1×10^5 conidia and incubated at 25°C shaking at 150 rpm under a 14 h light/10 h dark cycle. For fumonisin assay and RNA isolation (for QRT-PCR analysis), fungal strains were also

grown on cracked-corn medium as previously described (Shim & Woloshuk, 1999). To study colony morphology and growth of fungal strains, we used diluted (0.2×) potato dextrose agar (0.2×PDA) (Difco, Sparks, MD, USA). For macroconidia and microconidia counts, agar blocks (0.5 cm in diameter) were inoculated at the center of V8 juice agar and allowed to grow for 7 days, and the condinia were harvested in 0.1% triton and counted using a hemacytometer.

Nucleic acid isolation and manipulation. Bacterial plasmid DNA and fungal genomic DNA were extracted with Wizard miniprep DNA purification system (Promega, Madison, WI, USA) and OmniPrep Genomic DNA Extraction kit (G Biosciences, St. Louis, MO, USA), respectively. Total RNA for QRT-PCR was prepared with Trizol reagent (Invitrogen, Carlsbad, CA, USA) or with RNeasy plant mini kit (Qiagen, Valencia, CA, USA). Southern and northern analyses were performed as described previously (Sagaram *et al*., 2006a; Sambrook & Russell, 2001). The probes used in all hybridization experiments were ^{32}P-labeled with Prime-It random primer labeling kit (Stratagene, La Jolla, CA, USA). DNA sequencing was performed at Gene Technologies Lab, Texas A&M University (College Station, TX, USA).

PCR and quantitative real-time (QRT)-PCR. All primers used in this study are listed in Table 2.1. PCR amplifications were performed in a GeneAmp PCR system 9700 thermocycler (PE Applied Biosystems, Norwalk, CT, USA). PCR of DNA (except single-joint PCR) was performed in 25 μL total volumes with *Taq* DNA polymerase (Promega). The PCR conditions were 2 min of pre-denaturation at 94ºC followed by 30 cycles of 45 s denaturation at 94ºC, 45 s annealing at 54-57ºC and 2 min extension at

Table 2.1. Primers used in *CPP1* characterization

Number	Name	Primer sequence (5' – 3')
1	CPP1-A	CTA GAT CAT GGC TTC ACT AGT* AGG CGT ACC
2	CPP1-B	CAC TTT GAC TTG ACT CCC GGG* TGT TCA CTG
3	CPP1-C	GTG TGG TCA GAT CCA AAG CTT* GAA GAT GTC
4	CPP1-D	ACC AAC TCT ACC CAA GGT ACC* TCC ATA ACC
5	CPP1-che-F	CAC ATA GAC CTT CCA TTG AAG G
6	CPP1-che-R	TGA TCA ATC GTC CTA ATC TCA GG
7	HPH-R2	CTG AAA GCA CGA GAT TCT TCG C
8	CPP1-SC-F	CAT GGT CAT AGC TGT TTC CTG** CGG CCT TGC TGC CCC GCC AGT G
9	CPP1-SC-R	CCT TCA TTC ACG GCA AGA TGG GTC AAT GG
10	CPP1-SC-R2	GAA CGA AGT GAT TAT CCT TGC TCG C
11	M13-F	TTG TAA AAC GAC GGC CAG TGA
12	M13-R	CAG GAA ACA GCT ATG ACC ATG
13	CPP1-LC-F	CAT GGT CAT AGC TGT TTC CTG** GAT GCC TTC GCA TCC TCC CAG
14	CPP1-LC-R	CCT TCA TTC ACG GCA AGA TGG GTC AAT GG
15	CPP1-LC-R2	CGC TGT TCA AGA GTT GGG CTT TCC
16	Gene-F	GCG AAT TGG AGC TCC ACC GC
17	FUM1-F	ATA ACC ATC TCG GCT CAA CG
18	FUM1-R2	GTA TCT GGT GGA CAA CTT TGG G
19	PKS1-F	GGA TAC ATC TCA ATG GCT GTT GAG G
20	PKS1-R	CCT CAC GAA GAT TAA AGT CGT CG
21	PKS2-F	GGA GTC AGT ATC AGA GTG TAG CTC
22	PKS2-R	CGT CCA TAC TTT GGA GGA GAA CC
23	PKS4-F	GCA TCA AGA CTA AGA TCA ACC AGG
24	PKS4-R	GGC AAT GTA TGC TTC GAG AGC
25	TUB2-F	CAG CGT TCC TGA GTT GAC CCA ACA G
26	TUB2-R	CTG GAC GTT GCG CAT CTG ATC CTC G
27	PPE1-com-F1	CAT GGT CAT AGC TGT TTC CTG** CTG TAG TCT TGT GGG CAT CG
28	PPE1-com-R1	GTG ACG ACC AGC GAA TCC CTG GTG
29	PPE1-com-R2	CTG GCT CTG GCT ATT TGT TGG ATG TTG G
30	PPE1-che-F1	GTC ATC ACA TCC GAG GAC ATC GAG

* Restriction enzyme sites were incorporated in the primers to insert amplicons into pBP15.

** M13-R primer sequence for single joint PCR application (Yu *et al*., 2004)

72ºC, unless specified otherwise. Single-joint PCR was performed using Expand Long Polymerase (Roche, Indianapolis, IN, USA) using the manufacturer's suggested protocol. QRT-PCR analyses were performed in a Cepheid Smart Cycler System (Cepheid, Sunnyvale, CA, USA) with QuantiTect SYBR Green RT-PCR kit (Qiagen). Concentration of RNA samples was adjusted to 100 ng μl^{-1} prior to QRT-PCR. QRT-PCR amplifications were carried out with 30 min of reverse transcription at 50ºC followed by 15 min of pre-denaturation at 95ºC and 35 cycles of 15 s of denaturation at 95ºC, 30 s of annealing at 55ºC and 30 s of extension at 72ºC. The expression of *F. verticillioides* β-tubulin gene (*TUB2*) (GenBank U27303) was used as a reference.

***F. verticillioides* transformation.** *F. verticillioides* protoplasts were generated using the protocol described by Shim & Woloshuk (2001), except that Mureinase (2 mg per ml) was replaced with Drieselase (5 mg mL^{-1}) (Sigma, St. Louis, MO, USA). The *CPP1* gene disruption vector, YEC2, was created by inserting 571-bp 5' and 479-bp 3' flanking regions of *CPP1* into pBP15 vector, which contains a hygromycin phosphotransferase (*HPH*) gene as a selectable marker (Fig. 2.1A) (Sagaram *et al*., 2006a). Primers CPP1-A, CPP1-B, CPP1-C, and CPP1-D were used to amplify the 5' and 3' regions, and subsequently cloned into pBP15 vector (Fig. 2.1A). The vector YEC2 was linearized with *Not*I prior to protoplast transformation. Hygromycin-resistant transformants were selected on regeneration agar medium amended with hygromycin (150 $\mu g\ mL^{-1}$) and screened for *CPP1* deletion by PCR and Southern analysis. For PCR, primers (CPP1-che-F, CPP1-che-R, and HPH-R2) that provide specific positive and negative amplification were used to detect homologous recombination events (Fig.

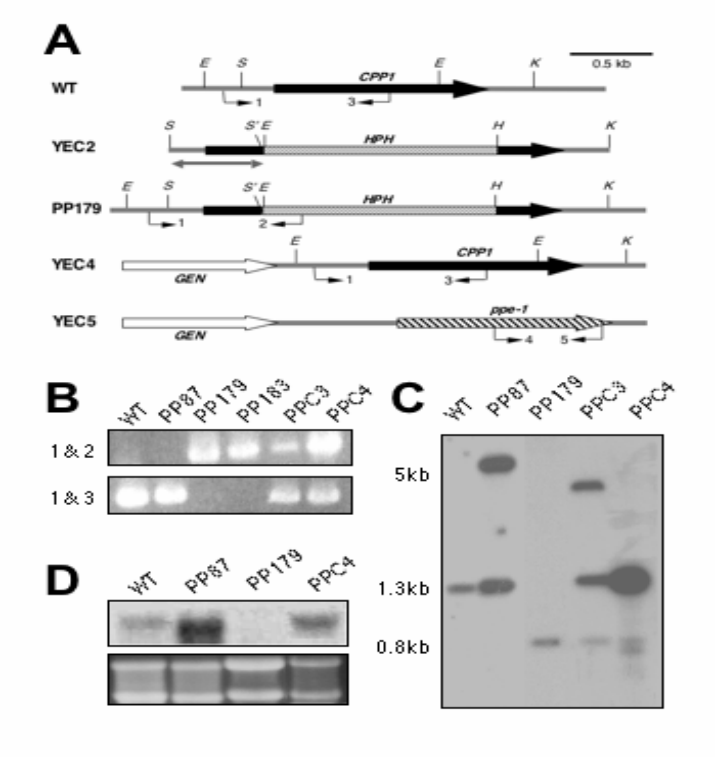

Fig. 2.1
Molecular characterization of *F. verticillioides CPP1*. **(A)** WT: Schematic representation of *CPP1* locus in the wild-type strain. YEC2: the *CPP1* disruption construct which harbors hygromycin phosphotranferase gene (*HPH*) as the selectable marker. PP179: schematic representation of *CPP1* locus in the knock-out strain after the homologous recombination event. YEC4: the construct with *CPP1* wild-type gene fused to the geneticin-resistance gene (*GEN*) that was used to complement PP179. YEC5: the construct with *Neurospora crassa ppe-1* gene fused to the geneticin-resistance gene (*GEN*) that was used to complement PP179. The double arrow on YEC2 indicates the fragment used as ^{32}P-labeled probe in Southern blot. The numbered arrows indicate the location of primers used for positive and negative PCR assays. S, *Spe*I; S', *Sma*I; H, *Hind*III; K, *Kpn*I. **(B)** PCR analysis of *CPP1* disruption and complementation using the primers described in Fig. 2A. WT: wild-type, PP87: ectopic-integration strain, PP179 and PP183: *CPP1* knock-out isolates, PPC3 and PPC4: YEC4-complemented strains. The number on the left indicates primer combinations for PCR amplifaction. **(C)** Southern blot analysis of transformants. Fungal genomic DNA was digested with *Eco*RI, and the blot was hybridized with ^{32}P-labeled DNA probe (shown in Fig. 2.1A). Molecular sizes are indicated on the left. **(D)** Northern blot analysis of the transformants probed with ^{32}P-labeled DNA fragment (Fig. 2.1A) to determine the expression of *CPP1*. Total RNA samples (15 μg) were subjected to electrophoresis in a 1.2% denaturing agarose gel. The gel was stained with ethidium bromide to confirm uniformity of loading (rRNA).

2.1A). For Southern analysis, fungal genomic DNA samples were digested with *Eco*RI before being subjected to electrophoresis in a 1% agarose gel. A 500-bp DNA fragment of YEC2, excised by double enzyme digestion (*Spe*I and *Sma*I), was ^{32}P-labelled as a probe (Fig. 2.1A).

The *CPP1* deletion mutant, PP179, was complemented with a wild-type *CPP1* gene fused to a geneticin-resistance gene (*GEN*). Two complementation constructs, YEC3 and YEC4, were made via single-joint PCR strategy (Sagaram *et al*., 2006a; Yu *et al.*, 2004). For YEC3, primers CPP1-SC-F and CPP1-SC-R were used to amplify full-length *CPP1* plus 400-bp 5' untranslated region (UTR) and 170-bp 3' UTR. The *GEN* marker was prepared as described previously (Sagaram *et al*., 2006a). Subsequently, the amplicons were mixed in a single tube and were joined by PCR. The final YEC3 construct was amplified with primers M13-F and CPP1-SC-R2 using Expand Long Polymerase (Roche). For YEC4, primers CPP1-LC-F and CPP1-LC-R amplified the complete *CPP1* gene plus 850-bp 5' UTR and 450-bp 3' UTR. This amplicon was fused with the *GEN* marker, and the final YEC4 construct was amplified using primers Gene-F and CPP1-LC-R2 (Fig. 2.1B). We then independently transformed YEC3 and YEC4 into PP179 protoplasts, and screened for colonies resistant to geneticin and hygromycin (Sagaram *et al*., 2006a). The introduction of YEC3 or YEC4 in geneticin-resistant strains was verified by PCR and Southern blot analyses.

Fumonisin B_1 analysis. *F. verticillioides* strains were grown in cracked-corm medium for 10 days for fumonisin production analysis. Fumonisin B_1 (FB_1), the major fumonisin produced by *F. verticillioides*, was extracted and analyzed by HPLC

following the method described by Shim & Woloshuk (1999). In addition to FB_1 HPLC analysis, QRT -PCR was used to investigate the relative expression of *FUM1* and other selected polyketide synthase (*PKS*) genes (Kroken *et al*., 2003) in the wild-type and mutant strains. Total RNA samples were prepared from wild-type, PP87, PP179, and PPC4 grown in cracked-corn medium for 10 days, and QRT - PCR analysis was performed with SYBR-Green® as the fluorescent reporter using gene specific primers for *FUM1* gene (FUM1-F and FUM1-R2). The expression of each gene was normalized to endogenous *TUB2* gene expression. The gene expression was calibrated using $2^{-\Delta\Delta Ct}$ method (Livak & Schmittgen, 2001); the range of expression was calibrated using $2^{-\Delta\Delta Ct-s}$ - $2^{-\Delta\Delta Ct+s}$, where s is the standard deviation of ΔCt value (Ct=Threshold Cycle). Subsequently, the total RNA samples of wild-type and PP179 strains were subjected to QRT-PCR analysis using gene specific primers for *FUM1* gene, *PKS1* gene (PKS1-F and PKS1-R), *PKS2* gene (PKS2-F and PKS2-R), and *PKS4* gene (PKS4-F and PKS4-R). Again, the gene expression was calibrated using $2^{-\Delta\Delta Ct}$ method with *TUB2* as the endogenous control.

Microscopy. Microscopic observations were made using an Olympus BX51 microscope (Olympus America Inc., Melville, NY, USA). A detailed description of features used for imaging from this microscope has been described previously (Shaw & Upadhyay, 2005). Imaging of hyphal growth phenotypes was performed using an Olympus DP70 camera and DP70-BSW software (version 01.01). Nuclei were stained with Hoechsts 33258 dye as described previously (Shaw & Upadhyay, 2005).

Complementation of PP179 strain with *Neurospora crassa PPE-1*.

Neurospora crassa ppe-1 (GenBank XM_951629) encodes a probable cell shape control protein phosphatase. The complementation construct, YEC5 was generated by single-joint PCR strategy (Fig. 2.1A) (Yu et al., 2004). Wild-type *ppe-1* (1.43-Kb *ppe-1* gene plus 1.6 Kb 5' UTR and 500 bp 3' UTR) was amplified from the *N. crassa* genomic DNA using the primers PPE1-com-F1 and PPE1-com-R1. These amplicons were fused to *GEN* by joint-PCR using PPE1-com-R2 and Gene-F primers. The final construct, YEC5 was introduced into the protoplasts of PP179, and the transformants were screened for geneticin resistance. The selected isolates were further analyzed by PCR using primers PPE1-che-F1 and PPE1-com-R2 to determine the presence of YEC5 in the genome.

RESULTS

***F. verticillioides CPP1* encodes a putative protein phosphatase 2A catalytic subunit.** The *Fusarium verticillioides* Gene Index (The Institute for Genome Research, http://www.tigr.org/tdb/tgi/) and *Fusarium Group* Database (Broad Institute of Harvard and MIT, http://www.broad.mit.edu/annotation/fgi/) were screened using the 300-bp EST sequence (ft536_ 0_M14) for matching cDNA and genomic DNA sequences. The Gene Index screen resulted in the identification of a 1468-bp TC (tentative consensus) 26726, which contains an 1,221-bp open reading frame (ORF). The *Fusarium* Group Database search revealed that supercontig 2.31, specifically sequence 195,426 to

196,803, harboring a matching genomic DNA sequence. Taken together, *in silico* analysis revealed that the *CPP1* gene is 1377 bp in length, contains three introns (53, 51, and 49 bps), and is predicted to encode a 407-amino-acid polypeptide (GenBank Accession DQ924537).

Sequence analysis of Cpp1 revealed a type 2A protein phosphatase catalytic domain (PP2Ac) between amino acid 32 and 385. This domain is present among a large family of serine/threonine phosphatases. Likewise Cpp1 displayed high similarity to PP2Ac domains in a number of eukaryotes, particularly those present in filamentous fungi (Fig. 2.2). Namely, Cpp1 shares significant similarity with PPE-1 protein, a probable cell shape control PP2Ac in *Neurospora crassa* (E value= 0.0), and SitA, a PP2Ac involved in TOR pathway of *Aspergillus nidulans* (E value= 8e-165) (Fitzgibbon *et al*., 2005). Significantly, these filamentous fungi PP2Ac proteins are orthologous to the *Schizosaccharomyces pombe* protein Ppe1 which plays a role in cell morphogenesis and mitosis (Shimanuki *et al*., 1993). We determined via northern blot analysis that there is no significant differential expression of *CPP1* during growth and FB_1 production, thereby concluding that *CPP1* is a constitutively expressed gene in *F. verticillioides* (data not shown).

Disruption of *CPP1* results in up-regulation of *FUM1* and over-production of FB_1. *F. verticillioides CPP1* gene knock-out strains were generated using a double homologous recombination strategy in order to test our hypothesis that *CPP1* is associated with FB_1 biosynthesis. Of the 243 hygromycin-resistant transformants, two strains, designated PP179 and PP183, were identified in which *CPP1* was replaced by

the YEC2 construct. Specific primers, designed to produce a PCR amplicon dependent upon homologous recombination, were used to confirm the homologous recombination event. PP179 and PP183 produced the expected band; whereas, no amplicon was observed for the wild-type or strain PP87, a strain with ectopic YEC2 integration (Fig. 2.1B). We selected PP179 for further molecular characterization. Southern blot analysis further confirmed that the *HPH* gene replaced 370-bp of DNA within *CPP1* gene. The 500-bp ^{32}P-labelled DNA probe hybridized to a 1.3-kb band in the wild-type and PP87 strains whereas to a 0.8-kb band in the PP179 strain (Fig. 2.1C). Northern blot analysis was performed using a 571-bp *CPP1* DNA fragment probe, which hybridized to the expected 1.35-kb transcript band in the wild-type and PP87 but did not in PP179 (Fig. 2.1D).

Measurement of the radial growth of *F. verticillioides* strains on 0.2×PDA plates revealed that PP179 has approximately a 40% reduction in growth rate when compared to the wild-type progenitor and the PP87 strain (Fig. 2.3). However, no significant difference in fungal mass (fresh wet weight) was observed when strains were grown in 0.2×PDB and YEPD broth. Subsequently wild-type, PP87, and PP179 strains were grown on cracked-corn medium and DL medium to test FB_1 production. TLC and HPLC analysis revealed that wild-type and PP87 did not differ in FB_1 production in either media tested, however, we observed a significant increase in FB_1 production in PP179. Specifically, FB_1 production on inoculated cracked corn medium was more than four times greater for PP179 than that of wild-type (Fig. 2.4A). To verify that the growth phenotype and increased FB_1 production of PP179 is due to the deletion of

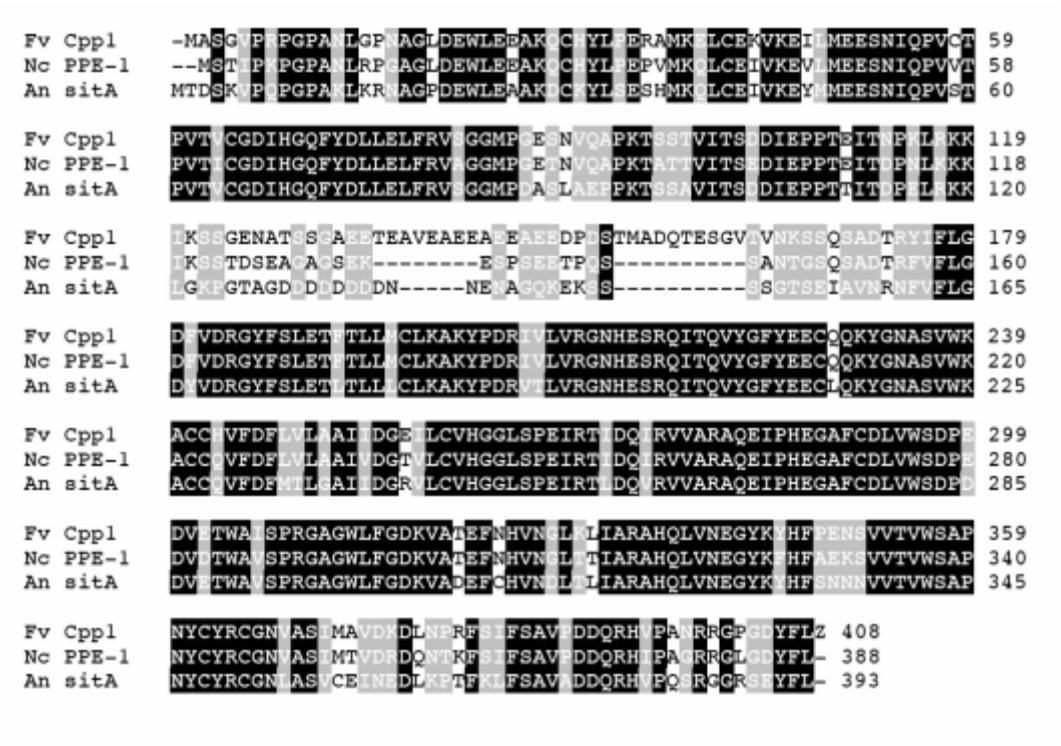

Fig. 2.2
Amino acid alignment of *F. verticillioides* Cpp1. Cpp1 was alignmed with *Neurospora crassa* PPE-1, and *Aspergillus nidulans* SitA via CLUSTALW. Amino acids common to all proteins are indicated by white letters on a black background. Similar amino acids are indicated by white letters on a gray background. Gaps introduced for alignment are indicated by dashes. Cpp1 shares significant similarity with PPE-1 (E value = 0.0) and SitA (E value = 8e-165).

CPP1, PP179 was complemented using vectors YEC3 and YEC4 which contain a wild-type copy of *CPP1* gene fused to the *GEN* (Fig. 2.1A). Following transformation, complemented strains were selected by testing growth on 0.2×PDA containing hygromycin and geneticin. Putative complemented strains containing YEC3 and YEC4 were designated as PPC3 and PPC4, respectively. We determined via PCR that both PPC3 and PPC4 contained the introduced *CPP1* gene (from YEC3 and YEC4) and the *HYG*-replaced mutant locus (Fig. 2.1B). Southern analysis verified the PCR data (Fig. 2.1C). However, northern blot analysis of PPC3 and PPC4 showed that *CPP1* gene expression is only detected in PPC4 (Fig. 2.1D). QRT-PCR analysis detected approximately 40% *CPP1* expression level in PPC3 when compared to the wild-type progenitor (data not shown). Based on the expression results, PPC4 was selected for further phenotypic analysis. Growth rate reduction and increased FB_1 reduction in PP179 were restored to the level of wild-type in the PPC4 strain, thus providing further evidence for roles of *CPP1* in growth rate and FB_1 production (Fig. 2.3 and 2.4A).

Increased FB_1 production in PP179 is due to up-regulation of *FUM1*, the FB_1-specific polyketide synthase gene. *FUM1* encodes a polyketide synthase that is critical to FB_1 biosynthesis (Proctor *et al*., 1999). Here, we asked the question whether the drastic increase in FB_1 production in PP179 is due to altered *FUM1* expression. Total RNA was harvested from wild-type, PP87, PP179, and PPC4 strains grown in cracked-corn medium, the culture condition used for FB_1 production. QRT-PCR analysis of *FUM1* revealed at least 11-fold higher *FUM1* expression in PP179 than that of the other strains tested (Fig.2.4B). Analysis of variance analysis (ANOVA) of the

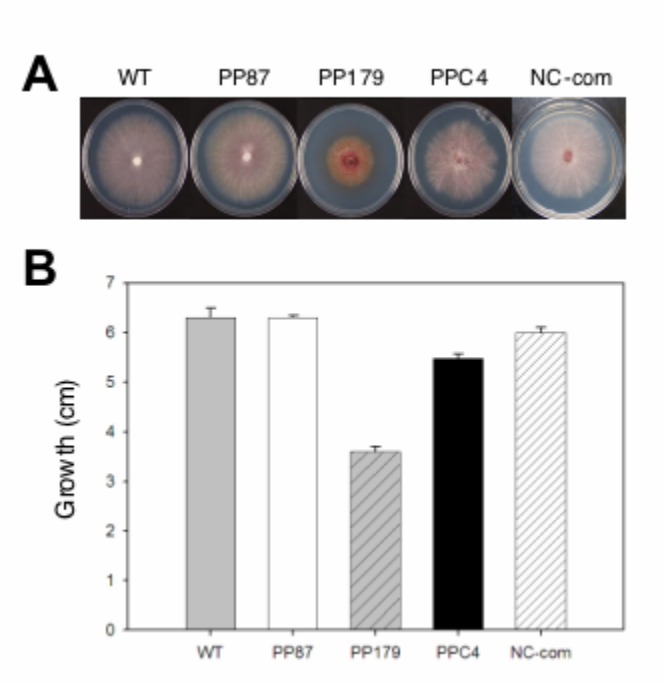

Fig. 2.3
Colony morphology and growth of the wild-type and mutants grown on 0.2×PDA. **(A)** Wild-type, PP87, PP179, PPC4, and Nc-com strains were point inoculated with an agar block (0.5 cm in diameter) and incubated for 7 days at 25°C under a 14 h light/10 h dark cycle. Growth was significantly impaired in PP179 whereas in PPC4 and Nc-com strains the growth defect was restored to that of the wild-type progenitor. **(B)** Radial growth measured and presented as a bar graph. Results are means of three biological replications.

gene expression data from all four strains ($P<0.01$) suggested that *FUM1* expression levels in wild-type, PP87, and PPC4 strains were significantly different from that of PP179 strain. When the test was limited to wild-type, PP87, and PPC4, the resulting P value was 0.862 suggesting that the complementation of PP179 with *CPP1* gene restored wild-type level *FUM1* expression. The data provides molecular evidence that *CPP1* serves as a negative regulator of FB_1 biosynthetic genes in *F. verticillioides*.

As there are over 15 polyketide synthase (PKS) genes in *F. verticillioides* (Kroken *et al.,* 2003), we next investigated the specificity of *CPP1* to regulation of *FUM1*. Kroken *et al*. (2003) classified 15 type-I PKS genes present in *F. verticillioides* into major clades or subclades. To test the impact of *CPP1* deletion (*Δcpp1*) on the expression of PKS genes, we selected four PKS genes from different subclades: *PKS1* (reducing PKS clade II), *PKS2* (reducing PKS clade I), *PKS4* (non-reducing PKS clade I) and *PKS11* (=*FUM1,* reducing PKS clade III). QRT-PCR analysis of the four PKS genes revealed that only *FUM1* expression was up-regulated significantly in PP179 whereas *PKS1*, *PKS2, PKS4* were either down-regulated or unchanged (Fig. 2.4C). The t-tests for *FUM1*, *PKS1*, *PKS2*, and *PKS4* expression confirmed a significant difference in expression between wild-type and PP179. Our results showed that the major impact of *Δcpp1* was on *FUM1* expression suggesting that *CPP1* may have a specific function to regulate *FUM1* in *F. verticillioides*.

Fig. 2.4

Fumonisin B_1 (FB_1) analysis and *FUM1* expression. **(A)** Quantification of FB_1 production in wild-type (WT), PP87, PP179 and PPC4 strains. Sterile cracked corn (2 g) was inoculated with an agar block (0.5 cm in diameter) of WT and mutant strains. After 10 days of incubation at 25°C, FB_1 was extracted with 10 mL of 50% acetonitrile in water, purified through SPE C18 columns and eluted in 2 mL 70% acetonitrile in water and quantified by HPLC. All values represent means of three biological replications with standard deviations shown as error bars. **(B)** Expression of *FUM1* gene in WT, PP87, PP179 and PPC4 strains. Total RNA samples were prepared from fungal strains grown in cracked-corn medium for 10 days, and quantitative real-time (QRT) - PCR analysis was performed with SYBR-Green® as the fluorescent reporter. The levels of transcription were evaluated using the $2^{-\Delta\Delta C}{}_T$ method with *TUB2* as endogenous control. Data represent the fold differences in gene expression. Three biological replications were performed to obtain standard deviations. **(C)** Expression analysis of select PKS genes in the wild-type and PP179. Total RNA samples were prepared from fungal strains grown in cracked-corn medium for 10 days, and QRT - PCR analysis was performed with SYBR-Green® as the fluorescent reporter. The levels of transcription were evaluated using the $2^{-\Delta\Delta C}{}_T$ Method with *TUB2* as endogenous control. Data represent the fold differences in gene expression. Three biological replications were performed to obtain standard deviations. Black circle: WT; White square: PP179.

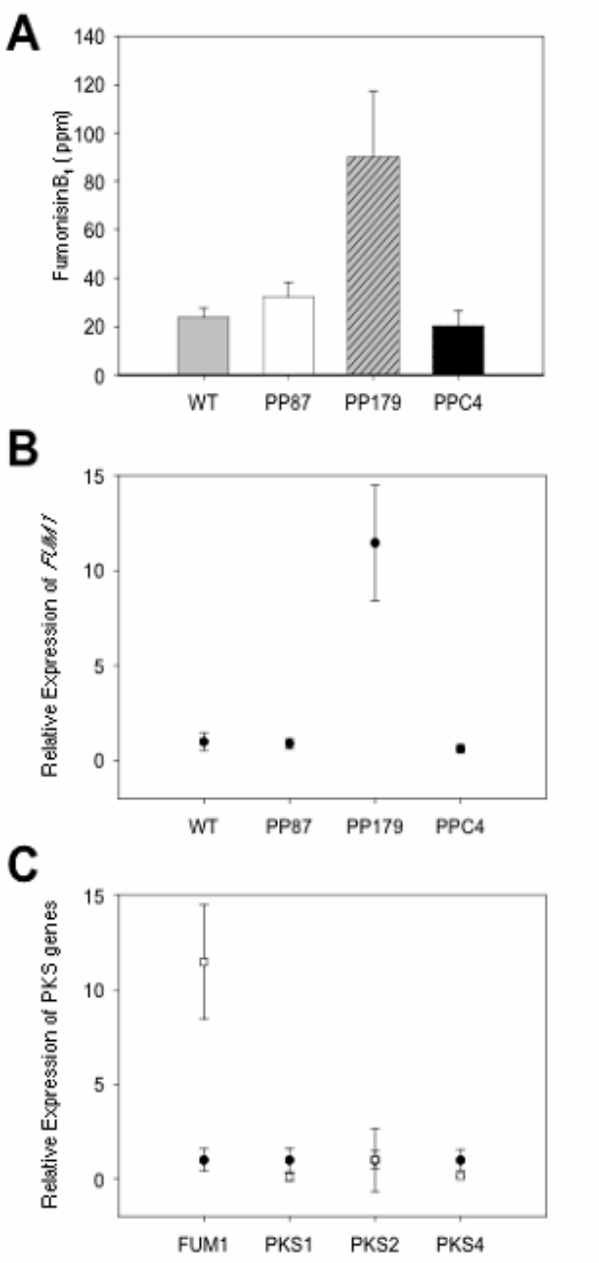
A
Fumonisin B1 (ppm)
140
120
100
80
60
40
20
0
WT
PP87
PP179
PPC4
B
Relative Expression of FUM1
15
10
5
0
WT
PP87
PP179
PPC4
C
Relative Expression of PKS genes
15
10
5
0
FUM1
PKS1
PKS2
PKS4

***CPP1* is required for hyphal polarity maintenance in *F. verticillioides*.** In contrast to wild-type and PP87, PP179 showed a distinguishable hyphal swelling when grown in liquid media (Fig. 2.5A). This phenotype in PP179 became more apparent in the late growth stages (data not shown). Nuclei staining was utilized to investigate whether the hyphal-swelling phenotype in PP179 was linked to defective cell cycle progression. Swollen hyphae of PP179 contained multiple nuclei, whereas nuclei in the wild-type strain were uniformly distributed along hyphae (Fig. 2.5B). This phenotype of PP179 suggested that cell cycle progression was not affected, but maintenance of hyphal polarity was impaired. Notably, suppression of hyphal swelling in PP179 occurred by the addition of sucrose (1 M) to the media (Fig. 2.5C), and this suppression was maintained for up to 10 days. PPC4 showed complete recovery from hyphal swelling demonstrating that this phenotype was due to *CPP1* deletion (Fig. 2.5A).

We next identified well-characterized *S. cerevisiae*, polarity genes *BNI1*, *BUD3*, *BUD6* and *SPA2* (Amberg *et al*., 1997; Chant *et al*., 1995; Sagot *et al*., 2002; Sheu *et al.*, 1998), and tested the transcriptional level of *F. verticillioides* genes homologous to *BNI1*, *BUD3*, *BUD6* and *SPA2* in wild-type and PP179 strains. However, we found no significant difference between wild-type and PP179 in expression levels of these genes (data not shown).

***CPP1* is involved in microconidia-macroconidia equilibrium and conidia germination in *F. verticillioides*.** One striking feature of PP179 was the high percentage of macroconidia production on V8 agar medium. In *F. verticillioides*, the formation of macroconidia has previously been shown under a few select conditions,

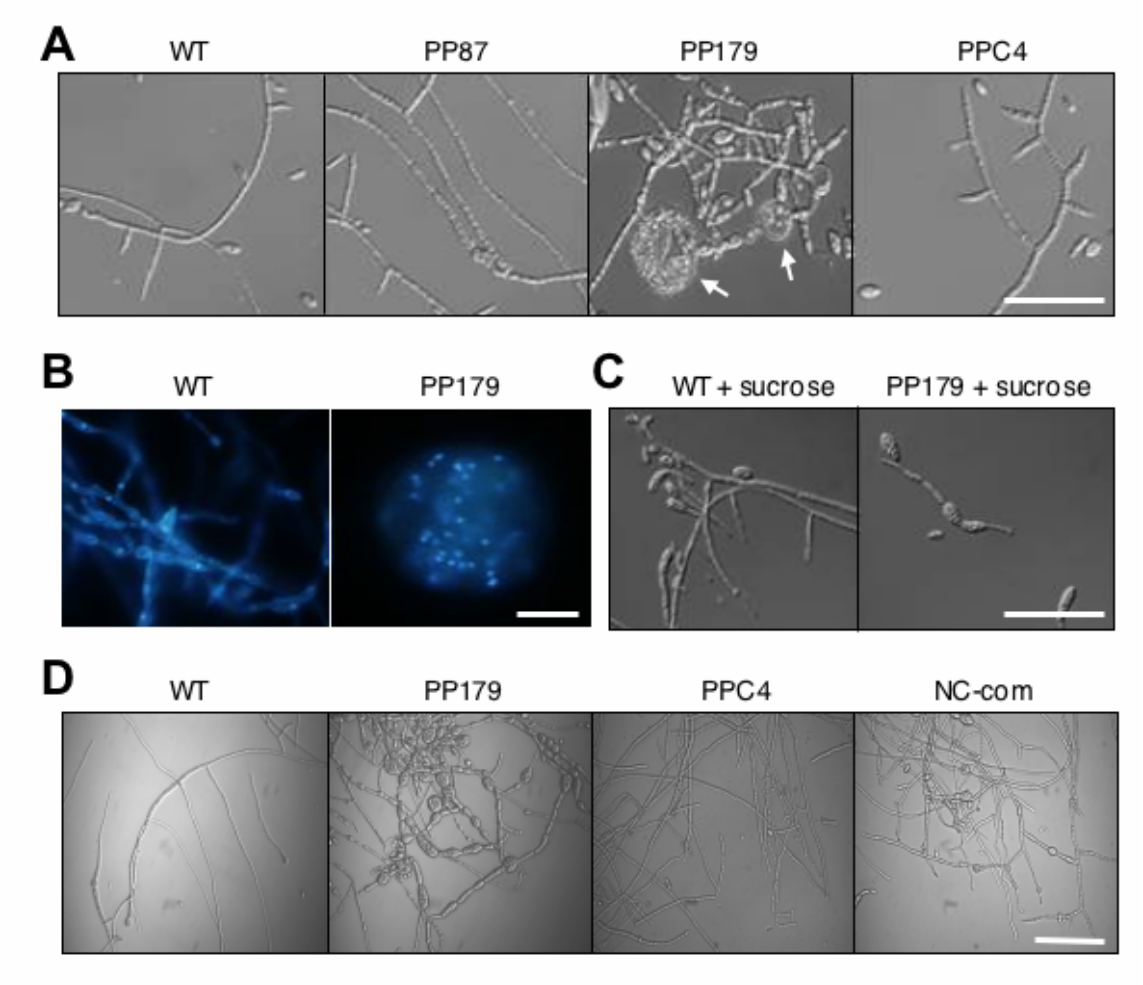

Fig. 2.5
Hyphal swelling phenotype associated with Δ*cpp1* mutation in *F. verticillioides*. **(A)** Each strain was inoculated in DL medium with same amount of conidia (1×10^5 conidia ml^{-1}). After 3 days of incubation, photos were taken under the microscope. The arrows indicate hyphal swelling in PP179. Hyphal-swelling phenotype was restored with YEC4 complementation (PPC4). Scale = 50 μM. **(B)** Nuclei staining was performed with Hoechsts 33258 dye in wild-type and PP179. Multiple nuclei in single swollen hypae were observed in PP179, which was in contrast to uniformly distributed nuclei in the wild-type strain. Scale = 10 μM. **(C)** Suppression of hyphal swelling in PP179 with exogenous sucrose. Sucrose (1 M) supplemented to the DL medium and fungal strains (1×10^5 conidia ml^{-1}) were inoculated. The suppression of swelling in PP179 was maintained throughout the 10-day incubation period. Wild-type and PP179 photos were taken on the 10^{th} day. Scale = 50 μM. **(D)** Fungal strains were grown in DL medium for 14 days. Hyphal swelling phenotypes of PP179 were restored in both PPC4 and NC-com. Scale = 50 μM.

such as UV exposure (Nelson *et al*., 1983). The wild-type and PP87 strains produced microconidia, but not macroconidia on V8 agar. In contrast, approximately 44% of the conidia harvested from PP179 on V8 agar were macroconidia (Fig. 2.6A). The conidiation profile was as wild-type in PPC4. We also observed significant reduction of the conidia-germination rate in PP179. Wild-type and PP87 conidia (1×10^5), when re-suspended in DL medium, successfully germinated after 24-hour incubation (Fig. 2.6B). However, under the same conditions, PP179 germination rate was only 30% of that of wild-type and PP87 strain (Fig. 2.6B). The germination deficiency in PP179 was only partially recovered with the complementation by *CPP1* (Fig. 2.6B).

Complementation of PP179 with *Neurospora crassa ppe-1* results in phenotypic recovery to wild-type *F. verticillioides*. Since PPE-1 of *N. crassa* showed the highest similarity to Cpp1, we hypothesized that PPE-1 and Cpp1 are functionally conserved and that the wild-type *ppe-1* gene could restore the phenotypic characteristics of the PP179 strain. Complementation construct, YEC5 containing wild-type *ppe-1* with 5' and 3' UTR (Fig. 2.1A), was transformed into PP179 protoplasts, and the transformants were selected by geneticin and hygromycin resistance. Isolates were further tested by PCR to demonstrate the presence of wild-type *ppe-1*. No amplicon of *ppe-1* was detected in wild-type and PP179 strains, whereas amplicons of the expected size (1.5kb) was observed in the YEC5-complemented isolates (data not shown). One isolate was selected and designated as NC-com and further analyzed. Interestingly, the complementation of PP179 with YEC5 resulted in restorations of wild-type morphology,

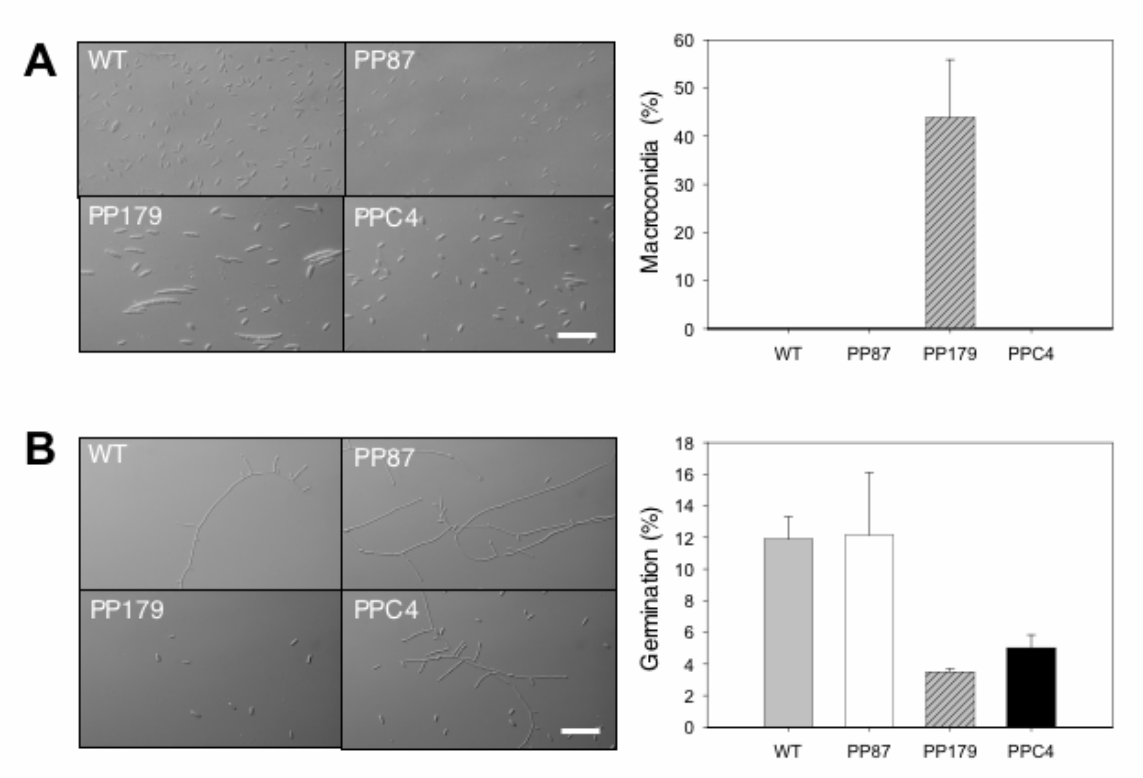

Fig. 2.6
Macroconidia production and conidia germination deficiency in PP179. **(A)** Wild-type (WT) and PP179 strains were spot inoculated with an agar block (0.5 cm in diameter) on a V8 juice agar and incubated for 7 days at 25°C under a 14 h light/10 h dark cycle. Conidia were harvested and quantified with a hemocytometer. The percentage of macrocondia is presented in the figure. Three biological replications were performed to obtain standard deviations. Scale = 50 μM. **(B)** Germination efficiency in the WT, PP87, PP179, and PPC4. Germination of conidia was observed 24 hours after inoculation. The percentage of germination is shown. Three biological replications were performed to obtain standard deviations. Scale = 50 μM.

and the reduced growth rate of PP179 was restored to wild-type level in NC-com (Fig. 2.3). Notably, the hyphal swelling phenotypes of PP179 were less apparent in NC-com (Fig. 2.5D). Macroconidia production by PP179 was completely eliminated in NC-com (data not shown). Elevated FB_1 production in PP179 was significantly reduced in NC-com similar to the wild-type level (data not shown). These results strongly support the hypothesis that *N. crassa* PPE-1 and *F. verticillioides* Cpp1 are functionally conserved across the two species.

DISCUSSION

In eukaryotic cells, reversible protein phosphorylation provides an important means to regulate various cellular functions in response to external signals. While protein kinases take part in phosphorylation, protein phosphatases catalyze the dephosphorylation of proteins, thereby exerting a fundamental role in regulating cellular processes (Dickman & Yarden, 1999). It has been suggested that about one-third of the eukaryotic proteins are regulated by reversible phosphorylations of specific serine, threonine and/or tyrosine residues (Ceulemans & Bollen, 2004). To date, the major group of Ser/Thr protein phosphatases are encompassed by two different structural families. PP1, PP2A, PP2B, and PP5 are classified as members of the PPP family, while PP2C is a member of Mg^{2+}-dependent PPM family (Dickman & Yarden, 1999). Each protein phosphatase has specific or overlapping roles in regards to regulating cellular functions. Despite their central roles in regulating a wide variety of cellular function, including signal transduction and gene expression, limited information is available on the functions of protein phosphatases in filamentous fungi.

F. verticillioides Cpp1 belongs to one of the six major protein phosphatase groups, PP2A. In general, fungi have a larger number of protein kinases than protein phosphatases in their genome. For instance, *S. cerevisiae* has approximately 6,000 genes, of which 113 encode protein kinase genes but only 31 encode protein phosphatases (Dickman & Yarden, 1999; Sakumoto *et al*., 1999; Stark, 1996). Considering the deviation in prevalence between protein kinases and protein phosphatases, it is likely that Cpp1 has broad substrate specificity and interacts with multiple protein kinases in several signaling pathways. Further complicating the process, a 36-kDa PP2A catalytic subunit combines with a 65-kDa regulatory subunit to form a PP2A holoenzyme dimer, with a third variable subunit, known as the B subunit, responsible for substrate specificity (Stark, 1996; Mayer-Jaekel & Hemmings, 1994). Since *CPP1* encodes catalytic subunit of PP2A, the broad specificity of substrates of *CPP1* may be compensated with additional protein phosphatase subunit components. These additional subunits may determine the activity and substrate specificity (Mayer-Jaekel & Hemmings, 1994). In this study, we hypothesized that *CPP1* serves as a putative FB_1 regulatory gene, perhaps in a negative or suppressive manner. Consistent with our hypothesis, we detected elevated FB_1 production in PP179 via TLC and HPLC analyses (Fig. 2.4A), and subsequent QRT-PCR analysis suggested this increased FB_1 production is a result of an elevated *FUM1* expression (Fig. 2.4B). *PKS1* and *PKS2* were classified, along with *FUM1*, as reducing PKSs, whereas *PKS4* resided in a separate group of non-reducing PKSs (Kroken *et al*., 2003). Interestingly, deletion of *CPP1* did not have a drastic effect on the expression of other *PKS* genes, suggesting that the regulatory role of

CPP1 is specific to *FUM* genes and FB_1 biosynthesis (Fig. 2.4C). An expanded transcriptional profiling study is necessary to help us better understand the role of *CPP1* in *F. verticillioides* secondary metabolism pathways.

Multiple PP179 phenotypes suggest that *CPP1* is involved in multiple downstream signaling pathways of *F. verticillioides*. Type 2A protein phosphatases are associated with cell differentiation and development in eukaryotes, including filamentous fungi (Dickman & Yarden, 1999; Hunter, 1995; Mayer-Jaekel & Hemmings, 1994; Shenolikar, 1994). *CPP1* gene deletion in strain PP179 revealed a phenotype of hyphal swelling; thereby indicating the functional role of *CPP1* in morphogenesis. We hypothesized that hyphal swelling in PP179 is caused by random deposition of cell wall components leading to impaired hyphal polarity. In yeast, genes regulating polarity and proper cell development, such as *BNI1*, *BUD3*, *BUD6* and *SPA2,* have been identified (Amberg *et al*., 1997; Chant *et al*., 1995; Sagot *et al*., 2002; Sheu *et al*., 1998). Mutation in these genes could trigger cell-polarity phenotypes. We found that expression levels of *F. verticillioides* genes homologous to *BNI1*, *BUD3*, *BUD6* and *SPA2* were not affected by *Δcpp1* (data not shown). This result suggests that hyphal swelling in PP179 is not due to transcriptional defect in *BNI1*, *BUD3*, *BUD6* and *SPA2* genes and that unknown genes or pathways downstream of *CPP1* are involved in maintaining hyphal polarity and growth. We also investigated whether exogenous application of protein phosphatase inhibitors would induce hyphal swelling in the wild-type strain. We applied okadaic acid, which inhibits preferentially PP2A activity (Kinoshita *et al*., 1993; Yatzkan *et al*., 1998; Shenolikar, 1994; Yatzkan *et al*., 1998), but

did not observe any morphological deficiency in the okadaic acid (up to 400nM)-treated wild-type strain (data not shown).

In *S. cerevisiae*, PP2A related genes were identified and designated as *PPH21*, *PPH22*, *PPH3*, *SIT4*, and *PPG1* (Zabrocki *et al*., 2002). A phylogenic tree containing the well-characterized protein phosphatases in *S. cerevisiae* clearly indicated that Cpp1 has the highest homology with Sit4 (data not shown). Sit4 is a component of the conserved TOR (the target of rapamycin) signaling pathway (Di Como & Arndt, 1996) that interacts with Tap42, the phosphatase regulatory subunit of the TOR pathway, in response to nutrient stress (Cutler *et al*., 2001). Considering the similarity between Sit4 and Cpp1, we hypothesized that hyphal swelling in PP179 may be caused by the defect in nutritional stress response (Fig. 2.5A and 2.5B). The hyphal swelling phenotype in PP179 was particularly apparent in the later stages of growth perhaps when the fungus is under nutritional stress. In contrast, the hyphal swelling could be reversed in PP 179 by osmotic remediation by sucrose (Fig. 2.5C). In *A. nidulans*, protein phosphatase catalytic subunit Sit4 is implicated in the G_1 to S transition (Jiang, 2006), which leads us to presume that growth and germination defects in PP179 are the consequence of defect in cell cycle progression (Fig. 2.3 and 2.6B). In *A. nidulans*, an amino acid change in PP2A protein (PphA) led to a growth defect, lack of germ tube, and mitotic defect (Kosmidou *et al*., 2001). In *N. crassa*, the transcript levels of PP1 gene (*ppp-1*) were increased during hyphal germination and elongation (Zeke *et al*., 2003). We also speculate that the germination defect in PP179 may be linked to hyphal swelling. The

hyphal polarity defect caused by *Δcpp1* may have initially affected germination and later led to hyphal swelling.

A previous report by Yatzkan & Yarden (1999) suggested a link between PP2A regulatory subunit *rgb-1* and macroconidiation in *N. crassa*; inactivation of *rgb-1* led to a failure in the formation of mature macroconidia. In contrast, we observed that macroconidiation was activated in PP179 (Fig. 2.6A). Since macroconidia production occurs rarely in *F. verticillioides* under the laboratory conditions (Nelson *et al*., 1983), it is reasonable to presume that *CPP1* play a role in suppressing macroconidia production in the wild-type strain. Recently, characterization of the *F. verticillioides FvVE1* revealed that deletion of this gene results in macroconidiation and growth defect phenotypes similar to those of PP179 (Li *et al*., 2006). The molecular genetic linkage between *CPP1* and *FvVE1* has not been determined to date.

N. crassa ppe-1 encodes a probable cell shape control protein phosphatase that showed the highest similarity to Cpp1 (E value= 0.0) among the proteins identified in filamentous fungi. PPE-1 and Cpp1 are protein phosphatase 2A catalytic subunits that show 80% identity in amino acid alignments (Fig. 2.2). By complementing PP179 with wild-type *N. crassa ppe-1,* we were able to restore the phenotypic alterations caused by the *cpp1* gene deletion, including the radial growth defect (Fig. 2.3), hyphal swelling (Fig. 2.5D), FB_1 production (data not shown), and macroconidia production (data not shown). Our results provide experimental evidence that that *N. crassa* PPE-1 and *F. verticillioides* Cpp1 are functionally conserved and that Cpp1 is the protein phosphatase 2A catalytic subunit that regulates multiple cellular functions in *F. verticillioides*. Based

on our findings, we anticipate additional proteins, such as additional protein phosphatase subunit components and Cpp1-interacting proteins, are involved in regulating secondary metabolism and fungal development in *F. verticillioides*. Identification and functional characterization of these proteins will help us unravel the complex regulatory mechanisms associated with Cpp1.

CHAPTER III

IDENTIFICATION OF DIFFERENTIALLY EXPRESSED PROTEINS IN WILD-TYPE AND Δ*FCC1* MUTANT STRAINS OF THE MYCOTOXIN-PRODUCING FUNGUS *FUSARIUM VERTICILLIOIDES* BY PROTEOMIC ANALYSIS*

INTRODUCTION

Fusarium verticillioides (Sacc.) Nirenberg (teleomorph *Gibberella moniliformis* Wineland) is a plant pathogenic fungus of maize that produces fumonisins, a group of polyketide-derived mycotoxins, on maize and maize-based products (Munkvold & Desjardins, 1997; Nelson *et al*., 1983). Fumonisin-contaminated food and feeds have been linked to a variety of human and animal illnesses, including leukoencephalomalasia in horses and neural tube defects in humans (Gelderblom *et al*. 1988; Missmer *et al*., 2006). Studies have shown that these toxic effects are due to the fact that fumonisins can inhibit ceramide synthase and ultimately disrupt sphingolipid metabolism in animals (Merrill *et al*., 1996; Tolleson *et al*., 1996). Significantly, a possible link between fumonisin-contaminated food and human illnesses, such as esophageal cancer and neural tube defects, has raised food safety and public health concerns (Missmer *et al*., 2006,

* Reprinted with permission from "Identification of genes associated with fumonisin biosynthesis in *Fusarium verticillioides* via proteomics and quantitative real-time PCR" by Choi, Y. E. & Shim, W. B, 2008b. *J Microbiol Biotechnol*, Copyright [2008] by Journal of Microbiology and Biotechnology. (in press)

Yoshizawa *et al*., 1994). Due to these concerns, a guideline for fumonisin levels in food and feeds was implemented by the US Food and Drug Administration in 2001 (Park & Troxell, 2002). In particular, fumonisin B_1 (FB_1), which is the predominant fumonisin found in nature, has been analyzed and closely monitored in foods and feeds.

While researchers have invested substantial efforts to understand the chemistry, toxicology, and biology of fumonisin since its discovery, current research focus is centered around the molecular mechanism associated with fumonisin biosynthesis in *F. verticillioides.* Proctor *et al* (1999) isolated and characterized *FUM1*, a gene encoding a polyketide synthase in *F. verticillioide*. *FUM1* was the first gene identified in what is now determined as the fumonisin biosynthetic (*FUM*) gene cluster, which contains at least 15 co-regulated genes (Proctor *et al*., 2003). It is interesting to note that a pathway-specific regulatory gene has not been characterized in the *FUM* gene cluster to date and that the regulatory mechanisms involved in fumonisin biosynthesis is considered complex (Sagaram *et al*., 2006b). A number of genes regulating fumonisin biosynthesis have been isolated and characterized but none of these genes are present in the *FUM* gene cluster (Sagaram *et al*., 2006b). Molecular characterization of these regulatory genes demonstrated that these genes are critical for fumonisin biosynthesis in *F. verticillioides* (Flaherty *et al*., 2003; Flaherty & Woloshuk, 2004; Shim & Woloshuk, 2001). In addition, the fact that physiological and nutritional conditions, notably acidic pH and nitrogen stress, favor or perhaps trigger fumonisin biosynthesis suggests that mechanism associated with fumonisin biosynthesis a complex biological process (Flaherty *et al*., 2003; Shim & Woloshuk, 1999).

A variety of molecular genetic approaches including restriction enzyme-mediated integration (REMI) mutagenesis, degenerate PCR cloning, and suppressive subtraction hybridization (SSH) were employed to isolate genes associated with FB_1 regulatory mechanism (Flaherty *et al*., 2003; Shim & Woloshuk, 2001). To date, regulatory genes such as *PAC1, FCC1, ZFR1*, and *GBP1* were identified as genes associated with FB_1 biosynthesis (Flaherty *et al*., 2003; Flaherty & Woloshuk, 2004; Sagaram *et al*., 2006a; Shim & Woloshuk, 2001). In particular, *FCC1* has been identified as a gene regulating early signal transduction events that trigger FB_1 biosynthesis in *F. verticillioides* (Shim & Woloshuk, 2001). To further our understanding of this complex regulatory mechanism, genomics strategies have been applied to accrue more comprehensive information. Pirttilä *et al* (2004) constructed microarrays with expressed sequenced tags (ESTs) from wild-type and the *FCC1* deletion mutant (*Δfcc1*) *F. verticillioides* strains and identified genes that are expressed concomitantly with fumonisin production. The study identified 19 genes displaying expression profiles similar to the *FUM* genes. Furthermore, Brown *et al* (2005) reported generating over 87,000 ESTs from *F. verticillioides*. Analysis of this extensive collection of ESTs, which is estimated to represent over 80% of the expressed genes in the fungus, revealed eight tentative consensus (TC) sequences that are likely to regulate fumonisin biosynthesis. Further functional characterization of these putative regulatory genes will provide additional insight into fumonisin regulation in *F. verticillioides*.

However, while transcriptional profiling is a commonly accepted strategy for identifying genes associated with certain biological processes, it is important not to

discount its limitations. The mRNA levels of a certain gene represent short-term changes in the expression and may influence down-stream gene regulation and ultimately cellular function. One the other hand, mRNA abundance may not be indicative of a gene's regulatory or metabolic potential. In some instances, pathway regulations occur at the post-transcriptional level, and therefore activity of the final gene product, the protein, may provide better evaluation of a gene's functional role. Thus, to complement these approaches and isolate genes with potential involvement in FB_1 biosynthesis, we analyzed the proteomic changes that are due to *Δfcc1* mutation in *F. verticillioides.* Deletion of *FCC1* in *F. verticillioides* resulted in drastic reduction of fumonisin biosynthesis and conidia production in BSAL medium (Shim & Woloshuk, 2001). Also, one of the key reasons we selected the Δ*fcc1* strain for proteome analysis, in comparison with the wild-type strain, is the availability of the gene expression profile in two strains during FB_1 biosynthesis and fungal development (Pirttilä *et al*., 2004).

The objective of this study was to identify proteins that are differentially regulated in either the wild-type genetic background or *Δfcc1* genetic background. Our premise is that these differentially expressed proteins are associated with fumonisin biosynthesis or conidiation in *F. verticillioides*. To perform direct comparative analysis of the gene expression profile versus the proteome profile, we incubated the wild-type and *Δfcc1* strains in the same culture condition, BSAL medium which is conducive to fumonisin biosynthesis, as described previously (Pirttilä *et al*., 2004). We also isolated corresponding gene sequences and investigated their transcriptional profiles via

quantitative real-time PCR in order to identify protein-gene pairs that show concomitant expression patterns during FB_1 biosynthesis.

METHODS

Fungi and culture media. The wild-type *F. verticillioide* strain 7600 (also designated M-3125**,** Fungal Genetics Stock Center, Kansas City, KS) and the fumonisin-deficient mutant *Δfcc1* strain (Shim & Woloshuk, 2001) were stored in 30 % glycerol at -80 ºC. The fungi were grown on V8 agar (200 mL V8 juice, 3 g $CaCO_3$, 20 g agar per liter) for inoculum. For protein and total RNA extraction, the fungal strains were grown in BSAL medium (22mM KH_2PO_4, 2.5mM $MgSO_4$, 85 mM NaCl, 117 mM sucrose, and 1g/L bovine serum albumin) adjusted to pH 6 (Pirtillä *et al*., 2004). A Erlenmyer flask containing 100-ml BSAL medium was inoculated with 1×10^7 conidia and incubated on a rotary shaker (150 rpm) at 24 ºC for 7 days before harvesting fungal tissue. The culture filtrates were analyzed for FB_1 using HPLC (Shim & Woloshuk, 1999).

Proteins sample preparation. Protein extracts were prepared by grinding *F. verticillioides* tissues with grinding buffer (50 mM NaCl, 1% SDS, 10 mM Tris (pH 7.4), and 1 mM EDTA) in liquid nitrogen. The homogenized fungal tissues were centrifuged, and the recovered supernatants were mixed with cracking buffer (3.8 g Tris (pH 6.8), 5 g SDS, 5 ml β-mercaptoethanol, 5 mg Bromophenol Blue, and 50 ml glycerol per liter). The extracted protein suspension was heated at 100 °C for 3 min prior to SDS-Polyacrylamide Gel Electrophoresis (PAGE). Protein concentration was determined by

the Bradford method (Bio-Rad, Hercules, CA). Protein samples (20 mg) were separated in 7.5% and 18% polyacrylamide gels, and subsequently stained with coomassie brilliant blue.

Two-dimensional polyacrylamide gel electrophoresis (2D-PAGE). All the reagents used for 2D-PAGE were analytical grade and purchased from Amersham Pharmacia Biotech Korea Ltd (Seoul, Korea) unless described otherwise. Sequencing grade trypsin and α-cyano-4-hydroxycinamic acid was purchased from Promega (Madison, WI) and Sigma (St. Louis, MO), respectively. Trifluoroacetic acid (TFA) and acetonitrile were purchased from Merck (Piscataway, NJ). The protein sample supernatants were mixed with an equal volume of 20% trichloroacetic acid (TCA), incubated for 30 min on ice, and centrifuged at 16,000 rpm at 4°C for 15 min. The supernatants were carefully removed, and the pellets were mixed with cold acetone (300 ml) and centrifuged for 5 min at 4 °C. The pellet was dried and then resuspended in lysis buffer (7 M urea, 2 M thiourea, 40 mM DTT, 4% CHAPS). 2D-PAGE was performed by vertical electrophoresis, IPGPhor was used for the first dimensional isoelectric focusing with immobiline DryStrip (24 cm, pH 4-7), and the Ettan DALT system was used for the second dimensional SDS-PAGE (11% gel). The protein samples (350 μg) were loaded to the IPG strips (Immobilized pH 4-7 linear gradient) by cup loading with the use of IPGphor (24 cm). Isoelectric focusing was carried out successively at 500V for 1h, 1,000 V for an h, and 8,000 V for 5 h. After isoelectric focusing, strips were incubated with equilibration buffer 1 (50 mM Tris-HCl (pH 8.8), 6 M urea, 30% glycerol, 2% SDS, and BPB, 2% DTT) and buffer 2 (50 mM Tris-Hcl (pH 8.8), 6 M urea, 30% glycerol, 2%

SDS, BPB, 2% DTT, 2.5% iodoacetamide) for 15 min each. The equilibrated strip was placed on a polyacrylamide gradient slab gel (10-15% gradient). Separation was continued at 20 mA/gel in running buffer (25 mM Tris (pH 8.8), 198 mM glycine, and 0.1% SDS) until BPB reached the bottom of gel. The gel was then treated with fixing solution (40% methanol, 10 % acetic acid) for 1 h. After fixing, the gel was treated with rehydration solution (30% ethanol) for 30 min, twice, and with sensitizing solution (0.02% sodium thiosulfate) for 1 min, before washing with deionized water. Subsequently, the gel was treated with $AgNO_3$ solution (0.2% AgNO3, 0.02% HCOH) for 30 min, washed with deionized water, and was incubated with developing solution (3 % sodium carbonate, 0.05% HCOH) for 3-5 min. Finally, stop solution (0.5% glycine) was added.

Image analysis and mass spectrometry (MS). The silver stained gels were scanned with a densitometer 800 (Bio-Rad). Two protein spots that showed similar expression levels in the two gels were identified as control proteins (Fig. 3.1). The digitized image was analyzed using PDQUEST software (V. 6.1, Bio-Rad). Differentially expressed (greater than 5×) proteins were selected for further mass spectrometry analyses. Proteins were identified by MALDI-TOF MS (Jensen *et al*., 1997) and QTOF-MS/MS. Selected protein spots were cut from gels with a spot cutter (Bio-Rad), and the excised gel spots were de-stained with 100 µl of destaining solution (30 mM potassium ferricyanide (Sigma), in 100 mM sodium thiosulfate (Merck)) with shaking for 5 min. After the de-staining, the gel spots were incubated with 200 mM ammonium bicarbonate (Sigma) for 20 min. The gel pieces were dried in a speed

vacuum concentrator for 5 min and then re-hydrated with 20 μl of 50 mM ammonium bicarbonate containing 0.2 μg modified trypsin (Promega) for 45 min on ice. After removal of solution, 30 μl of 50 mM ammonium bicarbonate was added and the digestion was performed overnight at 37 °C. The peptides were desalted and concentrated using C18 nanoscale (porus C18) columns (In2Gen, Seoul, Korea).

For analysis by MALDI-TOF MS (peptide-mass fingerprinting method), the peptides were eluted with 0.8 μl of matrix solution (70 % acetonitrile (Merck), 0.1% TFA (Merck), 10 mg/ml alpha-cyano-4-hydroxycinamic acid (Sigma)), and were spotted onto a stainless steel target plate. Masses of peptides were determined using MALDI-TOF MS (Model M@LDI-R; Micromass, Manchester, UK). Calibration was performed using internal mass of trypsin auto digestion product (m/z 2211.105). For analyses by QTOF-MS/MS, 15 μL of the peptide solutions from the digestion supernatant were diluted with 30 μL 5% formic acid, loaded onto the column, and washed with 30 μL of 5% formic acid. Peptides were eluted with 2 μL methanol/H_2O/formic acid (50/49/1, v/v/v) directly into a pre-coated borosilicate nanoelectrospray needles (EconoTip^{TM}, New Objective, USA). MS/MS of peptides generated by in-gel digestion was performed by nano-ESI on a Q-TOF2 mass spectrometer (Micromass, Manchester, UK). The source temperature was 80 °C. A potential of 1 kV was applied to the precoated borosilicate nanoelectrospray needles in the ion source combined with a nitrogen back-pressure of 0–5 psi to produce a stable flow rate (10–30 nL/min). The mass spectrometer operated in an automatic data-dependent MS/MS to collect ion signals from the eluted peptides. In this mode, the most abundant peptide ion peak with a double- or triple-

charged ion in a full scan mass spectrum (m/z 400–1500) was selected as the precursor ion. Finally, an MS/MS spectrum was recorded to confirm the sequence of the precursor ion using collision-induced dissociation (CID) with a relative collision energy dependant on molecular weight. The cone voltage was 40 V. The quadrupole analyzer was used to select precursor ions for fragmentation in the hexapole collision cell. The collision gas was Ar at a pressure of 6~7 x 10^{-5} mbar and the collision energy was 20–30 V. Product ions were analyzed using an orthogonal TOF analyzer, fitted with a reflector, a micro-channel plate detector and a time-to-digital converter. The data were processed using a Mass Lynx Windows NT PC system.

To identify the protein, protein masses from MALDI-TOF MS were matched with the theoretical molecular weight of peptides for proteins in the NCBI nr database using MASCOT software. Also, all MS/MS spectra recorded on tryptic peptides derived from spot were searched against protein sequences from NCBI nr and the *F. verticillioides* Gene Index (http://compbio.dfci.harvard.edu/tgi/), and the *F. verticillioides* genome database (http://www.broad.mit.edu/annotation/genome /fusarium_verticillioides/Home.html) using the MASCOT search program (www.matrixscience.com).

Expression profiles of genes corresponding to the expressed proteins. Total RNA for QRT-PCR was prepared with Trizol reagent (Invitrogen, Carlsbad, CA) or with RNeasy plant mini kit (Qiagen, Valencia, CA) as per the manufacturers' protocols. All the QRT-PCR reactions were performed in Cepheid Smart Cycler System (Cepheid, Sunnyvale, CA) with QuantiTect SYBR Green RT-PCR kit (Qiagen). All primers used in

this experiment are listed in Table 3.1. Amplification and quantification were performed as described by Sagaram *et al*. (2006a). Briefly, QRT-PCR reactions were carried out with 30 min of reverse transcription at 50ºC followed by 15 min of pre-denaturation at 95ºC and 35 cycles of 15 s of denaturation at 95 ºC, 30 s of annealing at 55ºC and 30 s of extension at 72ºC. All QRT-PCR were technically repeated three times. The gene expression was calibrated using $2^{-\Delta\Delta Ct}$ method (Livak & Schmittgen 2001) with the β-tubulin gene (*TUB2*) (GenBank U27303) expression as a reference. The range of expression was calibrated using $2^{-\Delta\Delta Ct-s}$ - $2^{-\Delta\Delta Ct+s}$ where s is the standard deviation of ΔCt value (Ct=Threshold Cycle).

RESULTS

Computational 2D-PAGE comparison of differentially expressed proteins in the wild-type and *Δfcc1 F. verticillioides* strains. Protein was extracted from 7-day-old *F. verticillioides* wild-type and *Δfcc1* mutant mycelia grown in BSAL, a medium conducive to FB_1 biosynthesis (Shim & Woloshuk, 2001), and were prepared for 2D-PAGE. The protein extracts from three independent biological replications were resolved on 1D SDS-PAGE to visualize a reproducible protein separation pattern before proceeding to 2D-PAGE analysis (data not shown). In addition, HPLC analysis verified FB_1 production in the wild-type culture but not in the *Δfcc1* culture (data not shown).

We selected two biological replications and generated three reproducible 2D-PAGE gels displaying the differentially expressed proteins in two fungal strains per

Table 3.1. Primers used in proteomics

Protein	Forward primer sequence (5' – 3')	Reverse primer sequence (5' – 3')
W3	GGA CTA TCT CCA GGA GAT GAA GAC	GCT CAC AGA CCT TCC AAG C
W4	CCT GTG GAT TGG AAG AAG ACT GG	CCA TAT TTC CAC GAG AAC GGA CC
W10	GAC CTT GCT TCC AGC TGA AGC	CCT TGG TCT TCG AGC TGA GC
W19	CAT CAA GTA CGC CCT CGA G	CAG CCT TGT TGA CGA TCT CC
W20	GTC ACG GCG TGT TGA ATG G	CGA TAT TGG CAC CCT GGT CC
F1	CTG CAC CTT ATG ATG CCA CC	GTG ACG ATC TGA AGC CAG TGG
F8	CTG TCA AGG ACG CTC ACA CTG	CTA CCG TCT TCA TTC TTG CGA ATC G
F10	CTC CCA AGC CTT ACC ATA TTC TAC TC	GCA TCA AAG TTT GCG CCA GC
F11	CTC CTT CGT CTC GTC AAC GG	GAG ATG CTT GAT CAC TCT GCG AC
F15	CGA TTC AAC TCC ACC AAG TCC	GAA CTC CTT GAG CTG AGT CAT GG
F19	GTG CCC CAG TTA ATG ACC TCC	GAC AAG AAC TCT GGC ACT CTG
W1915	GGT ATC AAT GCA CTC CCA ACA ACG TC	CCT CCT CAC TCA TTC TTC CAC C
W3110	CGA TCA CGA ATC AGC GCT C	CCA TAC TTC TCG ACA AGG TTA TAG ACC
W5111	GAG AAG AGC CCC TAT GTC AGC	GTG CTC CAG GGG TGA ATA GC
F148	GCA CCA GAC TTC TCG ATG C	CGA CAA GAT CAA GGC CAA GG
F2719	CAA GGT CGA GGA GAA GAA GTA CG	GCG TTG CAG GAC TTG AGC TC
F5611	GGA CAA GAT CGC TGA TCA GG	CTC GAG AGC CTT CTC GTA GTG
F5906	CCT TAT TGC CAT CTG GGA CGA C	CTG TTT GAT ATC GTC GGC CTT GAG

biological replication (data not shown). Approximately 1,150 protein spots were separated in the pH 4-7 range and their images were digitized and analyzed using PDQUEST software (Fig. 3.1). We performed quantitative comparison of the proteins that are uniquely and differentially regulated in the wild-type and the *Δfcc1* strains. Based on the results from the 2D-PAGE gels, we selected 48 proteins for MS analysis. Twenty of these proteins were expressed only in the wild-type, twenty were expressed only in the *Δfcc1* strain, and eight exhibited a difference (greater than 5×) in expression between the two strains (Fig. 3.2).

Identification of differentially expressed proteins in the wild-type and the *Δfcc1* genetic background and functional classification. A total of forty-eight differentially-expressed proteins were initially analyzed via MALDI-TOF MS. Twenty-nine proteins that did not provide significant database matches were further analyzed via QTOF MS. In the end, thirty-seven out of forty-eight selected proteins resulted in interpretable MS data. Subsequently, the best homologs for each protein were identified via searches against protein sequences from NCBI nr, the *F. verticillioides* Gene Index at the Dana Farber Cancer Institute and the *F. verticillioides* genome database at the Broad Institute using the MASCOT MS/MS Ion Search. The protein sequences were grouped in three categories: proteins expressed only in the wild-type, proteins expressed only in the *Δfcc1* mutant, and proteins differentially expressed in wild-type and *Δfcc1*.

Thirteen proteins that were expressed only in the wild-type strain were identified (Table 3.2). Seven protein spots did not yield informative data due to failed sequencing

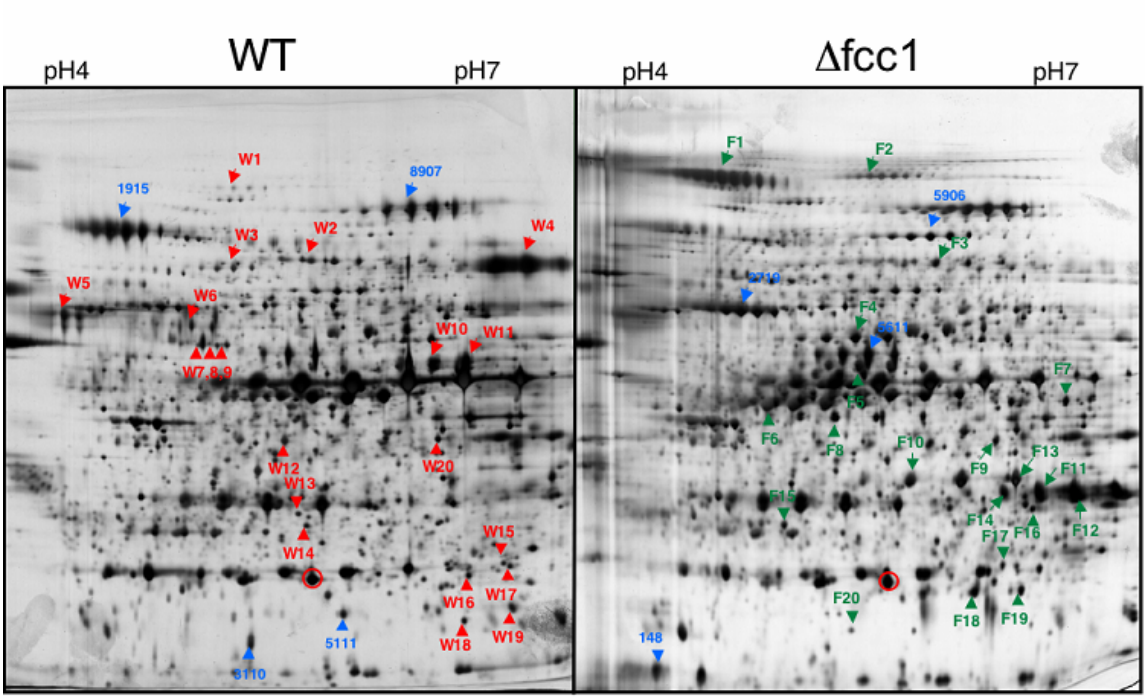

Fig. 3.1
Silver-stained protein expression profile of *F. verticillioides* wild-type and *Δfcc1* mutant strains. Both strains were grown in culture medium conducive to FB_1 biosynthesis for 7 days and total proteins from fungal mycelia were extracted. Protein samples (350 µg) were applied to two-dimensional polyacrylamide gel electrophoresis for separation. Here, a representative figure from three technical and two biological replicates is shown for wild-type and *Δfcc1*. Wild-type specific proteins are labeled with red numbers and arrows in the WT gel. *Δfcc1* mutant specific proteins are labeled with green numbers and arrows in the *Δfcc1* gel. Proteins that are differentially produced in both gels are indicated with blue numbers and lines (solid line indicates up-regulation and dotted line indicates down-regulation).

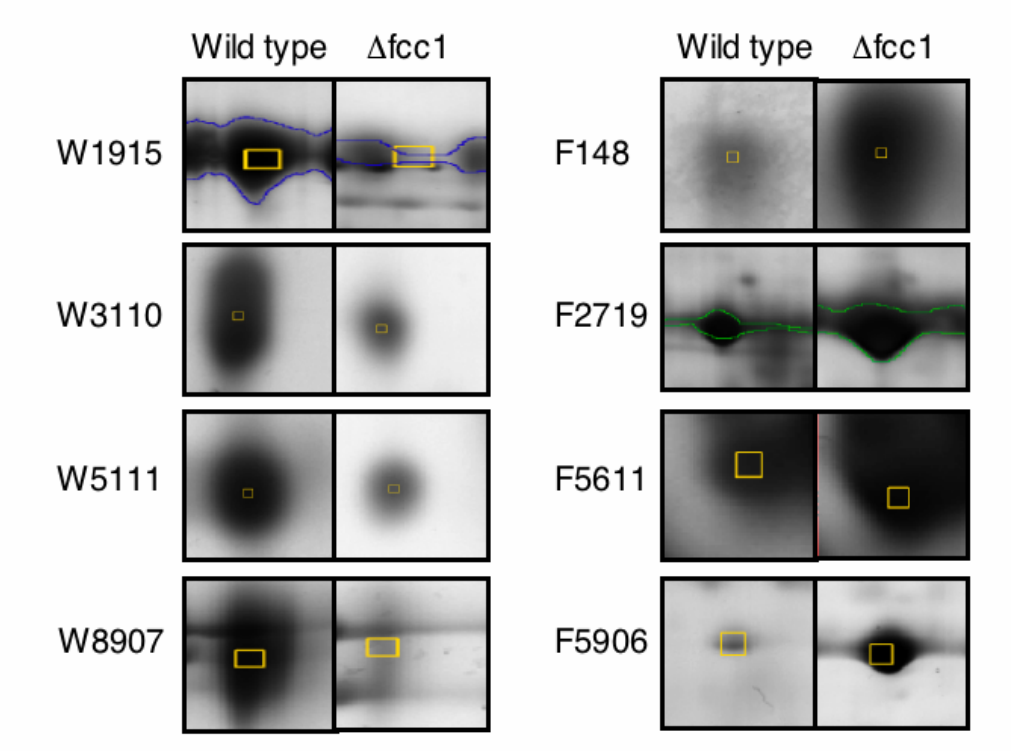

Fig. 3.2
Two-dimentional gel electrophoresis close-up image of differentially expressed proteins in *F. verticillioides* wild-type and Δ*fcc1*mutant strains. Silver stained gel was scanned and the digitized images were compared using PDQUEST software. Proteins that show greater than 5-fold increase were selected. Proteins W1915, W3110, W5111, and W8907 are proteins up-regulated in wild-type strain, and proteins F148, F2719, F5611, and F5906 are proteins up-regulated in Δ*fcc1* strains.

Table 3.2. Proteins uniquely expressed in wild-type protein samples

Spot No.	MS Mascot Method Score[d]	Fv EST or Sequence Fg locus match[a] Coverage[e]	Putative Function	Mol. Mass[c]	pI [c]
W1	Q-TOF	No match			
W2	MALDI 100	FVEG_05069.3 31	pyruvate decarboxylase	63.541	5.60
W3	Q-TOF 208	FVEG_04358.3 30	alpha-glucosidase	36.867	7.46
W4	Q-TOF 79	FVEG_11127.3 32	serine-type carboxypeptidase precursor	27.298	8.66
W5	Q-TOF 39	FVEG_14045.3 3	carboxypeptidase Y precursor	62.181	5.45
W6	Q-TOF 52	FVEG_06027.3 3	putative peptidase	41.789	5.28
W7	MALDI	No match			
W8	MALDI 75	FVEG_11605.3 19	saccharopine dehydrogenase	42.424	5.09
W9	MALDI	No match			
W10	Q-TOF 122	FVEG_12529.3 22	O-acetylhomoserine	28.430	6.21
W11	Q-TOF 122	FVEG_12529.3 22	O-acetylhomoserine	28.430	6.21
W12	MALDI 88	FVEG_04128.3 15	elongation factor 2	91.849	6.45
W13	MALDI 80	FVEG_02960.3 32	proteasome subunit alpha type 6	27.933	5.69
W14	Q-TOF	No sequence			
W15	Q-TOF 69	FVEG_12529.3 9	O-acetylhomoserine	33.636	6.70
W16	Q-TOF	No sequence			
W17	MALDI	No match			
W18	Q-TOF	No sequence			
W19	Q-TOF 33	FVEG_10153.3 7	phosphoglycerate kinase	18.586	6.95
W20	Q-TOF 113	FVEG_03355.3 8	chaperone protein hchA	33.272	5.21

a) Gene locus numbers presented in the BROAD institute (http://www.broad.mit.edu/annotation/genome/fusarium_verticillioides/Home.html)

b) Descriptions of putative function were obtained from *F. verticillioides* Gene Index (http://compbio.dfci.harvard.edu/tgi/) and NCBI (www.ncbi.nlm.nih.gov).

c) Theoretical molecular mass (kDa) and pI were calculated using the ExPASy Compute pI/Mw tool (http://ca.expasy.org/tools/pi_tool.html).

d) Probability Based Mowse Score is -10×Log(P), where P is the probability that the observed match is a random event. Only peptides with individual scores greater than 30, which is indicative of significant homology, are presented in this table.

e) Percent of protein sequence covered by matched peptides.

or lack of a significant match in the database. Of the thirteen proteins that we sequenced, six proteins matched an EST in the *F. verticillioides* Gene Index, while seven other proteins shared highest similarity to *F. verticillioides* auto-annotated genes. We also performed BLASTP analysis against NCBI database to obtain putative function of these genes in *F. verticillioides*. Ironically, when the protein sequences were searched against the NCBI nr database, no protein was suggested to play a direct role in fungal secondary metabolism. However, we did observe a high number of sequences that are associated with protein metabolism. A group of proteins that could be the target of further investigation is peptidases. Peptidases are involved in a variety of cellular functions, including protein turnover, development, and gene signaling (Rao *et al*., 1998).

Table 3.3 describes proteins that are expressed only in the *Δfcc1* strain. Four protein spots did not yield informative data due to failed sequencing or lack of a significant match in the database. Of the sixteen proteins that we obtained sequence from nine peptides matched ESTs in the *F. verticillioides* Gene Index. Seven proteins shared highest similarity to *F. verticillioides* auto-annotated genes. Again, we performed BLASTP analysis against NCBI nr database to obtain putative function of these genes in *F. verticillioides.* Four of the identified proteins play a role in fungal secondary metabolism. Another significant category of proteins listed in Table 3.3 is proteins involved in stress response, such as heat shock protein and superoxide dismutase.

Sequencing results of eight proteins that are differentially expressed, four from the wild-type strain and four from the *Δfcc1* strain, are provided in Table 3.4. Imaging

Table 3.3. Proteins uniquely expressed in *Δfcc1* protein samples

Spot No.	MS Mascot Method Score[d)]	Fv locus match[a)] Sequence Coverage[e)]	Putative Function	Mol. Mass[c)]	pI [c)]
F1	Q-TOF 40	FVEG_12358.3 10	putative laccase	29.359	6.62
F2	MALDI 80	FVEG_10369.3 8	elongation factor 3	116.738	5.58
F3	MALDI 146	FVEG_12776.3 38	pyruvate kinase	59.784	5.81
F4	MALDI 180	FVEG_10153.3 39	phosphoglycerate kinase	44.882	5.91
F5	Q-TOF	No match			
F6	Q-TOF	No match			
F7	Q-TOF 48	FVEG_00289.3 2	reductase or Zn-dependent oxidoreductase	33.824	7.85
F8	MALDI 85	FVEG_01253.3 14	nitrogen metabolite repression-(nmr)-protein	94.215	4.50
F9	MALDI 108	FVEG_09479.3 37	minor allergen Alt a 7	36.328	6.10
F10	Q-TOF 459	FVEG_07201.3 38	oxidoreductase	31.746	6.52
F11	Q-TOF 173	FVEG_10626.3 18	methyltransferase	31.290	6.44
F12	Q-TOF	No sequence			
F13	Q-TOF 41	FVEG_05159.3 9	60S acidic ribosomal protein P0	24.462	5.14
F14	Q-TOF	No sequence			
F15	Q-TOF 69	FVEG_07470.3 4	heat shock protein 90	79.818	4.93
F16	Q-TOF 89	FVEG_00186.3 8	glutathione-S-transferase	28.371	10.76
F17	Q-TOF	No match			
F18	Q-TOF	FVEG_11192.3	superoxide dismutase, mitochondrial precursor		
F19	Q-TOF 43	FVEG_11192.3 8	superoxide dismutase, mitochondrial precursor	22.474	9.06
F20	Q-TOF	No match			

a) Expressed in wild-type protein sGene locus numbers presented in the BROAD institute (http://www.broad.mit.edu/annotation/genome/fusarium_verticillioides/Home.html)

b) Descriptions of putative function were obtained from *F. verticillioides* Gene Index (http://compbio.dfci.harvard.edu/tgi/) and NCBI (www.ncbi.nlm.nih.gov).

c) Theoretical molecular mass (kDa) and pI were calculated using the ExPASy Compute pI/Mw tool (http://ca.expasy.org/tools/pi_tool.html).

d) Probability Based Mowse Score is -10×Log(P), where P is the probability that the observed match is a random event. Only peptides with individual scores greater than 30, which is indicative of significant homology, are presented in this table.

e) Percent of protein sequence covered by matched peptides.

Table 3.4. Proteins differentially expressed in wild-type and *Δfcc1* protein samples

Spot No.	MS Mascot Method Score[d]	Fv EST or Sequence Fg locus match[a] Coverage[e]	Putative Function	Mol. Mass[c]	pI [c]
W1915	Q-TOF 142	FVEG_04402.3 26	serine carboxypeptidase	32.073	6.32
W3110	Q-TOF 302	FVEG_01921.3 54	aminopeptidase	28.010	6.01
W5111	Q-TOF 160	FVEG_12529.3 21	O-acetylhomoserine	28.430	6.21
W8907	Q-TOF	No match			
F148	Q-TOF 55	FVEG_01986.3 16	Probable peroxisomal membrane protein	13.722	7.93
F2719	Q-TOF 76	FVEG_01481.3 27	enolase	47.538	5.01
F5611	MALDI 93	FVEG_00882.3 22	S-adenosylmethionine synthetase 2	44.271	5.71
F5906	MALDI 86	FVEG_02780.3 15	transketolase 1	74.824	5.53

a) Gene locus numbers presented in the BROAD institute (http://www.broad.mit.edu/annotation/genome/fusarium_verticillioides/Home.html)

b) Descriptions of putative function were obtained from *F. verticillioides* Gene Index (http://compbio.dfci.harvard.edu/tgi/) and NCBI (www.ncbi.nlm.nih.gov).

c) Theoretical molecular mass (kDa) and pI were calculated using the ExPASy Compute pI/Mw tool (http://ca.expasy.org/tools/pi_tool.html).

d) Probability Based Mowse Score is -10×Log(P), where P is the probability that the observed match is a random event. Only peptides with individual scores greater than 30, which is indicative of significant homology, are presented in this table.

e) Percent of protein sequence covered by matched peptides

analysis showed that these proteins are expressed at greater than 5× level in either wild-type or *Δfcc1* strain (Fig. 3.2). Only three protein spots from the wild-type strain gave sequence information, and those sequenced all matched significantly to the EST in the *F. verticillioides* Gene Index. All four proteins in the *Δfcc1* mutant were sequenced. One sequence matched the EST in the *F. verticillioides* Gene Index whereas three others shared highest similarity to *F. verticillioides* auto-annotated genes.

Transcriptional profile of genes that correspond to the differentially-expressed proteins. After the identification differentially-expressed proteins, we tested the transcription level of each corresponding gene with QRT-PCR. *F.verticillioides* EST sequences corresponding to the 18 identified proteins were selected for gene expression study. Of the five proteins identified in the wild-type 2DE, only W3 and W4 showed higher transcription levels in the wild-type strain (Table 3.5). Three other sequences (W10, W19, and W20) showed contradictory transcriptional and translational expression patterns. Of the six proteins identified from the *Δfcc1* 2DE, four sequences (F1, F10, F11, and F19) showed higher mRNA and protein expression in the *Δfcc1* strain (Table 3.5). Notably, F10 and F11 showed greater than 100-fold transcriptional up-regulation in the mutant. Genes encoding F8 and F15, on the other hand, showed higher gene expression in the wild-type. When transcriptional patterns of genes corresponding to the differentially-expressed proteins (Table 3.4) were analyzed, we observed that no significant transcriptional-translational correlation is present (Table 3.5). This study demonstrates to us that the level of protein expression in a fungal cell is not directly dependent upon gene expression level.

Table 3.5. Transcription levels of genes corresponding to selected protein spots.[a,c)]

Protein spots	Gene expression in wild-type	Gene expression in *Δfcc1*
W3	1.0 (0.83-1.2)[b)]	0.5 (0.41-0.6)[b]
W4	1.0 (0.9-1.1)	0.23 (0.18-0.29)
W10	1.0 (0.37-2.71)	1.83 (1.71-1.95)
W19	1.0 (0.63-1.58)	1.46 (1.16-1.84)
W20	1.0 (0.23-4.43)	2.26 (1.58-3.25)
F1	1.0 (0.62-1.61)	18.9 (7.57-47)
F8	1.0 (0.78-1.28)	0.58 (0.56-0.62)
F10	1.0 (0.64-1.57)	133.44 (116.97-152.22)
F11	1.0 (0.62-1.61)	7082.29 (5752.61-8719.32)
F15	1.0 (0.72-1.39)	0.8 (0.78-0.83)
F19	1.0 (0.6-1.68)	2.08 (2.03-2.14)
W1915	1.0 (0.69-1.45)	0.08 (0.07-0.09)
W3110	1.0 (0.71-1.41)	0.27 (0.16-0.47)
W5111	1.0 (0.53-1.88)	1.12 (0.81-1.54)
F148	1.0 (0.83-1.2)	0.66 (0.63-0.68)
F2719	1.0 (0.83-1.2)	1.83 (1.5-2.23)
F5611	1.0 (0.52-1.93)	0.48 (0.35-0.68)
F5906	1.0 (0.92-1.09)	0.43 (0.37-0.5)

a) Total RNA samples were prepared from fungal strains grown on BSAL medium (Pirttilä et al., 2004). Quantitative real-time (QRT) - PCR analysis of gene expression was performed with SYBR-Green® as the fluorescent reporter. The expression of each gene was normalized to endogenous β-tubulin (*TUB2*) (GenBank U27303) gene expression.

b) The gene expression was calibrated using $2^{-\Delta\Delta Ct}$ (Livak and Schmittgen, 2001). Data represent the fold differences where gene expression in wild-type is standardized to 1.0. The range of expression was calibrated using $2^{-\Delta\Delta Ct-s}$ - $2^{-\Delta\Delta Ct+s}$ where s is the standard deviation of ΔCt value. Ct=Threshold Cycle.

c) Each value is the mean of three technical replicates from one biological experiment. The experiment was repeated with similar results.

DISCUSSION

The premise of this investigation was that by identifying proteins that are differentially translated in wild-type and *Δfcc1*, we would gain additional molecular genetic information associated with FB_1 biosynthesis and fungal development in *F. verticillioides*. In our study, we were able to obtain corresponding gene sequences of 42 proteins that were differentially expressed (>5 folds) in wild-type and *Δfcc1* strains. Differential expressions of these proteins were verified by two biological replications and three independent technical replications of 2D-PAGE before performing protein spot isolation and subsequent MS analyses. Of the 42 proteins that were sequenced, 16 proteins were unique to the wild-type, 17 were unique to *Δfcc1*, 4 were up-regulated in the wild-type, and 4 were up-regulated in *Δfcc1*. Based on the sequence information retrieved, we categorized the proteins into putative functional groups, e.g., protein metabolism, secondary metabolism, stress response, and signal transduction. Contrary to our anticipation, we did not observe a high number of proteins associated with secondary metabolism in the wild-type. This result is noteworthy since it is in contrast to the transcriptional data obtained in SSH and microarray studies, where a number of *FUM* genes were identified in the wild-type samples (Pirttilä *et al*., 2004; Shim & Woloshuk 2001). A relatively high number of protein sequences that are associated with fungal stress responsiveness were identified in *Δfcc1* strain, and this observation is in agreement with the previous SSH and microarray studies (Pirttilä *et al*., 2004; Shim & Woloshuk, 2001) where a high number of stress responsive genes were

identified in the mutant genetic background. Our results reaffirm the importance of a functional *FCC1* for *F. verticillioides* to cope with ambient environmental stress factors.

In the wild-type strain, proteins with functional role in FB_1 biosynthesis were not identified but rather a relatively high number of proteins known to be associated with protein metabolism. Among the proteins identified in the wild-type strain proteome were protein peptidases (W6, W1915, W3110). Protein peptidases are known to perform a wide variety of cellular functions, such as protein turnover, enzyme modification, and regulation of gene expression (Rao *et al*., 1998). Moreover, recent published reports suggest that post-translational modification of enzymes associated with secondary metabolite biosynthesis may play an important role than previously anticipated (Fujii *et al*., 2004; Liu *et al*., 2006; Yu *et al*., 2005). For example, *Aspergillus fumigatus* protein Ayg1, which contains a serine protease-type hydrolytic motif, is involved in formation of a pentaketide 1,3,6,8-tetrahydroxynaphthalene (T4HN), which is a key precursor of 1,8-dihydroxynaphthalenemelanin, an important virulence factor in pathogenic fungi (Fujii *et al*., 2004). We anticipate that protein peptidases identified in this study may possess proteolytic activities on putative enzymes that influence FB_1 biosynthesis. In addition, proteolytic modification of enzyme precursors may help activate particular functions or enable proper protein-trafficking, which will ultimately contribute to regulating secondary metabolism and cellular development in *F. verticillioides*.

Our proteomic analysis also revealed several interesting genes in the *Δfcc1* strain that are candidates for further investigation. One example is the superoxide dismutase identified in Table 3 (F18, F19). Reactive oxygen species are generated under stress

conditions and in many organisms superoxide dismutase plays an indispensable role in protecting organisms from the reactive oxygen species. The importance of this enzyme in biological systems was clearly demonstrated in a study by Li *et al*. (1995) in which a null mutation of superoxide dismutase in mice led to lethality. It is also reported that Mn^{2+}-containing superoxide dismutase is involved in the protection of *Candida albicans* during the stationaty growth stage when a dramatic burst of reactive oxygen species is known to occur (Lamarre *et al*., 2001). Hence, the up-regulation of the putative superoxide dismutase in *Δfcc1* strain suggests that the mutant is actively responding to internal or external stress. Moreover, reactive oxygen species are known to affect sexual development in *Aspergillus nidulans* (Lara-Ortíz *et al*., 2003), and therefore we can hypothesize that the superoxide dismutase is negatively impacting conidiation in *Δfcc1* strain (Shim & Woloshuk, 2001). Another interesting protein identified in *Δfcc1* proteome is glutathione S-transferase (F16). While glutathione S-transferase is widely used as an enzyme to purify protein of interest, it cellular function is to act as a detoxification enzyme. All eukaryotes possess multiple glutathione S-transferase isozymes, which underscores the importance of this enzyme in cellular detoxification process (Hayes *et al*., 1995). In *A. nidulans*, glutathione S-transferase contributes to resistance against heavy metal and xenobiotic stress (Fraser *et al*., 2002). Perhaps similar to superoxide dismutase, the role of glutathione S-transferase is to relieve endogenous (or exogenous) stress in the Δ*fcc1* mutant. On the other hand, it has been shown in parsley (*Petroselinum crispum*) that glutathione S-transferase is involved in flavonoid production gene signaling (Loyall *et al*., 2000). Further functional characterization is

necessary to verify the role of glutathione S-transferase in *F. verticillioides* secondary metabolism.

Notably, we also identified a protein (F8) that is highly similar to *F. fujikuroi* nitrogen metabolite repression-responsible protein (Table 3.3). Nitrogen metabolite repression is a global regulatory mechanism for the selection of preferred nitrogen source. Significantly, nitrogen metabolite repression and secondary metabolism in filamentous fungi have been closely linked, including fumonisin biosynthesis (Candau *et al*., 1992; Shim & Woloshuk, 1999; Tudzynski *et al*., 1998). While our understanding of how nitrogen metabolite repression impacts fungal secondary metabolism gene signaling pathways in fungi is far from complete, it is reasonable to anticipate that elevated expression of the nitrogen metabolite repression-responsible protein is having a negative impact on FB_1 biosynthesis in *Δfcc1* strain. Also, proteins known to play a role in secondary metabolism, oxidoreductase (F10) and methyltransferase A (F11), were identified in *Δfcc1* strain. Oxidoreductase and methyltransferase are similar to enzymes involved in aflatoxin biosynthesis in *Aspergillus parasiticus* and *A. flavus* (Cary *et al*., 2006; Keller *et al*., 1993). Differential expression of these enzymes is not totally surprising since *F. verticillioides* produce a variety of secondary metabolites other than FB_1, and it can be anticipated that these oxidoreductase and methyltransferase A identified in Δ*fcc1* mutant are involved in synthesizing other secondary metabolites, perhaps pigments or other mycotoxins. Comparative genomic analysis of secondary metabolite gene clusters in *Fusarium* species is in progress to help us associate these enzymes to certain secondary metabolism pathways.

We followed up *in silico* analysis with QRT-PCR to investigate the transcriptional pattern of genes that encode identified proteins. Correlation between transcription and translation is known to be less than 50% (King & Sinha 2001), and we observed a similar trend when we analyzed the transcription levels of identified proteins. Among the 18 proteins selected for the gene expression study, only 8 gene/protein samples (44.4%) showed consistent up-regulation in both mRNA and protein expression. We grouped the proteins into three categories according to gene expression-protein expression pattern: positive correlation, negative correlation, and no significant correlation. While we anticipate that gene-protein pairs that show positive correlation are primary candidates for functional analysis, we can not rule out the possibility that proteins that fall into other categories are associated with *F. verticillioides* secondary metabolism. In other work, we have been generating knock-out mutants of *F. verticillioides* genes discovered via microarray analysis (Pirtillä *et al*., 2004), but a relatively high number of these mutants show no deviation from the phenotype of wild-type progenitor (Choi & Shim, unpublished data). Currently, we are in the process of characterizing the functional role of genes identified in this study to assess their association with FB_1 biosynthesis.

To summarize, we used proteomic approach to elucidate additional genetic information that may have potential roles in fumonisin biosynthesis in *F. verticillioides*. *In silico* analysis suggests that several proteins identified in the 2DE gel may play a role in secondary metabolism and stress responsiveness. Moreover, we followed up the proteomic analysis with QRT-PCR analysis to perform comparative analyses of

transcriptional and translational expression in *F. verticillioides*. To our knowledge, this is first demonstration of utilizing a proteomic approach to isolate novel genes associated with secondary metabolism and development in *F. verticillioides*. Functional characterization of the identified genes/proteins is in progress to further validate of the functional role of the identified genes in *F. verticillioides* secondary metabolism.

CHAPTER IV

GAC1, A GENE ENCODING A PUTATIVE GTPASE-ACTIVATING PROTEIN, REGULATES BIKAVERIN BIOSYNTHESIS IN THE MAIZE PATHOGEN *FUSARIUM VERTICILLIOIDES*

INTRODUCTION

Fungi produce a wide variety of secondary metabolites, which are often complex in chemical structure. Some of the well-characterized fungal secondary metabolites, such as growth regulators, antibiotics, and mycotoxins, are known to impact plant and animal cellular functions (Yu & Keller, 2005). While it is clear that these secondary metabolites are of great importance to mankind, the biological role of vast majority of fungal secondary metabolites is still unknown (Calvo *et al*., 2002; Yu & Keller, 2005). Furthermore, the complex process in which these metabolites are synthesized in fungi is still open to discussion. It is generally perceived that ambient environmental factors, *e.g.* nitrogen, carbon, and pH, trigger secondary metabolism in fungi (reviewed by Sagaram *et al*., 2006b). However, our understanding of fungal secondary metabolism, particularly when coupled with fungal developmental processes, is far from complete.

The ascomycete *Fusarium verticillioides* (Sacc.) Nirenburg (teleomorph *Gibberella moniliformis* Wineland) has been the topic of extensive research because of its production of the mycotoxin fumonisin B_1 (FB_1) on corn. FB_1 is a potent carcinogen,

and ingestion of fumonisin-contaminated corn by humans and animals has been linked to a variety of illnesses, including leukoencephalomalasia and neural tube defects (Gelderblom *et al*., 1988; Marasas, 2001; Minorsky, 2002; Missmer *et al*., 2006). However, secondary metabolites from *F. verticillioides* are not limited to FB_1 and also include a wide variety of the other mycotoxins and pigments (Bacon *et al*., 2004; Nelson *et al*., 1993). Although recent studies have revealed some of the regulatory mechanisms associated with FB_1 biosynthesis, little is known about the biosynthetic processes of other secondary metabolites in *F. verticillioides*.

One of the pigments produced by *F. verticillioides* is bikaverin, which is mainly responsible for the red color that is present in cultures of *Fusarium* species (Linnemannstöns *et al*., 2002). Bikaverin belongs to polyketides with antiprotozoal and antifungal activities (Linnemannstöns *et al*., 2002). Specific conditions, such as nitrogen depletion and acidic pH, are required for bikaverin biosynthesis (Giordano *et al*., 1999). In *Fusarium fujikuroi*, it was found that *PKS4* encodes a polyketide synthase (PKS), a key enzyme necessary for bikaverin biosynthesis, and that *PKS4* is negatively associated with the global nitrogen regulator, *AREA* (Linnemannstöns *et al*., 2002). *F. verticillioides* harbors 15 type-I PKS genes (Kroken *et al*., 2003), one of which is *PKS4* involved in bikaverin production (Proctor *et al*., 2006). However, no further information is available regarding the regulatory mechanism associated with bikaverin biosynthesis in *Fusarium* species.

In this study, we employed REMI (Restriction Enzyme Mediated Integration) to explore the genes associated with *F. verticillioides* secondary metabolism. REMI is an

attractive molecular genetic tool for investigating gene function in filamentous fungi and lower eukaryotes (Kahmann *et al*., 1999; Maier *et al*., 1999). *F. verticillioides*, an ascomycete, spends most of its life cycle with a haploid genome, which makes it feasible for generating null mutants via REMI approach. For example, *FCC1*, one of the key regulatory genes for FB_1 biosynthesis, was initially identified by REMI mutant screenings for altered FB_1 production (Shim & Woloshuk, 2001). Here, we describe the isolation of a mutant strain, R647, which exhibits increased bikaverin biosynthesis. We show that a single gene, designated *GAC1* is responsible for this phenotype. We also demonstrate that transcriptional levels of *AREA* and *PKS4* are positively and negatively affected by *GAC1* mutation, respectively.

METHODS

Fungal strain and culture media. *Fusarium verticillioides* strain 7600 (Fungal Genetics Stock Center, University of Missouri, Kansas City, MO, USA) was stored in 20% glycerin at –80°C. Conidia were produced for inocula by growing the fungus on V8 juice agar (200 ml of V8 juice L^{-1}, 3 g of $CaCO_3$ L^{-1}, and 20 g of agar L^{-1}) at 25°C. For genomic DNA extraction, the fungus was grown in YPD medium (Difco, Detroit, MI, USA) on a rotary shaker (150 rpm). For RNA isolation, the fungus was grown in defined liquid (DL) medium, pH 6.0 (Shim & Woloshuk, 1999). The medium (100 ml) was inoculated with 1×10^5 conidia and incubated at 25°C, shaking at 150 rpm, under a 14 h light/10 h dark cycle. To test for bikaverin production, the fungus was grown on 0.2× potato dextrose agar (PDA) (Difco) (Shim & Woloshuk, 2001). For RNA isolation,

fungal strains were grown on plates filled with 0.2× potato dextrose broth (PBD) (Difco) without shaking.

Nucleic acid isolation and manipulation. Bacterial plasmid DNA and fungal genomic DNA were extracted with the Wizard Miniprep DNA Purification System (Promega, Madison, WI, USA) and the OmniPrep Genomic DNA Extraction Kit (G Biosciences, St. Louis, MO, USA), respectively. Total RNA for qRT-PCR or northern analysis was prepared using Trizol reagent (Invitrogen, Carlsbad, CA, USA) or via the RNeasy Plant Mini Kit (Qiagen, Valencia, CA, USA). Southern and northern analyses were performed as described previously (Sagaram et al. 2006a; Sambrook & Russell 2001). The probes used in all hybridization experiments were ^{32}P-labeled using the Prime-It Random Primer Labeling Kit (Stratagene, La Jolla, CA, USA).

PCR and quantitative real-time (qRT)-PCR. All primers used in this study are listed in Table 4.1. PCR amplifications were performed in a GeneAmp PCR System 9700 thermocycler (PE Applied Biosystems, Norwalk, CT, USA). PCR of DNA (except single-joint PCR) was performed in 25 μL total volumes with *Taq* DNA polymerase (Promega). The PCR conditions were 2 min of pre-denaturation at 94ºC followed by 30 cycles of 45 s denaturation at 94ºC, 45 s annealing at 54-57ºC and 2 min extension at 72ºC, unless specified otherwise. PCR reactions for amplicons larger than 2 kb were performed using Expand Long Polymerase (Roche, Indianapolis, IN, USA) using the manufacturer's suggested protocol.

qRT-PCR analyses were performed in a Cepheid Smart Cycler System (Cepheid, Sunnyvale, CA, USA) with the QuantiTect SYBR Green RT-PCR kit (Qiagen).

Table 4.1. All primers used in REMI

Number	Name	Primer sequence (5' – 3')
1	CSP1-F	GAA TAT ACT TGG CGA TAG CTT CTT GCT C
2	CSP1-R	CAG ATC GCT CAA CTT CTT GAC G
3	ACG1-F	CCC GAC TAC AAT GTC ATT CAT ATA GC
4	ACG1-R	CTA TGC AAA GCC AGA GTT CAC C
5	GAC1-F	GCC GAT TAG CCT CAC TTA GTC AC
6	GAC1-R	GGA AAA ATC GAC GGT GTC AGT G
7	GAC1-NOR-R	CTC CAT GTG ACC AGA GGA CAG
8	TUB2-F	TTCTGGCAAACCATCTCTGG
9	TUB2-R	ATC TGA TCC TCG ACC TCC TT
10	M13-F	TTG TAA AAC GAC GGC CAG TGA
11	M13-R	CAG GAA ACA GCT ATG ACC ATG
12	GAC-com-F1	CAT GGT CAT AGC TGT TTC CTG* CGC TCG ACT CAA TGA CG
13	GAC-com-R1	GTG TAA CGG TGA CCT AAC TTG CTG CTA GTG G
14	Gene-F	GCG AAT TGG AGC TCC ACC GC
15	GAC-com-R2	CAG ATT GTG ATA ACG AGA CGC TGC AGT CTA CC
16	AREA-F	CCA CAG GCG TTA CAC AGT GG
17	AREA-R	CAG CAG AAT GGT TTT GAG CAG C
18	PKS4-F	GCA TCA AGA CTA AGA TCA ACC AGG
19	PKS4-R	GGC AAT GTA TGC TTC GAG AGC
20	TUB2-rt-F	CAG CGT TCC TGA GTT GAC CCA ACA G
21	TUB2-rt-R	CTG GAC GTT GCG CAT CTG ATC CTC G

* M13-R primer sequence for single joint PCR application (Yu *et al*., 2004)

Concentrations of RNA samples were adjusted to 100 ng μl^{-1} prior to qRT-PCR. qRT-PCR amplifications were carried out with 30 min of reverse transcription at 50ºC followed by 15 min of pre-denaturation at 95ºC and 35 cycles of 15 s of denaturation at 95ºC, 30 s of annealing at 55ºC and 30 s of extension at 72ºC. The expression of *F. verticillioides* β-tubulin gene (*TUB2*) (GenBank U27303) was used as a reference.

***F. verticillioides* transformation.** *F. verticillioides* protoplasts were generated using the protocol described by Shim & Woloshuk (2001), except that Mureinase (2 mg per ml) was replaced with Drieselase (5 mg mL^{-1}) (Sigma, St. Louis, MO, USA). Mutations were performed using Restriction Enzyme Mediated Integration (REMI). The pBP15 vector, which contains a hygromycin phosphotransferase (*HPH*) gene as a selectable marker (Fig. 1A), was used for REMI screenings (Fig. 4.1A). The pBP15 vector was linearized with *Hind*III, prior to protoplast transformation. Hygromycin-resistant transformants were selected on regeneration agar medium amended with hygromycin (150 μg mL^{-1}) and screened for increased red pigment. For Southern analysis, fungal genomic DNA samples were digested with *Eco*RV before being subjected to electrophoresis in a 1% agarose gel. A 2-kb DNA fragment of the pBP15 vector, amplified by M-13 forward and reverse primers, was ^{32}P-labelled as a probe (Fig. 4.1A).

To identify the integration locus of pBP15, genomic DNA of REMI isolate R647 was extracted and digested with *Eco*RI. Subsequently, self-ligation reactions were performed and cloned into Top10 chemically competent cells (Invitrogen). Sequences

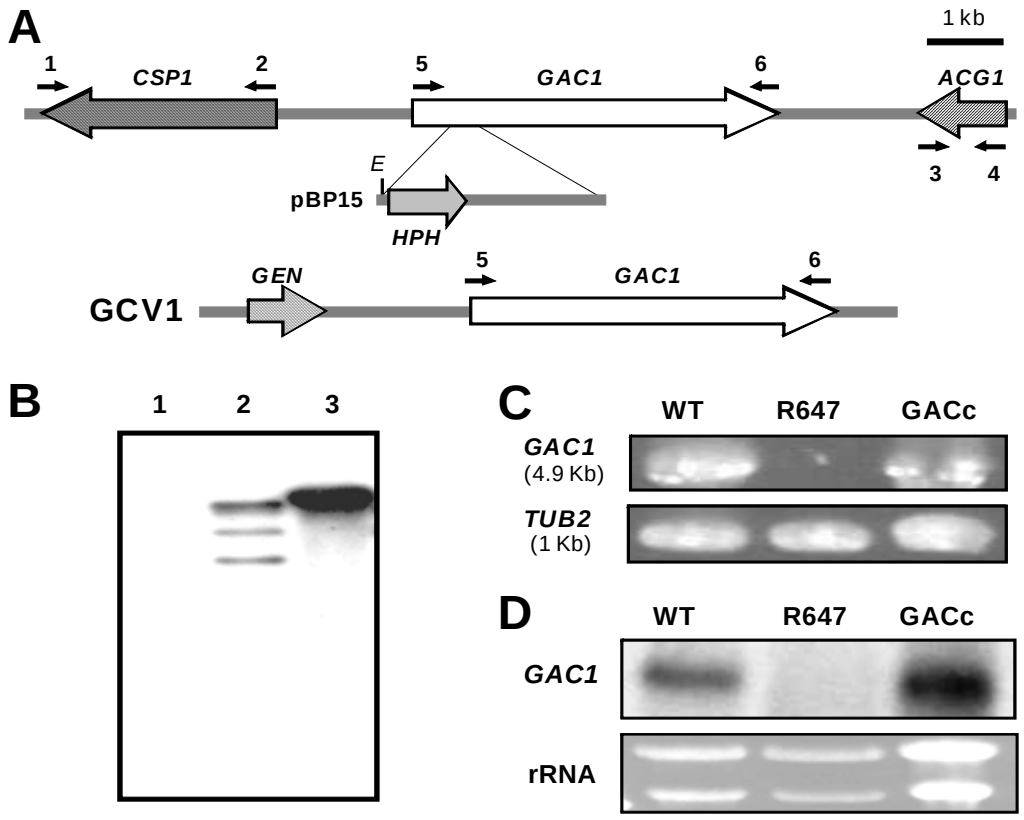

Fig. 4.1
Identification of REMI locus **(A)** Schematic representation of *GAC1* locus in the wild-type strain. Flanking genes of *GAC1* are *CSP1* and *ACG1*. In REMI strain, R647, pBP15 vector is integrated in *GAC1* locus. REMI vector, pBP15 harbors hygromycin phosphotranferase gene (*HPH*) as the selectable marker. GCV1 is the construct with *GAC1* wild-type gene fused to the geneticin-resistance gene (*GEN*) that was used to complement R647. The numbered arrows indicate the location of primers used for PCR assays of each gene (Table 4.1). The double arrow on pBP15 indicates the fragment used as ^{32}P-labeled probe in Southern blot. **(B)** Southern blot analysis of R647. Fungal genomic DNA was digested with *Eco*RV, and the blot was hybridized with ^{32}P-labeled DNA probe (shown in Fig. 4. 1A). (C) PCR analysis of *GAC1* using gene specific primers (5&6) described in Fig. 4.1A. WT: wild-type, R647: REMI strain, GACc: GCV1-complemented strain. As a control, we did PCR analysis with β-tubulin gene (*TUB2*). The amplified genes and sizes were shown on the left. (D) Northern blot analysis of the transformants probed with ^{32}P-labeled DNA fragment of *GAC1* to determine the expression of *GAC1*. Total RNA samples (15 μg) were subjected to electrophoresis in a 1.2% denaturing agarose gel. The gel was stained with ethidium bromide to confirm uniformity of loading (rRNA).

were retrieved with M-13 forward and reverse primers. DNA sequencing was performed at Gene Technologies Lab, Texas A&M University (College Station, TX, USA).

REMI isolates R647 was complemented with a wild-type *GAC1* gene fused to a geneticin-resistance gene (*GEN*). The complementation vector, GCV1 was made via a single-joint PCR strategy (Sagaram *et al*., 2006a; Yu *et al.*, 2004). For GCV1, primers GAC-com-F1 and GAC-com-R1 were used to amplify full-length *GAC1* plus a 1.17-kb 5' untranslated region (UTR) and a 640-bp 3' UTR. The *GEN* marker was prepared as described previously (Sagaram *et al*., 2006a). Subsequently, the amplicons were mixed in a single tube and were joined by PCR. The final GCV1 construct was amplified with primers Gene-F and GAC-com-R2 using Expand Long Polymerase (Roche). We then transformed GCV1 into R647 protoplasts, and screened for colonies resistant to geneticin and hygromycin (Sagaram *et al*., 2006a). The introduction of GCV1 in geneticin-resistant strains was verified by PCR analyses. Northern analysis was also used for verifying *GAC1* mutation and complementation. A 280-bp *GAC1* DNA fragment probe was amplified with primers (GAC1-F & GAC1-NOR-R) and ^{32}P-labeled for northern hybridization.

Fumonisin B_1 and bikaverin analysis. For fumonisin production analysis, *F. verticillioides* strains were grown in cracked-corn medium for 10 days. Fumonisin B_1 (FB_1), the major fumonisin produced by *F. verticillioides*, was extracted and analyzed by HPLC following the method described by Shim & Woloshuk (1999). Bikaverin was extracted from total mycelium grown on 0.2× PDA for 14 days following the suggested

protocol (Chávez-Parga *et al*., 2005; Giodano *et al*., 1999) and analyzed by UV-visible spectrophotometer (Agilent 8453) at 518 nm (Giodano *et al*., 1999).

qRT -PCR was used to investigate the relative expression of *PKS4* and *AREA* in the wild-type, R647, and GACc strains. Total RNA samples were prepared from wild-type, R647, and GACc grown on plates filled with 0.2× PDB. qRT - PCR analysis was performed with SYBR-Green® as the fluorescent reporter using gene specific primers for *PKS4* (PKS4-F and PKS4-R) and *AREA* genes (AREA-F and AREA-R). The expression of each gene was normalized to endogenous *TUB2* gene expression by using *TUB2* gene specific primers (TUB2-rt-F and TUB2-rt-R). The gene expression was calibrated using $2^{-\Delta\Delta Ct}$ method (Livak & Schmittgen 2001); the range of expression was calibrated using $2^{-\Delta\Delta Ct-s}$ - $2^{-\Delta\Delta Ct+s}$, where s is the standard deviation of ΔCt value (Ct=Threshold Cycle).

Visual anlysis of bikaverin production. To test bikaverin production under various conditions, we prepared agar plates with various nutrients and different pHs. Bikaverin production was tested using 0.2× PDA with pH 7.0 or 10.0. Agar plates with different nutrient components were made by supplementing water agar with either sucrose, glucose, ammonium acetate, $NaNO_3$, ethanol, or methanol at suggested concentrations. *F. verticillioides* was point inoculated with an agar block (0.5 cm in diameter) on the various plates and incubated for 7 days at 25°C under a 14 h light/10 h dark cycle.

RESULTS

Isolation of REMI mutant strain R647 in *F. verticillioides*. We generated over 2,000 *F. verticillioides* REMI mutants with the goal of studying fungal secondary metabolism and virulence, namely FB_1 production, maize stalk rot and ear rot pathogenicity. During the screening process, we identified a strain, designated R647, which showed a drastic increase in red pigment production on 0.2×PDA plates. The pigment production on 0.2×PDA by R647 became evident 4 days post-inoculation, whereas the wild-type progenitor showed lack of any pigment. This phenotype became more apparent after 14 days (Fig. 4.2A). We further analyzed R647 for additional phenotypes aberrant from the wild-type strain, namely conidiation, hyphal development, FB_1 production, and maize pathogenicity. However, we did not observe any significant differences in these characteristics between the wild-type and R647 (data not shown). We did observe a slight growth reduction, approximately 12%, on agar plates when we compared wild-type and R647 (Fig. 4.2C).

Identification of REMI locus, *GAC1* encoding a GTPase activating protein. To confirm that the REMI event in R647 occurred at a single locus, we performed Southern blot analysis using the hygromycin phosphotransferase (*HPH*) gene as a probe (Fig. 4.1A). The *HPH* probe did not hybridized to the wild-type genomic DNA whereas a single band was detected in R647 genomic DNA (Fig. 4.1B). This blot demonstrates that a single copy of the pBP15 vector was inserted into the wild-type genome, suggesting that a mutation in a single locus is responsible for R647 phenotype.

Fig. 4.2
Pigmentation and morphology in R647 **(A)** Colony morphology and pigmentation of the wild-type, R647, and GACc grown on 0.2×PDA and V8 agar plates. Wild-type, R647, and GACc were point inoculated with an agar block (0.5 cm in diameter) and incubated for 14 days at 25°C under a 14 h light/10 h dark cycle. **(B)** Radial growth on 0.2xPDA (Fig. 4.2A) was measured and presented as a bar graph. Results are means of three biological replications. **(C)** Quantification of bikaverin production in wild-type, R647, and GACc grown on 0.2×PDA (Fig. 4.2A). Bikaverin was extracted from total mycelium on 0.2x PDA with 5 ml of chloroform and quantified with molecular extinction coefficient (log ε=3.95) at 518 nm (Giodano *et al*. 1999). Results are means of three biological replications.

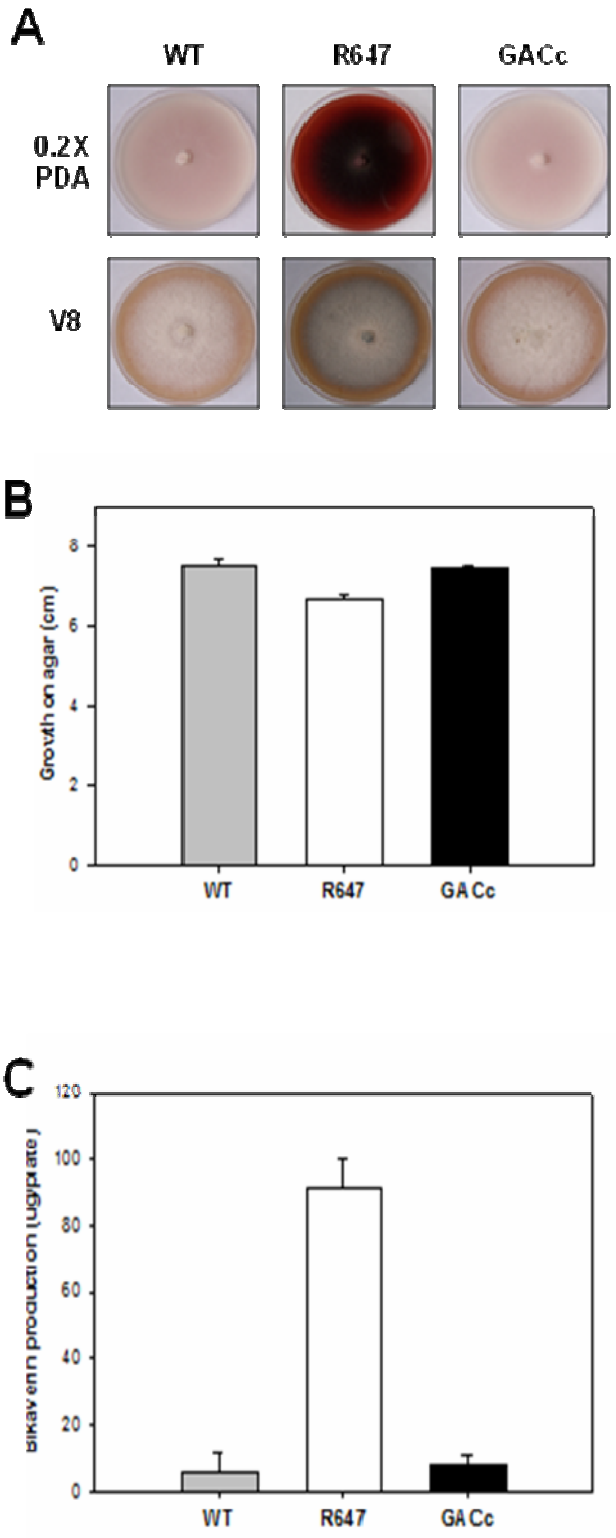
A
WT
R647
GACc
0.2X PDA
V8
B
Growth on agar (cm)
0
2
4
6
8
WT
R647
GACc
C
0
20
40
60
80
100
120
WT
R647
GACc

Subsequently, we recovered the DNA flanking the site of pBP15 integration in R647 by standard plasmid rescue technique (Shim *et al*., 2006). The genomic DNA of R647 was digested with *Eco*RI, self-ligated, and transformed into *E. coli*. The rescued plasmid containing the entire pBP15 vector and flanking *F. verticillioides* DNA was sequenced for the identification of the disrupted locus. A 70-bp DNA sequence was used to search the matching genomic DNA sequence in *F. verticillioides* (The *Fusarium Group* Database, Broad Institute of Harvard and MIT, http://www.broad.mit.edu/annotation/genome/fusarium_group). The search revealed that the 70-bp DNA sequence matched perfectly to sequence 714,918 to 714,988 in supercontig 10. This sequence was a part of a 4.9-kb open reading frame (ORF) encoding a putative GTPase activating protein. We designated this gene *GAC1*. Blast searches revealed that *GAC1* shares significant similarities with the putative GTPase activating protein in *Neosartorya fischeri* (E value= 0.0), *Aspergillus fumigatus* (E value= 0.0), and in *Candida albicans* (E value= 9e-95).

Next, we tested whether the REMI event also affected genes flanking *GAC1*. To do so, genes that flank *GAC1* in the *F. verticillioides* genome were identified in the *Fusarium Group* Database. A 3.2-kb gene encoding a putative chromosome segregation protein (supercontig 10, sequence 709,281 to 712,522) and a 1.2-kb gene encoding a putative beta-N-acetylglucosaminidase (supercontig 10, sequence 721,246 to 722,474) were identified, and were designated *CSP1* and *ACG1*, respectively (Fig. 4.1A). PCR analyses were carried out to determine whether these genes were affected by the REMI event. In wild-type and R647 strains, PCR with primers specific for *CSP1* and *ACG1*

resulted in expected amplicons for *CSP1* and *ACG1* (data not shown). However, no PCR product was observed in R647 when the reaction condition was optimized to amplify 4.9-kb *GAC1* amplicon, suggesting that *GAC1* was affected by the insertion of pBP15 in R647 (Fig. 4.1C). As a control, we amplified the β-tubulin gene (*TUB2*) and obtained the expected amplicons in both the wild-type and R647 (Fig. 4.1C).

Complementation analysis of *GAC1* in R647. Southern blot and PCR analyses showed that *GAC1* locus was disrupted by the insertion of pBP15. Consequently, northern blot analysis was performed using a 280-bp *GAC1* DNA fragment probe, which hybridized to the expected 5-kb transcript band in the wild-type but did not in R647 (Fig. 4.1D). The study confirmed that expression of *GAC1* was drastically suppressed by the REMI mutation. To further verify that the phenotypes exhibited by R647 was due to REMI mutation, we transformed R647 with vector GCV1, which contains an intact copy of the *GAC1* gene fused to *GEN* (Fig. 4.1A). Following the transformation, the complemented strains were selected by growth on 0.2× PDA containing hygromycin and geneticin. The putative complemented strain containing GCV1 was designated as GACc. We determined via PCR that GACc contained the introduced *GAC1* gene (Fig. 4.1C). Northern analysis also showed that expression of *GAC1* was restored in GACc (Fig. 4.1D). We then tested whether the R647 phenotypes were restored in GACc. The presence of *GAC1* completely restored R647 pigmentation levels to those of the wild-type (Fig. 4.2A). Likewise, GACc growth on agar plates was at wild-type levels (Fig. 4. 2B). Therefore, we concluded that the mutation of *GAC1* was responsible for the increased pigmentation and the growth reduction on agar plates in R647.

Identification of bikaverin and its production pattern on various agar plates. During the course of this study, the nature of the red pigment produced by R647 was ambiguous. Review of literature strongly suggested that the metabolite is likely bikaverin, which is the major red pigment produced by a variety of *Fusarium* species in culture (Linnemannstöns *et al*., 2002). We followed the extraction protocol specifically designed for bikaverin (Chávez-Parga *et al*., 2005; Giodano *et al*., 1999), and measured the concentration of bikaverin following the protocol described previously (Chávez-Parga *et al*., 2005; Giodano *et al*., 1999). We observed more than a 15-fold increase in bikaverin production in R647 culture when compared to that of the wild-type progenitor, and this increased was completely reverted to the wild-type level in GACc culture (Fig. 4.2C). This result suggests that the red pigment that is overproduced in R647 is bikaverin.

Next, we tested whether conditions known to enhance bikaverin production, such as lower pH and nitrogen stress, affect the overproduction of bikaverin in R647. Under higher pH conditions, bikaverin biosynthesis was inhibited in the wild-type and GACc strains, whereas no significant difference was observed in R647 (data not shown). We also tested the impact of different carbon or nitrogen sources on R647 bikaverin production. Interestingly, the presence of readily usable nitrogen sources, such as ammonium or nitrate, completely suppressed bikaverin production in the wild-type, GACc, and R647 strains (Fig. 4.3), suggesting that bikaverin biosynthetic mechanism is under nitrogen catabolite repression. Consequently, we argue that *AREA*, the global

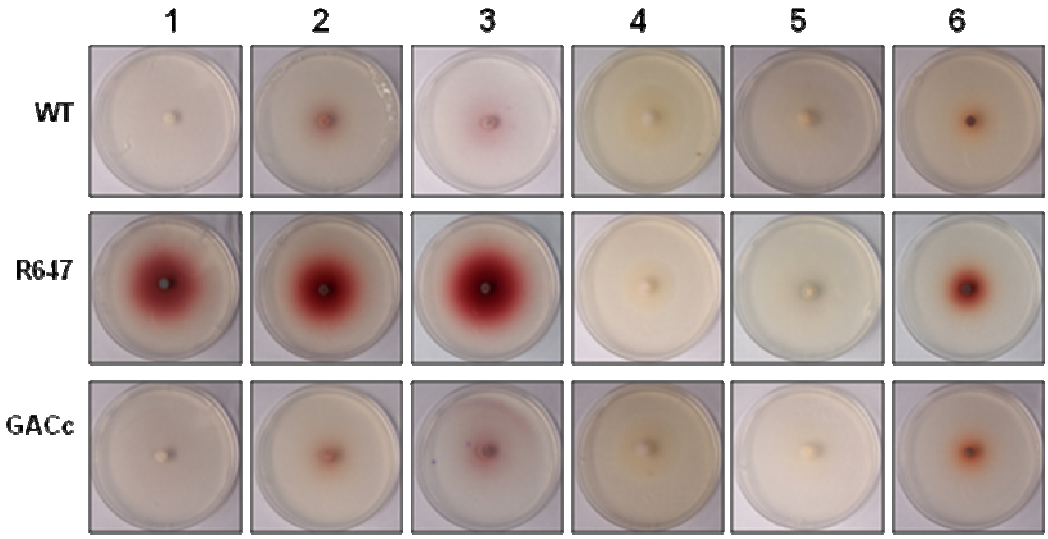

Fig. 4.3
Bikaverin production on a variety of agar plates. Wild-type, R647, and GACc were point inoculated with an agar block (0.5 cm in diameter) and incubated for 7 days at 25°C under a 14 h light/10 h dark cycle. All agar plates were made on the basis of water agars and added the suggested concentration of components 1: sucrose 0.01M, 2: sucrose 0.1M, 3: Glucose 0.1M, 4: $NH_4C_2H_3O_2$ 0.1M, 5: $NaNO_3$ 0.1M, 6: Ethanol 15ml/50ml.

nitrogen regulator is downstream of *GAC1*. Moreover, *PKS4* responsible for bikaverin biosynthesis is downstream of *AREA* in *F. fujikuroi* (Linnemannstöns *et al*., 2002).

***AREA* and *PKS4* are regulated *GAC1 in F. verticillioides*.** We investigated the impact of a *GAC1* mutation on the expression of *AREA* and *PKS4* genes using qRT-PCR analysis. Total RNA samples were prepared from fungal mycelia of wild-type, R647, and GACc strains grown in 0.2× PBD without agitation. qRT-PCR analysis revealed that *AREA* expression was two-fold down-regulated, whereas *PKS4* expression was up-regulated significantly in R647, compared to those of wild-type and GACc (Fig. 4.4). Analysis also showed that *GAC1* complementation restored *AREA* and *PKS4* expressions to the wild-type levels. Our data provide molecular evidence that *AREA* and *PKS4* are downstream genes of *GAC1* and they are under positive and negative regulation, respectively, by *GAC1* in *F. verticillioides*.

DISCUSSION

Bikaverin is a cyclic polyketide rendering deep red hues from the culture of *Fusarium* species and has been recognized as an undesirable byproduct of gibberellin production in *Fusarium fujikuroi* (Giordano *et al*., 1999; Linnemannstöns *et al*., 2002) as well as a fungal metabolite with anti-protozoal and antifungal activities (Linnemannstöns *et al*., 2002). Its biosynthesis requires a polyketide synthase (PKS)

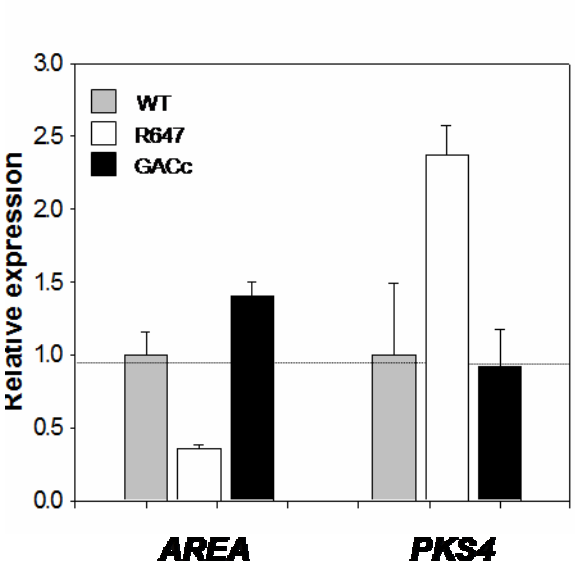

Fig. 4.4
Expression of *AREA* and *PKS4* genes in wild-type, R647, and GACc strains. Total RNA samples were prepared from fungal strains grown on 0.2x potato dextrose broth (BD) for 14 days, and quantitative real-time (qRT) - PCR analysis was performed with SYBR-Green® as the fluorescent reporter. The levels of transcription were evaluated using the $^{2-\Delta\Delta C_T}$ method with *TUB2* as endogenous control. Data represent the fold differences in gene expression. Three biological replications were performed to obtain standard deviations.

and, in *F. fujikuroi* and *F. verticillioides*, *PKS4* has been characterized as the PKS required for bikaverin production (Linnemannstöns *et al*., 2002; Proctor *et al*., 2006). However, little additional information is available on bikaverin biosynthesis, particularly the gene signaling pathways that control regulation of this secondary metabolite production.

The REMI mutagenesis study was aimed at identifying genes responsible for secondary metabolism and virulence in *F. verticillioides*. Unexpectedly, in this study we identified *GAC1*, which encodes a GTPase activating protein (GAP), that is not associated with fumonisin biosynthesis nor fungal virulence but with bikaverin biosynthesis. Investigation of R647 phenotypes suggested that *GAC1* is negatively associated with bikaverin biosynthesis. A database search using Gac1 protein sequence indicated that Gac1 is likely a Ran-GAP, which regulates Ran GTPase (Avis & Clarke, 1996). Ran-GTPase is involved in trafficking of proteins in or out of the nucleus by acting on GTP (Avis & Clarke, 1996). Ran-GAP takes part in turning off Ran-GTPase by hydrolysis of GTP, leading to transport of proteins from the nucleus to the cytosol. The counterpart of GAP is guanine nucleotide exchange factor (GEF), which turns on the G-protein again by making a GTP-bound form of the G proteins, and thereby it allows protein transport into nucleus (Avis & Clarke, 1996). We can speculate that the disruption of *GAC1* may have resulted in an imbalance of GAP and GEF, giving rise to increased GEF activity, and ultimately constitutive activations of yet-to-be determined G protein that led to over-production of bikaverin in *F. verticillioides*.

Further investigation is necessary to unambiguously determine the G-protein signaling pathway that directly regulates bikaverin biosynthesis.

While the questions regarding the G-protein directly downstream of Gac1 remain, we investigated other molecular and physiological factors are known to impact bikaverin production in *Fusarium* species, and how these factors are associated with each other. In *F. fujikuroi*, it has been demonstrated that the expression of *PKS4* is affected by the global nitrogen regulator *AREA*. Accordingly, we observed that the presence of ammonia or nitrate completely inhibited bikaverin production in the *GAC1* mutant strain, R647 (Fig. 4.3A). Based on these findings, we postulated that *AREA* and *PKS4* are downstream of *GAC1*, and to test our hypothesis we analyzed the expression levels of *AREA* and *PKS4* in R647 (Fig. 4.3B). Our data showed that *GAC1* mutation had a negative effect on *AREA* expression, which strongly suggests that *GAC1* is upstream of *AREA* in bikaverin regulatory pathway. This repression of *AREA* resulted in over-expression of *PKS4* in R647, suggesting that *AREA* plays a negative regulator role in bikaverin biosynthesis. However, the fact that *PKS4* is under negative regulation by *AREA* was not a surprise. Linnemannstöns *et al* (2002) previously suggested a model explaining how *AREA* and *PKS4* impact bikaverin biosynthesis in *F. fujikuroi*. In this model, it was postulated that *AREA* is directly interacting with an unidentified bikaverin specific repressor under nitrogen-rich conditions, which, in turn, could repress *PKS4* expression.

Another factor that is known to affect bikaverin production is pH, particularly acidic pH which is known to trigger bikaverin biosynthesis (Giordano *et al*., 1999).

However, when we observed R647 under different pH conditions, we did not see a difference in bikaverin production (data not shown). When wild-type *F. verticillioides* was grown on alkalic agar media, we did see a slight decrease in bikaverin production. Subsequently, we questioned whether *GAC1*-mediated bikaverin biosynthesis in *F. verticillioides* is controlled by a key pH regulator gene, *PAC1*. *PAC1,* homologous to *PACC* in *Aspergillus nidulans*, is activated under alkaline conditions repressing genes that require acidic conditions (Flaherty *et al*., 2003; Orejas *et al*., 1995). As anticipated, the mutation in *GAC1* did not affect *PAC1*, and therefore we concluded that the pH response pathway(s) in *F. verticillioides* are not associated with *GAC1*-mediated bikaverin biosynthesis.

In summary, using a REMI approach, we identified *F. verticillioides GAC1* gene, which encodes a GTPase activating protein, and demonstrated that *GAC1* is negatively associated with bikaverin production. Transcription levels of *AREA* and *PKS4* are under the control of *GAC1* positively and negatively, respectively. *GAC1* is also necessary for proper growth, as was indicated by a reduction of the growth rate in the *GAC1* mutant. Currently, our lack of knowledge of *F. verticillioides* gene network hinders us from unambiguously characterizing *GAC1*-mediated bikaverin biosynthesis regulatory mechanism. Here, we can conclude that *GAC1*, *AREA*, and *PKS4* play critical roles in bikaverin production. However, there is no doubt that additional genes, *e.g*. G proteins, are involved in this signaling pathway, and currently functional genomic tools, such as microarray and proteome analyses, are being utilized to identify additional genes that formulate this complicated signaling pathway.

CHAPTER V

ENHANCED HOMOLOGOUS GENE RECOMBINATION EFFICIENCY IN *FUSARIUM VERTICILLIOIDES* BY DISRUPTION OF *FVKU70*, A GENE REQUIRED FOR NON-HOMOLOGOUS END JOINING

Fusarium verticillioides (Sacc.) Nirenburg (teleomorph *Gibberella moniliformis* Wineland) causes severe stalk rot and ear rot of maize and is found in plant residues in almost every maize field at harvest (White, 1999). Fungal stalk rots, including Fusarium stalk rot, are the most devastating disease of maize in terms of average yield loss. Economic losses due to stalk rot come in several different forms including stalk breakage, lodging, premature death of the plant, and the interruption of the normal grain filling process. Recently, attention to maize diseases caused by *F. verticillioides* has increased due to the fact that the fungus produces fumonisins, a group of carcinogenic mycotoxins, in infested maize ears. Ingestion of fumonisin-contaminated maize by humans and animals has been linked to a variety of illnesses, including leukoencephalomalasia and neural tube defects (Gelderblom *et al*., 1988; Marasas, 2001; Minorsky, 2002; Missmer *et al*., 2006). Over the past decade, significant progress has been made in elucidating the molecular genetic mechanisms associated with fumonisin biosynthesis, maize ear rot, and stalk rot in *F. verticillioides*. And the in the process, the research community assembled a wealth of publicly available *F. verticillioides* molecular, genetic, and genomic resources. These include a genetic map consisting of

150 biochemical, molecular and morphological markers and 486 AFLP markers (Jurgenson *et al*., 2002; Xu & Leslie., 1996), the *F. verticillioides* Gene Index at Dana-Farber Cancer Institute (http://compbio.dfci.hsrvsrd.edu/tgi/cgi-bin/tgi/gimain.pl?gudb=f_verticill) and the *F. verticillioides* genome database at Broad Institute (http://www.broad.mit.edu/annotation/genome/fusarium_group/MultiHome.html).

Despite being equipped with these resources, however, gene disruption remains as the key experimental procedure to unambiguously determine the functional role of a gene in filamentous fungi. In *F. verticillioides*, protoplast generation methodology was successfully adopted from other fungal systems (Upchurch *et al*., 1991; Salch & Beremand, 1993) and we now can routinely transform the fungus (Proctor *et al*., 1999; Shim & Woloshuk, 2001). In addition, using double-joint PCR-based strategy gene disruption vector construction is no longer the bottleneck step in *F. verticillioides* gene knock-out procedure (Yu *et al*., 2004; Shim *et al*., 2006). Albeit these improvements, targeted gene disruption in *F. verticillioides* is a laborious process due to high number of ectopic integration events that occur during transformation. In filamentous fungi, homologous recombination (HR) is primarily utilized for generating targeted gene replacement mutants, and in *F. verticillioides*, like other fungi, HR frequency is quite low (generally < 2%) (Weld *et al*., 2006). In general, we typically screen hundreds of drug-resistant transformants via PCR and Southern blot analysis before we can identify a true knock-out mutant strain.

This high frequency of ectopic integration in filamentous fungi is perhaps attributable to the activity of the nonhomologous end-joining (NHEJ) pathway in the

event of double-strand break (DSB) repair (Hefferin & Tomkinson, 2005). When exogenous gene disruption DNA constructs are introduced to protoplasts, they are recognized as DSB and subjected to DSB repairs in fungal nucleus. Two independent pathways are involved in repairing DSB: (1) HR which depends on sequence similarity, and (2) NHEJ which integrates exogenous DNA fragments into the genome independent of sequence homology (Ninomiya *et al*., 2004). NHEJ is the predominante mechanism for repairing DSB in filamentous fungi whereas HR is the dominant strategy in *Saccharomyces cerevisiae* (Meyer *et al*., 2007). The mechanism of DSB repair via NHEJ involves binding of Ku proteins (Ku70-Ku80 heterodimer) to foreign DNA fragment (Hefferin & Tomkinson, 2005; Ninomiya *et al*., 2004). Recent reports demonstrate drastic improvement in HR frequency in filamentous fungi by disrupting Ku70 or Ku80, (Goin *et al*., 2006; Haarmann *et al*., 2007; Krappmann *et al*., 2006; Meyer *et al*., 2007; Nayak *et al*., 2006; Ninomiya *et al*., 2004; Ueno *et al*., 2007). In this study, we hypothesized that *F. verticillioides* HR efficiency can be improved by disrupting NHEJ. To test this hypothesis, we generated a gene deletion mutant of *F. verticillioides KU70* homolog (*FvKU70*) and analyzed HR frequency in the mutant strain (SF41). We also investigated the impact of *FvKU70* deletion on the biology of the organism by investigating key *F. verticillioides* phenotypes, e.g., development, secondary metabolism, and virulence, in SF41. All primers used in this study are listed in Table 5.1.

The *F. verticillioides FvKU70* sequence was identified by screening the *Fusarium Group* Database. The search revealed that supercontig 4, specifically sequence 2,393,440 to 2,395,474, harbors 2,035-bp *FvKU70* gene sequence (FVEG_04235.3).

Table 5.1. Primers used in this study

Number	Name	Primer sequence (5' – 3')
1	KU-che-F	GATAAGCACCAGATCCTTCTGACCCTTGG
2	Gene-R	GAGAACCTGCGTGCAATCCATCTTGTTC
3	KU70-A	GAGTACTGAGGATATTGTGTGAATGCGACAG
4	KU70-B*	TCACTGGCCGTCGTTTTACAAGATACGATTGATGTC TGTTGCTCTTAGTG
5	KU70-C*	CATGGTCATAGCTGTTTCCTGGAATTGATCGAGAGA ATCGAGG
6	KU70-D	GTACTCCCATCGGTTGAGCTGATTGTCG
7	KU70-nest-F	CTCGGCGTTTTGGTATTCAGACCACTTTCGG
8	KU70-nest-R	CGATGTTGTTTAGGCTCTCGAGTGTCCC
9	CPP-F	CACATAGACCTTCCATTGAAGG
10	HPH-R2	CTGAAAGCACGAGATTCTTCGC
11	CMG-F	CAAGATCGACGAGATGCTCATTGTTCC
12	HPH-R2	CTGAAAGCACGAGATTCTTCGC
13	CPE-F	GTGGCCCATAGCTCTTACCAAGG
14	HPH-R	TGTAGAAGTACTCGCCGATAG
15	ORD-F	GAGAGCGAGCTTCCATTCTTGG
16	HPH-R	TGTAGAAGTACTCGCCGATAG

* M13-Forward and M13-Reverse primer sequences (underlined) were incorporated for double joint PCR application (Yu *et al*., 2004)

Conceptually translated FvKU70 protein shares significant similarity with *Neurospora crassa* MUS-51 (E value= 0.0) and *Claviceps purpurea* Ku70 (E value= 0) (Haarmann *et al*., 2007; Ninomiya *et al*., 2004), and is predicted to encode four key domains that are characteritic of Ku70 proteins, *i.e*., the Ku70/Ku80 N-terminal alpha/beta domain, the Ku70/Ku80 beta-barrel domain, the Ku70/Ku80 C-terminal arm, and the SAP (SAF-A/B, Acinus and PIAS) domain (Fig. 5.1A). A gene disruption vector (DKU1) containing a geneticin-resistance gene (*GEN*) as a selectable marker (Fig. 5.1B) was constructed via double-joint PCRs strategy as described previously (Sagaram *et al*., 2006a; Yu *et al.*, 2004). First, 950-bp 5' and 1000-bp 3' flanking regions of *FvKU70* were amplified from *F. verticillioides* genomic DNA (strain 7600, Fungal Genetic Stock Center, University of Missouri-Kansas City) using *Taq* DNA polymerase. The primers KU70-A and KU70-B were used to amplify 5' flanking region and primers KU70-C and KU70-D were used to amplify 3' flanking region. Simultaneously, the geneticin (G418)-resistant gene (*GEN*) was amplified from plasmid vectors pBS-G respectively using the primers M13-F and M13-R using Expand Long Polymerase, which has proof reading activity (Sagaram *et al*., 2007). Subsequently, the three amplicons were mixed in a single tube in a 1:3:1 (5' fragment: Marker: 3' fragment) molar ratio and joined by PCR without using any primers. Finally, nested primers KU70-nest-F and KU70-nest-R were used to amplify the 4.0-kb DKU1 construct (Fig. 5.1B). *F. verticillioides* transformation was performed as described (Sagaram *et al*., 2007), and the geneticin-resistant transformants were screened for *FvKU70* gene deletion by PCR and Southern blot

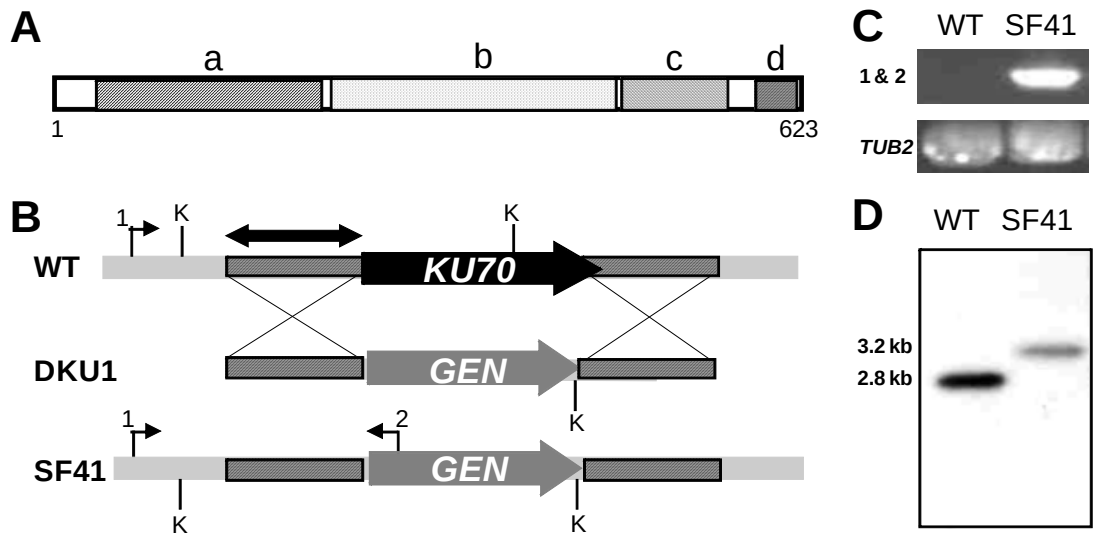

Fig. 5.1
Molecular characterization of *F. verticillioides FvKU70* gene. **(A)** Schematic representation of the putative 623-amino acid (aa) FvKU70 protein. Box a represents Ku70/Ku80 N-terminal alpha/beta domain, box b represnts Ku70/Ku80 beta-barrel domain, box c represents Ku70/Ku80 C-terminal arm, and box d represnts SAP (SAF-A/B, Acinus and PIAS) domain. **(B)** WT is a representation of *FvKU70* locus in the wild-type strain. DKU1 is the *KU70* disruption construct harboring a geneticin-resistance gene (*GEN*) as the selectable marker. SF41 is a schematic representation of *KU70* locus in the knock-out strain after the homologous recombination event. Shaded box represents the region where homologous recombination occurred. The double arrow on DKU1 indicates the fragment used as ^{32}P-labeled probe in the Southern blot. The numbered arrows indicate the location of primers used for PCR assays. K: *Kpn*I restriction site. **(C)** PCR analysis of *KU70* disruption using the primers described in Fig. 5.1A. WT: wild-type, SF41: *FvKU70* knock-out mutant. The number on the left (upper panel) indicates primer combinations for PCR amplification. Beta-tubulin gene PCR was used as a control. **(D)** Southern blot analysis of wild-type (WT) and SF41 strains. Fungal genomic DNA was digested with *Kpn*I, and the blot was hybridized with ^{32}P-labeled DNA probe (shown in Fig. 5.1A). Molecular sizes are indicated on the right.

analysis. Primers KU-che-F and Gene-R, designed to produce an amplicon only in the event of HR, were used to confirm the gene replacement. Of the 45 transformants screened, one isolate, designated SF41, produced the expected band (2.1 kb) whereas no amplicon was observed in the wild-type (Fig. 5.1C). Southern blot analysis further confirmed that the *GEN* gene replaced *FvKU70* in SF41. The 950-bp ^{32}P-labelled DNA probe hybridized to a 2.8 kb band in the wild-type, whereas to a 3.2 kb band in the SF41 strain (Fig. 5.1D).

Subsequently, we analyzed the impact of *FvKU70* deletion on key *F. verticillioides* phenotypes using methods described previously (Sagaram *et al*., 2007). We first assessed whether the mutation impacts growth and development by growing wild-type and SF41 on potato dextrose agar and V-8 agar. We did not observe any difference in colony morphology or growth rate (Fig. 5.2A and 5.2B). Conidia harvested from V-8 agar cultures showed no significant difference in asexual reproduction. We also successfully performed sexual cross using strain 7598 (Fungal Genetic Stock Center) as the opposite mating type (data not shown). Next, we tested whether SF41 is affected in virulence and fumonisin production (Sagaram *et al*., 2007). Internodal regions of 8-week-old B73 maize stalks were punctured with sterile needle and 10^4 spores of wild-type and SF41 were inoculated into the wound, and disease symptoms were observed by splitting open stalks longitudinally after 10-day incubation (25°C, 40% humidity). The stalk rots induced by wild-type and SF41 were indistinguishable. The result led us to conclude that deletion of *FvKu70* does not influence stalk rot virulence in *F. verticillioides* (Fig. 5.1D). A fumonisin assay was performed as described

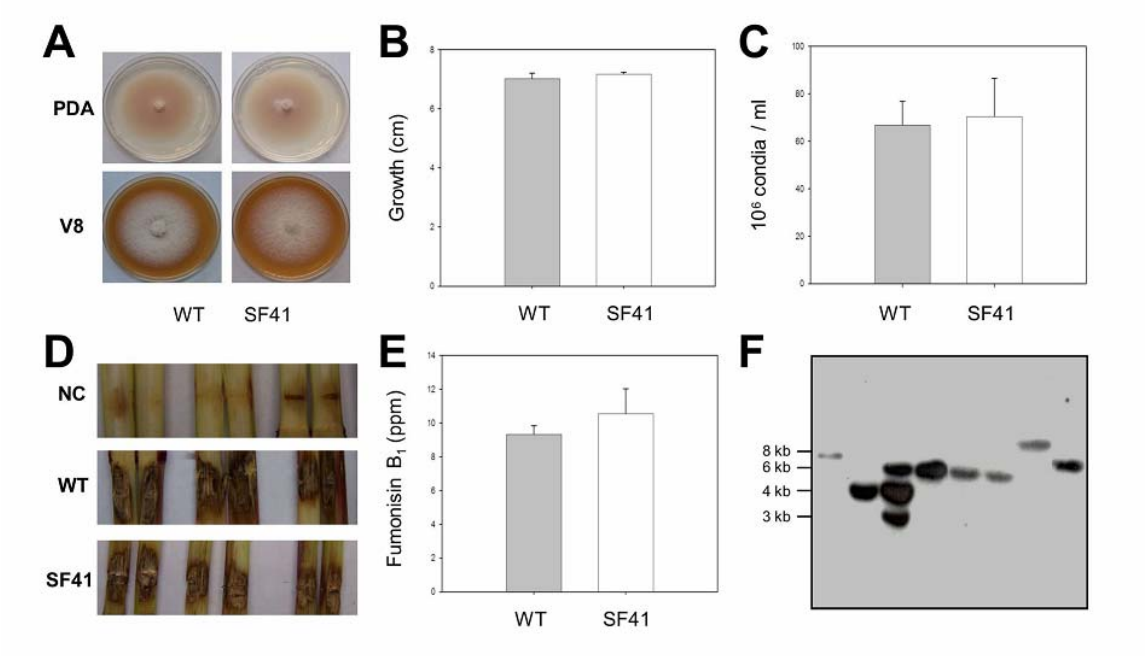

Fig. 5. 2
Phenotypic analysis of SF41 strain. **(A)** Colony morphology of the wild-type and SF41 strains grown on 0.2×PDA and V8 plates. Strains were point inoculated with an agar block (0.5 cm in diameter) and incubated for 7 days at 25°C under a 14 h light/10 h dark cycle. **(B)** Radial growth of strains grown on 0.2x PDA for 7 days was measured and presented as a bar graph. Results are means of three biological replications. **(C)** Conidia production was measured by harvesting conidia from 7-day-old carnation leaf agar as described previously (Sagaram *et al*., 2007). Mean number of conidia obtained from three biological replications is presented. **(D)** Fusarium stalk rot assay was performed as decribed by Shim et al. (2006). After incubation for 14 days, infected maize stalks were split longitudinally to assay the development of stalk rot. Three independent repetitions are shown. **(E)** Sterile cracked corn (1 g) was inoculated with wild-type and SF41, incubated for 14 days, and Fumonisin B_1 (FB_1) was analyzed by HPLC (Sagaram *et al*., 2007). All values represent means of three biological replications with standard deviations shown as error bars. **(F)** Southern blot analysis of eight randomly selected HR mutants with SF41 genetic background (Table 5.2). Molecular sizes are indicated on the left. Genomic DNA (10µg) samples were digested with *Eco*RV and were subjected to electrophoresis in 1.0% agarose gel. Blot was hybridized with ^{32}P-labeled *HPH* marker.

previously (Shim & Woloshuk, 2001; Sagaram *et al*., 2007). HPLC analysis of three biological replications revealed that there is no significant difference in fumonisin B1 production in wild-type and SF41 (Fig. 5.1E). Taken as a whole, we concluded that SF41 displays the same phenotypic traits as the wild-type strain and is therefore suitable for gene characterization studies as an alternative type strain.

To analyze the impact of *FvKU70* deletion on *F. verticillioides* HR frequency, we selected four genes, *CPP1* (FVEG_09543.3), *CMG1* (FVEG_12106.3), *CPE1* (FVEG_11127.3), and *ORD1* (FVEG_07201.3), for target gene disruption in wild-type and SF41 strains. Primers for DJ-PCR were designed and subsequently utilized to amplify gene-disruption constructs, harboring *HPH* gene as the selectable marker, as previously described (Choi & Shim, 2008a; Sagaram *et al*., 2007; Yu *et al.*, 2004). Wild-type and SF41 protoplasts were transformed with these constructs and selected hygromycin-resistant transformants. We then screened by PCR to determine the HR frequency in these transformants (Choi & Shim, 2008a; Sagaram *et al*., 2007). Primers for *CPP1* (CPP-F and HPH-R2), *CMG1* (CMG-F and HPH-R2), *CPE1* (CPE-F and HPH-R), and *ORD1* (ORD-F and HPH-R) would give rise to an amplicon only in the event of HR by gene-disruption constructs. The result demonstrated that the HR frequency in *F. verticillioides* was drastically increased by the deletion of *FvKU70*. In SF41 strain, we observed HR efficiency of 30~60%, which is a significant increase from 0.5~5% observed in the wild-type (Table 5.2); notably, we were able to increase *CMG1* HR frequency to 61% by using SF41, a dramatic increase from 1% in the wild-type strain. Subsequently, we randomly selected eight HR gene-disruption mutants, which

Table 5.2. Homologous recombination efficiency in the wild-type and SF41 strains

	Wild-type			SF41		
Genes	Transformants[a]	Mutants[b]	HR %[c]	Transformants[a]	Mutants[b]	HR %[c]
CPP1	180	2	1.1	13	5	38.5
CMG1	236	2	0.85	13	8	61.5
CPE1	40	2	5	12	4	33.3
ORD1	44	1	2.27	12	5	41.7

a) Total number of transformants screened for the homologous recombination (HR) event

b) The number of HR (knock-out) mutant isolates determined via PCR

C) HR percentages were calculated by dividing the number of HR mutant isolates with total number of transformants screened

were tested by PCR, and performed Southern analysis. Significantly, a high percentage of the mutants (7 out of 8) showed single disruption construct integration via HR (Fig. 5.2F). Also, we would like to note that four genes we tested are located on different chromosomes (I, IV, VIII, and IX), suggesting that the increased HR in SF41 is not restricted to certain loci. One negative effect of *FvKU70* deletion that we observed in this process was an overall decrease in the number of transformants. However, this was not surprising, and perhaps anticipated, since *FvKU70* deletion is not directly associated with improving HR process *per se* but rather eliminating or reducing NHEJ events that leads to frequent ectopic integration of disruption constructs during transformation (Hefferin & Tomkinson, 2005).

In summary, we demonstrated that HR efficiency in *F. verticillioides* can be improved significantly by using a NHEJ-deficient mutant strain SF41. Published reports show that HR frequency of 70-100% was observed in other filamentous fungi, e.g., *Neurospora crassa*, *Aspergillus fumigatus*, *A. nidulans, Cryptococcus neoformans*, *Sordaria macrospora*, and *Magnaporthe grisea* (Krappmann *et al*., 2006; Goin *et al*., 2006; Nayak *et al*., 2006; Ninomiya *et al*., 2004; Villalba *et al*., 2007). While the level of HR frequency was not as high as these filamentous fungi, increased HR frequency in SF41 is a drastic improvement from that of wild-type. In fungi where targeted gene disruption is considered difficult, such as *F. verticillioides* and *Claviceps purpurea* (Haarmann *et al*., 2007), HR frequency of 30-50% may have significant implications in future systemic gene function studies. SF41 strain is not impaired in key *F.verticillioides*

phenotypes, such as development, secondary metabolism, and pathogenicity, which render SF41 suitable for high-throughput gene function studies in *F. verticillioides*.

CHAPTER VI

CONCLUSION

Fusarium verticillioides poses a significant threat to human health and food safety by contaminating foods and feeds with various secondary metabolites. Of these secondary metabolites, FB_1 has received more attention due to its high toxicity. Therefore, research efforts have mainly focused on understanding the biosynthetic mechanism of FB_1. While our knowledge of FB_1 biosynthesis has increased, one of the remaining challenges is to characterize the regulatory mechanisms associated with FB_1 biosynthesis. Only a limited number of regulatory genes have been identified, and our understanding is still incomplete. Moreover, secondary metabolites produced by *F. verticillioides* are not limited to FB_1, and include a variety of other mycotoxins and pigments. Little is known about the biosynthesis mechanisms associated with other secondary metabolites in *F. verticillioides*.

My Ph.D. research has contributed to our understanding of *F. verticillioides* secondary metabolism in several ways. Characterization of a putative protein phosphatase gene *CPP1* as a negative regulator of FB_1 provides a new avenue for *Fusarium* secondary metabolism research. The fact that *CPP1* plays a key role in regulating not only secondary metabolism but also other key developmental phenotypes, such as macroconiation and hyphal morphogenesis, can lead us to exciting novel discoveries. Proteomics research is emerging as a practical tool to study fungal biology

and I have demonstrated that it can be applied to *F. verticillioides* secondary metabolism research. With the combination of qRT-PCR and proteomics, I identified a group of genes that are putatuve regulators of FB_1 biosynthesis. Forward genetics approach also enabled me to identify a novel gene *GAC1*, encoding a GTPase activating protein, serving as a negative regulator of bikaverin biosynthesis. Bikaverin biosynthesis in *F. verticillioides* is mostly unknown, and therefore this finding will provide a foundation for investigating the molecular mechanisms on bikaverin biosynthesis in *F. verticillioides*. Finally, *KU70* gene deletion mutant, SF41 strain, will help overcome low efficiency in HR and facilitate genome-scale functional studies in *F. verticillioides*.

There is no doubt that our knowledge of *F. verticillioides* secondary metabolisms is far from complete. There are only a handful of functionally characterized genes associated with FB_1 biosynthesis. Most of these regulatory genes show no clear epistatic relationships. Therefore, there is a need to study secondary metabolism signaling pathway(s) at the genome level, and further define inter-pathway relationships that control FB_1 biosynthesis. When signaling pathways that regulate other secondary metabolites are considered, the outlook of future research becomes far more complicated and intimidating. Conversely, this is an exciting era for *Fusarium* molecular genetics and genomics. I believe my research provided additional information and tools that will benefit *Fusarium* research community. It is my conviction that novel discoveries will be made in the near future, providing answers to decades old questions in fungal secondary metabolism.

REFERENCES

Avis, J. M. & Clarke, P. R. (1996). Ran, a GTPase involved in nuclear processes: its regulators and effectors. *J Cell Sci* **109,** 2423-2427.

Bacon, C. W., Hinton, D. M., Porter, J. K., Glenn, A. E. & Kuldau, G. (2004). Fusaric acid, a *Fusarium verticillioides* metabolite, antagonistic to the endophytic biocontrol bacterium Bacillus mojavensis. *Can J Bot* **82,** 878-885.

Bennett, J. W. & Bentley, R. (1989). What's in a name? Microbial secondary metabolism. *Adv Appl Microbiol* **34**, 1-28.

Bennett, J. W. & Ciegler, A. (1983). *Secondary Metabolism and Differentiation in Fungi*. New York: Marcel Dekker, Inc.

Blount, W. P. (1961). Turkey "X" disease. *J Br Turk Fed* **9**, 52-54.

Bluhm, B. H. & Woloshuk, C. P. (2005). Amylopectin induces fumonisin B_1 production by *Fusarium verticillioides* during colonization of maize kernels. *Mol Plant-Microbe Interact* **18**, 1333-1339.

Brown, D. W., Butchko, R. A., Busman, M. & Proctor, R. (2007). The *Fusarium verticillioides FUM* gene cluster encodes a Zn(II)2Cys6 protein that affects *FUM* gene expression and fumonisin production. *Eukaryot Cell* **6**, 1210-1218.

Brown, D. W., Cheung, F., Proctor, R. H., Butchko, R. A. E., Zheng, L., Lee, Y., Utterback, T., Smith, S., Feldblyum, T., Glenn, A., Plattner, R. D., Kendra, D. F., Town, C. D. & Whitelaw, C. A. (2005). Comparative analysis of 87,000 expressed sequence tags from the fumonisin-producing fungus *Fusarium verticillioides*. *Fungal Genet Biol* **42**, 848-861.

Brown, D. W., Yu, J. H., Kelkar, H. S., Fernandes, M., Nesbitt, T. C., Keller, N. P., Adams, T. H. & Leonard, T. J. (1996). Twenty-five coregulated transcripts define a sterigmatocystin gene cluster in *Aspergillus nidulans*. *Proc Natl Acad Sci* **93**, 1418-1422.

Bu'Lock, J. D. (1961). Intermediary metabolism and antibiotic synthesis. *Adv Appl Microbiol* **3**, 293-342.

Butchko, R. A. E., Plattner, R. D. & Proctor, R. H. (2003). *FUM13* encodes a short chain dehydrogenase/reductase required for C-3 carbonyl reduction during fumonisin biosynthesis in *Gibberella moniliformis*. *J Agric food chem* **51**, 3000-3006.

Calvo, A. M., Wilson, R. A., Bok, J.W. & Keller, N. P. (2002). Relationship between secondary metabolism and fungal development. *Microbio Mol Biol Rev* **66**: 447-459.

Candau, R., Avalos, J. & Cerda-Olmedo, E. (1992). Regulation of gibberellin biosynthesis in *Gibberella fujikuroi*. *Plant Physiol* **100**, 1184-1188.

Cary, J. W., Ehrlich, K. C., Bland, J. M. & Montalbano, B. G. (2006). The aflatoxin biosynthesis cluster gene, aflX, encodes an oxidoreductase involved in conversion of versicolorin A to demethylsterigmatocystin. *Appl Environ Microbiol* **72**, 1096-1101.

Ceulemans, H. & Bollen, M. (2004). Functional diversity of protein phosphatase-1, a cellular economizer and reset button. *Physiol Rev* **84,** 1-39.

Chant, J., Mischke, M., Mitchell, E., Herskowitz, I. & Pringle, J. R. (1995). Role of Bud3p in producing the axial budding pattern of yeast. *J Cell Biol* **129,** 767-778.

Chávez-Parga, M. del C., González-Ortega, O., Sánchez-Cornejo, G., Negrete-Rodríguez, M. de la L. X., González-Alatorre, G. & Escamilla-Silva, E. M.

(2005). Mathematical description of bikaverin production in a fluidized bed bioreactor. *World J Microbiol Biotechnol* **21**, 683-688.

Choi, Y. E. & Shim, W. B. (2008a). Functional characterization of *Fusarium verticillioides CPP1*, a gene encoding putative protein phosphatase 2A catalytic subunit. *Microbiol* **154,** 326-336.

Choi, Y. E. & Shim, W. B. (2008b). Identification of genes associated with fumonisin biosynthesis in *Fusarium verticillioides* via proteomics and quantitative real-time PCR. *J Microbiol Biotechnol*, in press.

Cooper, K. F., Mallory, M. J., Smith, J. B. & Strich, R. (1997). Stress and developmental regulation of the yeast C-type cyclin Ume3p (Srb11p/Ssn8p). *EMBO J* **16**, 4665-4675.

Cutler, N. S., Pan, X., Heitman, J. & Cardenas, M. E. (2001). The TOR signal transduction cascade controls cellular differentiation in response to nutrients. *Mol Biol Cell* **12,** 4103-4113.

Desjardins, A.E. (2006). *Fusarium Mycotoxins: Chemistry, Genetics, and Biology*. St. Paul, MN: APS Press.

Demain, A. L. & Fang, A. (2000). The natural functions of secondary metabolites. *Adv Biochem Eng Biotechnol* **69**, 1-39.

Dickman, M.B. & Yarden, O (1999). Serine/threonine protein kinases and phosphatases in filamentious fungi. *Fungal Genet Biol* **26**, 99–117.

Di Como, C. J. & Arndt, K. T. (1996). Nutrients, via the Tor proteins, stimulate the association of Tap42 with type 2A phophatases. *Genes Dev* **10,** 1904-1916.

Ding, Y., Bojja, R. S. & Du, L. C. (2004). Fum3p, a 2-ketoglutarate-dependent dioxygenase required for C-5 hydroxylation of fumonisins in *Fusarium verticillioides*. *Appl Environ Microbiol* **70**, 1931-1934.

Di Pietro, A., Madrid, M. P., Caracuel, Z., Delgado-Jarana, J. & Roncero, M. I. G. (2003). *Fusarium oxysporum*: exploring the molecular arsenal of a vascular wilt fungus. *Molecular Plant Pathology* **4,** 315-325.

Eaton, D & Groopman, J. (1998). *The Toxicology of Aflatoxins: Human Health, Vertinary, and Agricultural Significance*. San Diego: Academic Press.

Fitzgibbon, G., Morozov, I.Y., Jones, M.G. & Caddick, M.X. (2005). Genetic analysis of the TOR pathway in *Aspergillus nidulans*. *Eukaryot Cell* **4**, 1595–1598.

Flaherty, J. E., Pirttila, A. M., Bluhm, B. H. & Woloshuk, C. P. (2003). *PAC1*, a pH-regulatory gene from *Fusarium verticillioides*. *Appl Environ Microbiol* **69**, 5222-5227.

Flaherty, J. E. & Woloshuk, C. P. (2004). Regulation of fumonisin biosynthesis in *Fusarium verticillioides* by a zinc binuclear cluster-type gene, *ZFR1*. *Appl Environ Microbiol* **70**, 2653-2659.

Fraser, J. A., Davis, M. A. & Hynes, M. J. (2002). A gene from *Aspergillus nidulans* with similarity to *URE2* of *Saccharomyces cerevisiae* encodes a glutathione S-transferase which contributes to heavy metal and xenobiotic resistance. *Appl Environ Microbiol* **68**, 2802-2808.

Fujii, I., Yasuoka, Y., Tsai, H., Chang, Y. C., Kwon-Chung, K. J. & Ebizuka, Y. (2004). Hydrolytic polyketide shortening by Ayg1p, a novel enzyme involved in fungal melanin biosynthesis. *J Biol Chem* **279**, 44613-44620.

Gelderblom, W. C. A., Jaskiewicz, J., Marasas, W. F. O., Thiel, P.G., Horak, R. M., Vleggar, R., & Kriek, N. P. J. (1988). Fumonisins-novel mycotoxins with cancer-promoting activity produced by *Fusarium moniliforme*. *Appl Environ Microbiol* **54**, 1806-1811.

Giodano, W., Avalos, J., Cerdá-Olmedo, E. & Domenech, C. E. (1999). Nitrogen availability and production of bikaverin and gibberellins in *Gibberella fujikuroi*. *FEMS Microbiol Lett* **173**, 389-393.

Goins, C. L., Gerik, K. J. & Lodge, J. K. (2006). Improvements to gene deletion in the fungal pathogen *Cryptococcus neoformans*: Absence of Ku proteins increases homologous recombination and co-transformation of independent DNA molecules allows rapid complementation of deletion phenotypes. *Fungal Genet Biol* **43**, 531-544.

Haarmann, T., Lorenz, N. & Tudzynski, P. (2007). Use of a nonhomologous end joining deficient strain (Δku70) of the ergot fungus *Claviceps purpurea* for identification of a nonribosomal peptide synthetase gene involved in ergotamine biosynthesis. *Fungal Genet Biol* doi:10.1016/j.fgb.2007.04.008.

Hayes, J. D. & Pulford, D. J. (1995). The glutathione S-transferase supergene family: regulation of GST and the contribution of the isoenzymes to cancer chemoprotection and drug resistance. *Crit Rev Biochem Mol Biol* **30**, 445-600.

Hefferin, M. L. & Tomkinson, A. E. (2005). Mechanism of DNA double-stranded break repair by non-homologous end joining. *DNA Repair* **4**, 639-648.

Hunter, T. (1995). Protein kinases and phosphatases: The yin and yang of protein phosphorylation and signaling. *Cell* **80,** 225-236.

Jensen, O. N., Mortensen, P., Vorm, O. & Mann, M. (1997). Automation of matrix-assisted laser desorption/ionization mass spectrometry using fuzzy logic feedback control. *Anal Chem* **69**, 1706–1714.

Jiang, Y. (2006). Regulation of the cell cycle by protein phosphatase 2A in *Saccharomyces cerevisiae*. *Microbiol Mol Biol Rev* **70,** 440-449.

Jones, J.B., Jones, J. P. Stall, R. E. & Zitter. T. A. (1991). *Compendium of Tomato Diseases*. St. Paul, MN: APS Press.

Jurgenson, J. E., Zeller, K. A. & Leslie, J. F. (2002). Expanded genetic map of *Gibberella moniliformis* (*Fusarium verticillioides*). *Appl Environ Microbiol* **68**, 1972-1979.

Kahmann, R. & Basse, C. (1999). REMI (Restriction Enzyme Mediated Integration) and its impact on the isolation of pathogenicity genes in fungi attacking plants. *Eur J Plant Pathol* **105**, 221-229.

Keller, N. P., Dischinger, H. C., Bhatnagar, D. Jr., Cleveland, T. E. & Ullah, A. H. J. (1993). Purification of a 40-kilodalton methyltransferase active in the aflatoxin biosynthetic pathway. *Appl Environ Microbiol* **59**, 479-484.

King, H. C. & Sinha, A. A. (2001). Gene expression profile analysis by DNA microarrays: promise and pitfalls. *JAMA* **286**, 2280-2288.

Kinoshita, N., Yamano, H., Niwa, H., Yoshida, T. & Yanagida, M. (1993). Negative regulation of mitosis by the fission yeast protein phosphatase pps2. *Genes Dev* **7,** 1059-1071.

Kosmidou, E., Lunness, P. & Doonan, J. H. (2001). A type 2A protein phosphatase gene from *Aspergillus nidulans* is involved in hyphal morphogenesis. *Curr Genet* **39,** 25-34.

Krappmann, S., Sasse, C. & Braus, G. H. (2006). Gene targeting in *Aspergillus fumigatus* by homologous recombination is facilitated in a nonhomologous end-joining-deficient genetics background. *Eukaryot Cell* **5**, 212-215.

Kroken, S., Glass, N. L., Taylor, J. W., Yoder, O. C. & Turgeon, B. G. (2003). Phylogenomic analysis of type I Polyketide synthase genes in pathogenic and saprobic ascomycetes. *Proc Natl Acad Sci USA* **100,** 15670-15675.

Kung'u, J. N. & Jeffries P (2001). Races and virulence of *Fusarium oxysporum* f. sp. *cubense* on local banana cultivars in Kenya. *Ann Appl Biol* **139**, 343-349.

Lamarre, C., LeMay, J-D., Deslauriers, N. & Bourbonnais, Y. (2001). *Candida albicans* expresses an unusual cytoplasmic manganese containing superoxide dismutase (*SOD3* gene product) upon the entry and during the stationary phase. *J Biol Chem* **276**, 43784-43791.

Lara-Ortíz, T., Riveros-Rosas, H. & Aguirre, J. (2003). Reactive oxygen species generated by microbial NADPH oxidase NoxA regulate sexual development in *Aspergillus nidulans*. *Mol Microbiol* **50**, 1241-1255.

Li, S., Myung, K., Guse, D., Donkin, B., Proctor, R. H., Grayburn, W. S. & Calvo, A. M. (2006). *FvVE1* regulates filamentous growth, the ratio of microconidia to macroconidia and cell wall formation in *Fusarium verticillioides*. *Mol Microbiol* **62,** 1418-1432.

Li, Y., Huang, T. T., Carlson, E. J., Melov, S., Ursell, P. C., Olson, J. L., Noble, L. J., Yoshimura, M. P., Berger, C., Chan, P. H., Wallace, D. C. & Epstein, C. J. (1995). Dilated cardiomyopathy and neonatal lethality in mutant mice lacking manganese superoxide dismutase. *Nat Genet* **11**, 376-381.

Linnemannstöns, P., Schulte, J., del Mar Prado, M., Proctor, R. H., Avalos, J. & Tudzynski, B. (2002). The polyketide synthase gene *pks4* from *Gibberella fujikuroi* encodes a key enzyme in the biosynthesis of the red pigment bikaverin. *Fungal Genet. Biol* **37,** 134-148.

Liu, T. G., You, D. L., Valenzano, C., Sun, Y. H., Li, J. L., Yu, Q., Zhou, X. F., Cane, D. E. & Deng, Z. X. (2006). Identification of NanE as the thioesterase for polyether chain release in nanchangmycin biosynthesis. *Chem Biol* **13**, 945-955.

Livak, K. J. & Schmittgen, T. D. (2001). Analysis of relative gene expression data using real-time quantitative PCR and the $2^{-\Delta\Delta C}{}_{T}$ Method. *Methods* **25**, 402-408.

Loyall, L., Uchida, K., Braun, S., Furuya, M. & Frohnmeyer, H. (2000). Glutathione and a UV light-induced glutathione S-transferase are involved in signaling to chalcone synthase. *Plant Cell* **12**, 1939-1950.

Maier, F. J. & Shäfer, W. (1999). Mutagenesis via insertional- or restriction enzyme-mediated-integration (REMI) as a tool to tag pathogenicity related genes in plant

pathogenic fungi. *Biol Chem* **380**, 855-864.

Marasas, W. F. O. (2001). Discovery and occurrence of the fumonisins: A historical perspective. *Environ Health Perspect* **109,** 239-243.

Mayer-Jaekel, R. E. & Hemmings, B. A. (1994). Protein phosphatase 2A- a 'ménage á trios'. *Trends Cell Biol* **4,** 287-291.

McMullen, M., Jones, R. & Gallenberg, D. (1997). Scab of wheat and barley: A re-emerging disease of devastating impact. *Plant Dis* **81**, 1340-1348.

Merrill, A. H., Liotta, D. C. & Riley, R. T. (1996). Fumonisins: Fungal toxins that shed light on sphingolipid function. *Trends Cell Biol* **6**, 218-223.

Meyer, V., Arentshorst, M., El-Ghezal, A., Drews, A-C., Kooistra, R., van den Hondel, C. A. M. J. J. and Ram, A. F. J. (2007). Highly efficient gene targeting in the *Aspergillus niger kusA* mutant. *J Biotechnol,* **128**, 770-775.

Minorsky, P. V. (2002). The hot and the classic. *Plant Physiol* **129**, 929-930.

Missmer, S. A., Suarez, L., Felkner M., Wang E., Merrill Jr., A. H, Rothman, K. J., & Hendricks, K. A., (2006). Exposure to fumonisins and the occurrence of neural tube defects along the Texas-Mexico Border. *Environ Health Perspect* **114**, 237-241.

Munkvold, G. P. & Desjardins, A. E. (1997). Fumonisins in maize-Can we reduce their occurrence? *Plant Dis* **81**, 556-565.

Nayak, T., Szewczyk, E., Oakley, C. E., Osmani, A., Ukil, L., Murray, S. L., Hynes, M. J., Osmani, S. A. & Oakley, B. R. (2006). A versatile and efficient gene-targeting system for *Aspergillus nidulans*. *Genetics* **172**, 1557-1566.

Nelson, P. E., Desjardins, A. E., & Plattner, R. D. (1993). Fumonisins, mycotoxins

produced by Fusarium species: biology, chemistry, and significance. *Annu Rev Phytopathol* **31**: 233-252.

Nelson, P. E., Marasas, W. F. O., & Toussoun, T. A. (1983). Fusarium *species-An illustrated manual for identification*.University Park, PA: The Pennsylvania State University Press.

Ninomiya, Y., Suzuki, K., Ishii, C. & Inoue, H. (2004). Highly efficient gene replacements in *Neurospora* strains deficients for nonhomologous end-joining. *Proc Natl Acad Sci USA***101**, 12248-12253.

Orejas, M., Espeso, E. A., Tilburn, J., Sarkar, S., Arst Jr., H. N. & Penalva, M. A. (1995). Activation of the *Aspergillus* PacC transcription factor in response to alkaline ambient pH requires proteolysis of the carboxy-terminal moiety. *Genes Dev* **9**, 1622-1632.

Park, D. L. & Troxell, T. C. (2002). US perspective on mycotoxin regulatory issues. *Adv Exp Med Biol* **504**, 277-285.

Pelaez, F. (2005). *Handbook of Industrial Mycology*. New York: Marcel Dekker, INC.

Pirttilä, A. M., McIntyre, L. M., Payne, G. A. & Woloshuk, C. P. (2004). Expression profile analysis of wild-type and *fcc1* mutant strains of *Fusarium verticillioides* during fumonisin biosynthesis. *Fungal Genet Biol* **41**, 647-656.

Ploetz, R. C. (1994). Panama disease: Return of the first banana menace. *Int J Pest Man* **40**, 326-336.

Proctor, R., Desjardins, A., Plattner, R., & Hohn, T. (1999). A polyketide synthase gene required for biosynthesis of fumonisin mycotoxins in *Gibberella fujikuroi* mating population A. *Fungal Genet Biol* **27**, 100-112.

Proctor, R. H., Brown, D. W., Plattner, R. D., & Desjardins, A. E. (2003). Co-expression of 15 contiguous genes delineates a fumonisin biosynthetic gene cluster in *Gibberella moniliformis*. *Fungal Genet Biol* **38**, 237-249.

Rao, M. B., Tanksale, A. M., Ghatge, M. S. & Deshpande, V. V. (1998). Molecular and biotechnological aspects of microbial proteases. *Microbiol Mol biol Rev* **62**, 597-635.

Rheeder, J. P., Marasas, W. F. O., & Vismer, H. F. (2002). Production of Fumonisin analogs by *Fusarium* Species. *Appl Environ Microbiol* **68**, 2101-2105.

Rubella, S., Goswami & Kistler, H. C. (2004). Heading for disaster: *Fusarium graminearum* on cereal crops. *Mol Plant Pathol* **5**, 515-525.

Saez, A., Apostolova, N., Gonzalez-Guzman, M., Gonzalez-Garcia, M. P., Nicolas, C., Lorenzo, O. & Rodriguez, P. L. (2004). Gain-of function and loss-of-function phenotypes of the protein phosphatase 2C HAB1 reveal its role as a negative regulator of abscisic acid signaling. *The Plant Journal* **37,** 354-369.

Sagaram, U. S., Butchko, R. A. E., & Shim, W. B. (2006a). The putative monomeric G-protein *GBP1* is negatively associated with fumonisin B_1 production in *Fusarium verticillioides*. *Mol Plant Pathol* **7**, 381-389.

Sagaram, U. S., Kolomites, M & Shim, W. B. (2006b). Regulation of fumonisin biosynthesis in *Fusarium verticillioides*-Maize system, *Plant Pathol J* **22**, 203-210.

Sagaram, U. S., Shaw, B. D. & Shim, W. B. (2007). *Fusarium verticillioides GAP1*, a gene encoding a putative glycolipid-anchored surface protein, participates in conidiation and cell wall structure but not virulence. *Microbiol* **153**, 2850-2861.

Sagot, I., Rodal, A. A., Moseley, J., Goode, B. L. & Pellman, D. (2002). An actin nucleation mechanism mediated by Bni1 and profiling. *Nature Cell Biol* **4,** 626-631.

Sakumoto, N., Mukai, Y., Uchida, K., Kouchi, T., Kuwajima, Nakagawa, Y., Sugioka, S., Yamamoto, E., Furuyama, T., Mizubuchi, H., Ohsugi, N., Sakuno, T., Kikuchi, K., Matsuoka, I., Ogawa, N., Kaneko, Y. & Harashima, S. (1999). A series of protein phosphatase gene disruptants in *Saccharomyces cerevisiae*. *Yeast* **15,** 1669-1679.

Salch, Y. P. & Beremand, M. N. (1993). *Gibberella pulicaris* transformants: state of transforming DNA during asexual and sexual growth. *Curr Genet* **23,** 343-350.

Sambrook, J. & Russell, D.W. (2001). *Molecular Cloning*: *A Laboratory Manual.* Cold Spring Harbor, NY: Cold Spring Harbor Laboratory Press.

Seo, J. A., Proctor, R. H. & Plattner, R. D. (2001). Characterization of four clustered and coregulated genes associated with fumonisin biosynthesis in *Fusarium verticillioides*. *Fungal Genet Biol* **34**, 155-165.

Shaw, B. D. & Upadhyay, S. (2005). *Aspergillus nidulans swo*K encodes an RNA binding protein that is important for cell polarity. *Fungal Genet Biol* **42,** 862-872.

Shenolikar, S. (1994). Protein serine/threonine phosphatases-New avenues for cell regulation. *Annu Rev Cell Biol* **10,** 55-86.

Sheu, Y. -J., Santos, B., Fortin, N., Costigan, C. & Snyder, M. (1998). Spa2p interacts with cell polarity proteins and signaling components involved in yeast cell morphogenesis. *Mol Cell Biol* **18,** 4053-4069.

Shim, W. B., Flaherty, J. E. & Woloshuk, C. P. (2003). Comparison of fumonisin B_1 Biosynthesis in maize germ and degermed kernels by *Fusarium verticillioides*. *J Food Prot* **66**, 2116-2122.

Shim, W. B., Sagaram, U. S., Choi, Y. E., So, J., Wilkinson, H. H. & Lee, Y. W. (2006). *FSR1* is essential for virulence and female fertility in *Fusarium verticillioides* and *F. graminearum*. *Mol Plant-Microbe Interact* **19**, 725-733.

Shim, W. B. & Woloshuk, C. P. (1999). Nitrogen repression of fumonisin B1 biosynthesis in *Gibberella fujikuroi*. *FEMS Microbiol Lett* **177**, 109-116.

Shim, W. B. & Woloshuk, C. P. (2001). Regulation of fumonisin B_1 biosynthesis and conidiation in *Fusarium verticillioides* by a cyclin-Like (C-Type) gene, *FCC1*. *Appl Environ Microbiol* **67**, 1607-1612.

Shimanuki, M., Kinoshita, N., Ohkura, H., Yoshida, T., Toda, T. & Yanagida, M. (1993). Isolation and characterization of the fission yeast protein phosphatase gene ppe1+ involved in cell shape control and mitosis. *Mol Biol Cell* **4,** 303-313.

Stark, M. J. R. (1996). Yeast protein serine/threonine phosphatase: multiple roles and diverse regulation. *Yeast* **12,** 1647-1675.

Tag, A. G., Garifullina, G. F., Peplow, A. W., Ake Jr., C., Phillips, T. D., Hohn, T. M. & Beremand, M. N. (2001). A novel regulatory gene, *Tri10*, controls trichothecene toxin production and gene expression. *Appl Environ Microbiol* **67**, 5294-5302.

Tolleson, W. H., Melchior, W. B., Morris, S. M., McGarrity, L. J., Domon, O. E., Muskhelishvili, L., James, S. J. & Howard, P. C. (1996). Apoptotic and anti-proliferative effects of fumonisin B-1 in human keratinocytes, fibroblasts, esophageal epithelial cells and hepatoma cells. *Carcinogenesis* **17**, 239-249.

Tudzynski, B., Kawaide, H. & Kamiya, Y. (1998). Gibberellin biosynthesis in Gibbrella fujikuroi: cloning and characterization of the copalyl diphosphate synthase gene. *Curr Genet* **34**, 234-240.

Ueno, K., Uno, J., Nakayama, H., Sasamoto, K., Mikami, Y. & Chibana, H. (2007). Development of a highly efficient gene targeting system induced by transient repression of *YKU80* expression in *Candida glabrata*. *Eukaryot Cell* **6**, 1239-1247.

Upchurch, R. G., Walker, D. C., Rollins, J. A., Ehrenshaft, M. & Daub, M. E. (1991). Mutants of *Cercospora kikuchii* altered in cercosporin synthesis and pathogenicity. *Appl Environ Microbiol* **57**, 2940-2945.

Villalba, F., Collemare, J., Landraud, P., Lambou, K., Brozek, V., Cirer, B., Morin, D., Bruel, C., Beffa, R. & Lebrun., M. (2008). Improved gene targeting in *Magnaporthe grisea* by inactivation of *MgKU80* required for non-homologous end joining. *Fungal Genet. Biol* (In Press, doi:10.1016/j.fgb.2007.06.006).

Viljoen, A. (2002). The status of Fusarium wilt (Panama disease) of banana in South Africa. *S Afr J Sci* **98**, 341-344.

Weld, R. J., Plummer, K. M., Carpenter, M.A. & Ridgway., H. J. (2006). Approaches to functional genomics in filamentous fungi. *Cell Res* **16**, 31-44.

White, D. G. (1999). *Compendium of Corn Disease*. St. Paul, MN: APS Press.

Xu, J. R. & Leslie, J. F. (1996). A genetic map of *Gibberella fujikuroi* mating population A (*Fusarium moniliforme*). *Genetics* **143**, 175-189.

Yatzkan, E., Szöor, B., Fehér, Z., Dombrádi, V. & Yarden, O. (1998). Protein phosphatase 2A is involved in hyphal growth of *Neurospora crassa*. *Mol Gen Genet* **259,** 523-531.

Yatzkan, E. & Yarden, O. (1999). The B regulatory subunit of protein phosphatase 2A is required for completion of macroconidiation and other developmental processes in *Neurospora crassa*. *Mol Microbiol* **31,** 197-209.

Yoshizawa, T., Yamashita, A. & Luo, Y. (1994). Fumonisin occurrence in corn from high-risk and low-risk areas for human esophageal cancer in china. *Appl Environ Microbiol* **60**, 1626-1629.

Yu, F. G., Zhu, X. C. & Du, L. C. (2005). Developing a genetic system for functional manipulations of FUM1, a polyketide synthase gene for the biosynthesis of fumonisins in *Fusarium verticillioides. FEMS Microbiol Lett* **248**, 257-264.

Yu, J. H. & Keller, N. (2005). Regulation of secondary metabolism in filamentous fungi. *Annu Rev Phytopathol* **43**, 437-458.

Yu, J. H., Hamari, Z., Han, K. H., Seo, J. A., Reyes-Domínguez, Y. & Scazzocchio, C. (2004). Double-joint PCR: a PCR-based molecular tool for gene manipulations in filamentous fungi. *Fungal Genet Biol* **41,** 973-981.

Zabrocki, P., Van Hoof, C., Goris, J., Thevelein, J. M., Winderickx, J. & Wera, S. (2002). Protein phosphatase 2A on track for nutrient-induced signaling in yeast. *Mol Microbiol* **43,** 835-842.

Zeke, T., Kókai, E., Szöor, B., Yatzkan, E., Yarden, O., Szirák, K., Fehér, Bagossi, P., Gergely, P. & Dombrádi, V. (2003). Expression of protein phosphatase 1 during the asexual development of *Neurospora crassa*. *Comp Biochem Physiol B Biochem Mol Biol* **134,** 161-170.

VITA

Name:	Yoon E. Choi
Address:	3419 Cheswick Court Apt. F2, West Lafayette, Indiana, 47906
Email Address:	yechoi74@yahoo.com
Education:	B.S., Forest resources & environmental science, Korea University, 2000.
	M.S., Division of Molecular & Life Science, Pohang University of Science and Technology, Korea, 2002.
	Ph.D., Plant pathology and microbiology, Texas A&M University, 2008.